ATMOSPHERIC TEMPERATURE STRUCTURE FROM THE MICROWAVE EMISSION OF OXYGEN

by

B. RICHARD FOW
B.S., Drexel Institute of Technology
(1961)

SUBMITTED IN PARTIAL FULFILLMENT
OF THE REQUIREMENTS FOR THE
DEGREE OF MASTER OF SCIENCE

at the

MASSACHUSETTS INSTITUTE OF TECHNOLOGY
January, 1964

Signature of Author _____
Department of Meteorology,
20 January 1964

Certified by _____
Thesis Supervisor

Accepted by _____
Chairman, Departmental Committee
on Graduate Students

ATMOSPHERIC TEMPERATURE STRUCTURE FROM THE MICROWAVE EMISSION OF OXYGEN

by

B. Richard Pow

Submitted to the Department of Meteorology on January 20, 1964 in partial fulfillment of the requirements for the degree of Master of Science.

ABSTRACT

Previous work relating to the subject of the determination of atmospheric temperature profiles by radiometric soundings at infrared and microwave frequencies is reviewed. An attempt is made to show the progress and development of knowledge in this field. As suggested by Meeks and Lilley (1963) the microwave emission of atmospheric oxygen is investigated as a possible tool for the determination of the atmospheric temperature profile from zero to fifty kilometers. An iterative method for solving the integral equation relating the kinetic temperature profile and the emission measurements is proposed. Investigations designed to determine the best frequencies and nadir angles at which to make the measurements are undertaken. The iterative solution technique is compared with a simpler zero order solution and the former is demonstrated to be superior. A near limit in realizable accuracy of the iterative solution or inversion technique is determined. The effects of boundary conditions and the initial guess on the final result are explored. The iterative inversion technique is applied to ideal data from realistic model atmospheres. The results are seen to be quite good. Uncertainties and instrumental effects are then considered. The iterative inversion technique is applied to non-ideal data. The results obtained indicate the bandwidth and stability limitations that will be necessary in the radiometers ultimately to be built to make emissions measurements. The effects of uncertainties at different frequencies is explored. Experiments are performed to see if there is any difference between errors of the same magnitude but different sign.

Thesis Supervisor: Reginald E. Newell

Title: Assistant Professor of Meteorology

Research Supervisor: M. Littleton Meeks

Title: Staff Member, Lincoln Laboratory

TABLE OF CONTENTS

SECTION I

INTRODUCTION AND REVIEW OF PREVIOUS WORK

Meteorology is essentially pragmatic science. The ultimate purpose of scientific studies made in the name of meteorology is to extend the range and accuracy of weather forecasts or, more generally, predictions of the state of the entire atmosphere.. Most meteorologists would agree that before truly long range and accurate forecasts can be made, the forecaster must know the initial conditions of the atmosphere over the entire globe.

The density of weather observation sites is generally related to population density. North America, Europe, parts of Asia, and Australia are adequately covered while South America, Africa and in general the oceanic regions are poorly covered. In fact, there exist large expanses of ocean areas which are completely without any type of meteorological reporting stations.

It is virtually impractical and also very costly to provide world-wide coverage by conventional techniques.[1]

---

[1] Conventional techniques include balloon-radiosondes for soundings in the lowest 30 km of the atmosphere and rocket radiosonde and rocket grenade soundings for the region from about 30 km to 80 km. The radiosonde sensors are direct measuring and simple devices. The temperature sensor is a thermistor, the pressure sensor an aneriod capsule and the humidity sensor a relative humidity sensitive resistor. The rocket grenade method determines temperature and winds through measured time differences in the arrival of the sound waves at ground based receivers. At the present time rocket grenade firings are limited in number because of the large expense involved.

The cost of operating a weather ship for one year is of the order of several million dollars and several hundred such ships would be required to give even marginal coverage of the oceans. Additional land stations, though not as expensive as ships are nevertheless very costly. The use of airplanes or balloons to make direct measurements similar to those that are made by ground stations or ships is equally expensive.

The development of artificial earth satellites as observation platforms and the success of the TIROS weather satellite program have given impetus to the idea of using satellites to fill the void in our data acquisition network. It now appears that satellites can cover large areas of the earth's atmosphere in a short time and at a reasonable cost. However, since the satellite must operate outside the earth's atmosphere, most of what today is considered meteorologically useful information, that is temperature, pressure water vapor, and other trace substance distributions, must be measured by indirect methods. Unfortunately, the most useful meteorological information, the wind field, does not at present appear to be measureable to any satisfactory degree by indirect means. However, in all but the tropical and part of the subtropical latitudes, at least the geostrophic[2] wind

---

[2] In the middle latitudes, i.e., 30° to 60° North or South, the horizontal pressure gradient in the atmosphere and the coriolis force essentially balance one another. Hence at a given altitude, the horizontal wind can be calculated from the horizontal pressure gradient, density and coriolis parameter. This is known as the geostrophic approximation. For more details on this subject any introductory text in dynamic meteorology may be consulted.

field can be reasonably well deduced from the temperature, pressure and humidity distributions.

Since the geostrophic scale theory indicates that the approximation of a hydrostatic atmosphere is quite tenable, our primary interest is directed to the determination of the temperature and humidity distributions and the ground level pressure. Here we are indeed fortunate, because these three parameters are intimately associated with the electromagnetic radiation emanating from the earth's atmosphere.

In this work we shall be concerned with the determination of the vertical thermal structure of the atmosphere in the lowest fifty kilometers. We shall assume horizontal homogeneity of the atmosphere over relatively small square areas of about eighty kilometers or fifty miles on a side. It might be added at this point that the usefulness of the temperature structure is not limited to weather forecasting. It is a vital aspect of our environment and as such effects many human endeavours.

Before proceeding to examine the previous work in this subject, let us briefly review the theoretical foundations of the determination of temperature structure from the radiative emission of the atmosphere. The thermal radiation in the earth's atmosphere may be calculated from the differential equation of radiative transfer. A derivation and general discussion of this equation may be found in Steinberg et Lequeux (1960). We shall assume the radiative transfer equation in the following form:

$$\frac{d}{dz}(I_\nu) = -K_\nu (I_\nu) + \epsilon_\nu \qquad (1)$$

where I_ν = monochromatic intensity of radiation emerging from the atmosphere

K_ν = monochromatic absorption coefficient

ε_ν = monochromatic emission per unit length

z = vertical coordinate.

We next define the following quantity

$$\tau_\nu(z) = \int_0^{\tau_\nu(z)} d\tau_\nu = -\int_H^z K_\nu \, dz = \int_z^H K_\nu dz$$

as the monochromatic optical depth of the atmosphere when looking down from a height H to a height z. Using the definition of optical depth, we apply the integrating factor $e^{-\tau_\nu}$ to equation (1) and solve it obtaining the very general result

$$I_\nu(H) = I_\nu(z)\, e^{-\tau_\nu(z)} + \int_0^{\tau_\nu(z)} \frac{\varepsilon_\nu}{K_\nu}\, e^{-\tau_\nu}\, d\tau_\nu \qquad (2)$$

If we now assume that local thermodynamic equilibrium obtains and z is ground level; i.e. z = 0, then equation can be written as

$$I_\nu(H) = I_\nu(0)\, e^{-\tau_\nu(0)} + \int_0^{\tau_\nu(0)} J_\nu(\tau_\nu)\, e^{-\tau_\nu}\, d\tau_\nu \qquad (3)$$

where $J_\nu(\tau_\nu) = \dfrac{\varepsilon_\nu}{K_\nu n_\nu^2}$ = source function; i.e. Planck radiation function.

Equation (3) says that the intensity that we measure at altitude H is the sum of the intensity of a source lying underneath the atmosphere

$I_\nu(0)$ diminished by the negative exponential of the optical depth of the atmosphere plus the self emission of all infinitesimal layers between H and the ground each diminished by the negative exponential of the optical depth between it and H. Equation (3) was derived with the assumption that the observer is at an altitude H looking down to the ground. A similar equation results if the observer looks up from H. That equation is

$$I_\nu(H) = I_\nu(\infty)\, e^{-\tau_\nu(\infty)} + \int_0^{\tau(\infty)} J_\nu(\tau_\nu)\, e^{-\tau_\nu}\, d\tau_\nu \qquad (4)$$

where $I_\nu(H)$ is now the downward flux at H and $I_\nu(\infty)$ is the intensity of a source just above the atmosphere.

Now the optical depth τ_ν is a function of altitude and the monochromatic absorption coefficient. But the monochromatic absorption coefficient is a function of the temperature profile, pressure profile, and the composition profile of which the water vapor profile is a part. We have already stated that the hydrostatic assumption is generally a very good assumption, therefore, we shall employ it. We shall now further assume that the concentration profiles and ground level pressure are known. Hence the pressure profile with height may be expressed exclusively by the temperature profile. Thus the monochromatic absorption coefficient and in the case of thermodynamic equilibrium the monochromatic emissivity are functions of the temperature profile.

In this light let us reconsider the solution of equation (1). Hence we must solve the equation

$$\frac{dI_\nu}{dz} = - K_\nu\, I_\nu + \epsilon_\nu \qquad (5)$$

We apply the integrating factor $e^{K_\nu z}$ and obtain

$$\frac{d}{dz} \left(I_\nu e^{K_\nu z}\right) = \epsilon_\nu e^{K_\nu z} \tag{6}$$

Now for thermodynamic equilibrium we have

$$\epsilon_\nu = K_\nu J_\nu \tag{7}$$

where J_ν is the Planck black body radiation function. Substituting (7) into (6) and integrating from $z = 0$ to $z = H$ the height of the observation platform there obtains

$$I_\nu(H) = I_\nu(0)\, e^{-K_\nu H} + \int_0^H J_\nu K_\nu e^{-K_\nu(H-z)}\, dz \tag{8}$$

where the functional dependences of K_ν and J_ν on the temperature profile $T(z)$ are understood, i.e., $K_\nu = K_\nu(T(z))$ and $J_\nu = J_\nu(T(z))$. Equation (8) is a non-linear integral equation in the independent variable z, the parameter ν and implicitly the unknown function $T(z)$. That which is measured by the radiometric instrumentation on the satellite is $I_\nu(H)$ versus ν. If the complete $I_\nu(H)$ spectrum is known then a unique and exact $T(z)$ can be found which satisfies equation (8) for all ν.

Kaplan (1959) was the first one to propose the use of remote radiation measurements to deduce the thermal structure of the atmosphere. His proposed method required ten high resolution (10 cm^{-1} minimum resolution) measurements made from above the atmosphere at carefully selected frequencies in the 15 μ CO_2 vibrational band. The ten frequencies selected were on the high frequency side of the 15 μ resonance and the unit optical depths[3] corresponding to them ranged

[3] unit optical depth is the d which makes $\int_0^d K_\nu\, dz = 1$

from near zero to distances greater than the height of the observing platform. Thus the emission at each of the ten frequencies would be characteristic of the emission from each of ten layers of a cloudless atmosphere ranging from the ground to the very top layer of the atmosphere. Clouds were assumed to be black bodies and hence the tops were considered to be the lowest level from which radiation emanated.

In this proposal, it was concluded that the measurement of the emission into space at ten frequencies would permit the determination of the mean temperature of each of the ten layers, subject to the following provisions: (1) that within each layer the relative variation of temperature with height is specified; (2) that the temperature of the underlying surface be determined by measurements further out in the band wing where the unit optical depth is very large; and (3) that for a given frequency the emission should originate from approximately the same atmospheric layer for all temperature profiles.

In his next work (1960), Kaplan discusses in more detail the interpretation of the radiation measurements in terms of the departures of temperatures from some standard atmosphere with pressure as the independent variable. He divided the atmosphere into six layers and specified several possible constant lapse rates within each layer. This gave him a library of continuous temperature distributions from 1000 mb (assumed to be ground level) to 50 mb above which the atmosphere was considered to be isothermal. He also assumed a CO_2 concentration of 2.6 mm per mb at standard temperature and pressure. Each model atmosphere emits radiation, $\underline{S}_o$, whose frequency dependence

is a function of the temperature dependence. Given a set of actual radiation readings, $\underline{S}$, taken by a satellite spectroscope, the model which "best fits" the observed data is chosen as the one for which $(\underline{S} - \underline{S}_{\partial})^2$ is a minimum.

A more detailed solution is then obtained using a perturbation technique by expanding the fractional departures of the observed radiation from that of the "best fitting" model in terms of the temperature departures in each layer. The first order or linear departures are solved for directly from the resulting set of linear equations. These results are then used to obtain the quadratic or second order departures. The process is repeated iteratively until a satisfactory convergence is obtained. Third and higher order departures can be neglected if there are a sufficient number of models to obtain a reasonable first approximation.

Kaplan tested the method by using one of his models as assumed observations. He chose the following seven frequencies: 675, 685, 695, 700, 705, 710 and 730 cm^{-1}. He did not obtain convergent solutions in all the test cases of his method. The results of the cases that did converge were quite good.

Some experiments with systematic and random errors were also performed. It was found that temperature errors were approximately proportional to the magnitude of the systematic noise. However, the inclusion of random errors produced temperature errors that were much worse and oscillatory. Kaplan felt that a better selection of frequencies might reduce the effects of the random errors and if this was not sufficient, the number of atmospheric layers would have to be reduced.

Other conclusions reached by Kaplan were as follows. If ground reflectivity at 15 μ can be neglected, then the outgoing radiation for an overcast condition is the same with an isothermal layer from the top of the clouds to the ground. Hence the method can yield the level and temperature of cloud tops. With the addition of cloud pictures, the partially overcast case could be handled. Finally, the most accurate results will be obtained for each layer if the entire atmosphere is sounded.

King (1959, 1963) examines the radiative transfer equation and the solutions given by equations (3) and (4) in the light of modern mathematical concepts. He shows that if

$$e^{-\tau(0)} \ll 1 \quad \text{or} \quad e^{-\tau(\infty)} \ll 1$$

then (3) or (4) respectively are Laplace transforms of J_ν (τ_ν); the transform variable being τ_ν, the optical depth or in the case of a horizontally stratified atmosphere $\tau_\nu \sec \theta$, where θ is the zenith or nadir angle (see Fig. 1). Hence with the transform variable a function of frequency through τ_ν or a function of sec θ, the inversion may be performed in terms of frequency or sec θ. He further points out that since such a transformation is an integration operation, its inversion must be in essence a differentiation operation. Hence a multiplicative effect on errors in the data might be expected. Thus King's great contribution to this subject is to bring to light such theoretical mathematical considerations as are involved in this problem.

Wark (1961) proposed an abbreviated version of Kaplan's experiment. He started with the equation of radiative transfer in the following form:

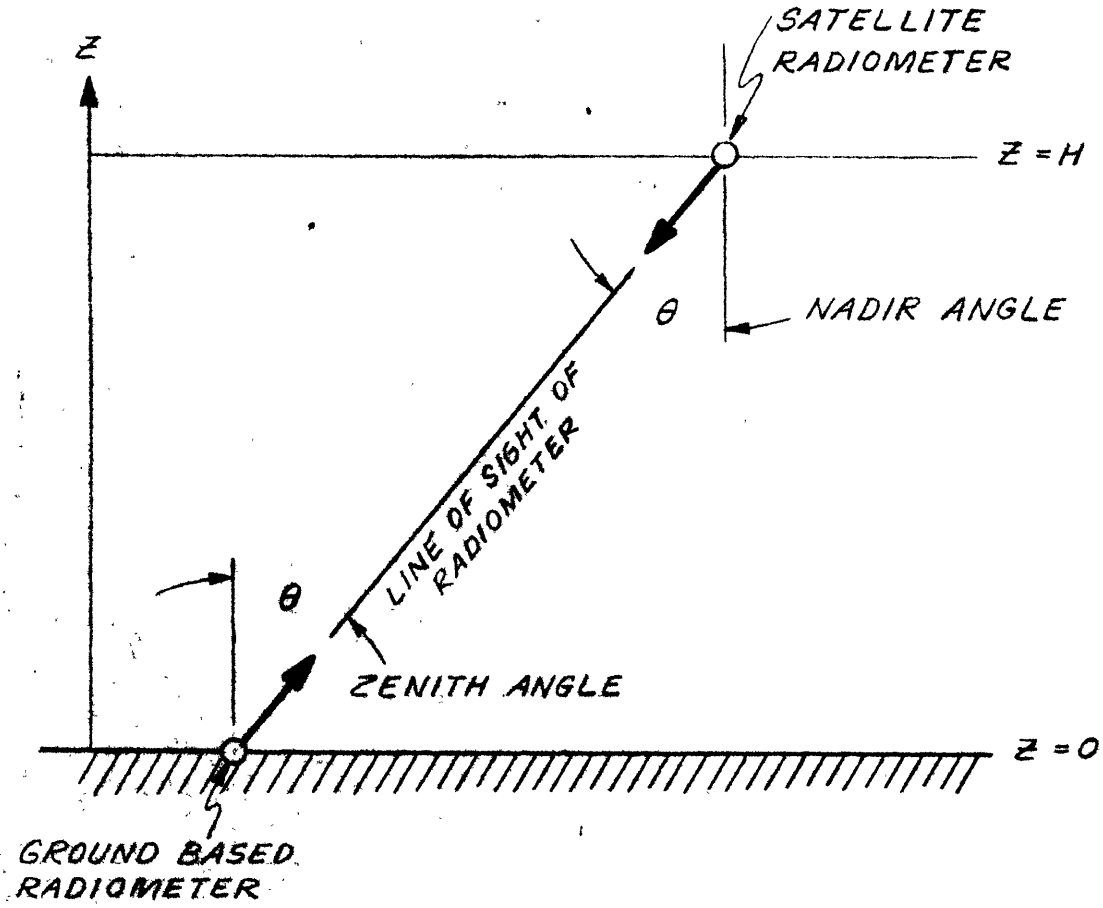

FIG. 1 RELATIONSHIP OF ALTITUDE AND PATH LENGTH FOR A HORIZONTALLY STRATIFIED ATMOSPHERE

$$I_\nu(H) = J_\nu(T_2) + \int_{T_2}^{T_o} \tau_\nu \frac{\partial[J_\nu(T)]}{\partial T} dt \tag{9}$$

where $\tau_\nu = e^{-\int_z^H K_\nu dz}$ = transmission function

T_2 = kinetic temperature at $z = H$

T_o = kinetic temperature at a point below where $\tau_\nu \sim 0$

Equation (9) is easily derived from equation (3) after assuming that the $\tau_\nu(0)$ of equation (3) is essentially infinite for the frequencies under consideration. He limits the investigation to the stratosphere and divides this region into three layers. Now if we use pressure instead of temperature as the dependent variable, we can rewrite equation (9) as

$$I_\nu(H) = J_\nu(T_2) + \int_{P_2}^{P_1} \tau_\nu \left[\frac{\partial J_\nu}{\partial(\log P)} \right] d(\log P) + \int_{P_1}^{P_o} \tau_\nu \left[\frac{\partial J_\nu}{\partial(\log P)} \right] d(\log P) \tag{10}$$

The layers are then assumed to be isothermal which is expressed by

$$\frac{\partial J_\nu}{\partial(\log P)} = \text{constant} = A \tag{11}$$

It is then further assumed that since the frequency range of the measurements is small, we can write for the chosen three frequencies (i.e. 680 cm^{-1}, 690 cm^{-1}, and 695 cm^{-1})

$$\begin{aligned} J_2 &= \beta_2 J_1 \\ J_3 &= \beta_3 J_1 \end{aligned} \tag{12}$$

where β_2 and β_3 are constants which are computed for $T = 250^\circ$ K. Substitution of (11) and (12) into (10) at the three frequencies yields

$$\begin{aligned} I_1 &= J_1'(T_2) + A' D_1' + A'' D_1'' \\ I_2 &= \beta_2 J_1'(T_2) + A' D_2' + A'' D_2'' \\ I_3 &= \beta_3 J_1'(T_2) + A' D_3' + A'' D_3'' \end{aligned} \tag{13}$$

where the D's are the integrals of the form $\int_0^P \tau d(\log P)$ which results from the substitution of (11) into (10). $J_1(T_2)$, A' and A'' are obtained from the solution of (13). From $J_1(T_2)$ we obtain T_2 and it can be shown that from A' and A'' we can obtain $\partial T/\partial(\log P)$, the temperature lapse rate.

Wark computed emissions for three assumed atmospheres and then used these as inputs to his method. His results also were quite good. There was no indication in Wark's work as to whether or not he made any analysis of the effects of random or systematic errors in the input data.

Fryberger and Uretz (1961) also made a study of the determination of the atmospheric temperature profile. They developed an equation

relating the radiometric profile to the temperature profile from concepts and terminology familiar to electrical engineers. They were concerned with the thermal structure in the lowest 10,000 feet of the atmosphere. They assumed a horizontally stratified atmosphere and chose to invert the transfer equation using zenith angle rather than frequency as the transform variable. Radiometric profiles were computed for several atmospheres. A solution for the temperature profile of the form

$$T = \begin{cases} T_1 = T_o + k_1 h & 0 \le h < 500 \\ T_2 = T_o + k_1 500 + k_2(h - 500) & 500 \le h < 1000 \\ & \\ T_{2-} = T_o + k_1 500 + \dots + k_{20}(h - 9500) & 9500 \le h < 10000 \end{cases} \tag{14}$$

where h is the altitude in feet, was assumed. The transform equation they dealt with was essentially equation (8) integrated from the ground up to 10000 feet instead of from H down to 0, generalized to a horizontally stratified atmosphere (i.e. heights were multiplied by sec θ), and with the resulting first term $e^{-K_\nu(10000)}$ considered to be negligible. They then substituted equation (14) into their expression for J_ν and used an assumed standard profile in K_ν. Thus equation (8) is linearized and tractable. They then solved the resulting linear system for the coefficients k_i in equation (14). The profile corresponding to these coefficients then served as the second approximation which is used in K_ν and the process is repeated iteratively until the k_i's converge.

They performed their inversions in infrared spectrum, but the frequency was not specified. Their results were good; the derived temperature profiles reproduced the temperature profiles from which the radiometric profiles were obtained well except where the original temperature profile had considerable and varying curvature. They did not indicate whether or not a systematic and/or random error analysis was performed.

Yamamoto (1961) described another approach to solving the so called Kaplan problem. We shall now consider his method in some detail for it is the method employed in this work. Observations are assumed to be made from above in the following four band regions of the 15 μ CO_2 band: 665-670, 675-680, 686-691 and 692-697. A uniform CO_2 distribution is assumed. Equation 3 may then be written as

$$I_\nu(0) = -\int_0^{p_s} J_\nu(p) \frac{d\tau_\nu(p)}{dp} dp \tag{15}$$

where the independent variable is pressure with p_s the surface pressure. τ_ν of equation (15) is the transmission function as defined in equation (9). Also as in equation (9) the monochromatic optical depth at the lower limit of the sounding is essentially infinite. Also, since all measurements are made at frequencies near the center of the 15 μ band, it is assumed that

$$J_\nu(p) = \alpha_\nu J(p) \tag{16}$$

where the α_ν's are constants and $J_\nu(p)$ is the Planck function at a wave number near the center of the band. Substituting (16) into

(15) there obtains

$$I'_\nu(0) = -\int_0^{p_s} J(p) \frac{d\tau_\nu(p)}{dp} \, dp \tag{17}$$

where $I'_\nu = \frac{I_\nu}{\tau_\nu}$

Yamamoto's technique is to express $J_\nu(p)$ by a polynomial of a limited number of terms (actually 4) each term having one unknown parameter, its coefficient. He then computes the transmission function using the ICAO standard atmosphere. Hence by inserting the assumed form of $J(p)$ into equation (17), its constants can be determined by inverting the linear system

$$I_{\nu_1}(0) = -a_1 \int_0^{p_s} P_1(p) \frac{d\tau_{\nu_1}}{dp} \, dp - a_2 \int_0^{p_s} P_2(p) \frac{d\tau_{\nu_1}}{dp} \, dp$$

$$- a_3 \int_0^{p_s} P_3(p) \frac{d\tau_{\nu_1}}{dp} \, dp - a_4 \int_0^{p_s} P_4(p) \frac{d\tau_{\nu_1}}{dp} \, dp \tag{18}$$

where the $P(p)$'s are the polynomial terms with coefficients a_1, a_2, a_3 and a_4 respectively. It should be emphasized at this point that the integrals can be evaluated since a temperature profile (i.e. ICAO Standard Atmosphere) has been assumed insofar as the computation of

$d\tau_\nu/dp$ is concerned. The process may be repeated with the temperature profile corresponding to the derived coefficients used in computing $d\tau_\nu/dp$, and so on iteratively. Yamanoto suggested this but did not do it.

His main concern in this work was to determine a variable by which the Planck function corresponding to the atmospheric temperature distribution, in general, could best be represented by a polynomial of as few terms as possible. He also tried different representations for the transmission function, for example, numerical values, Legendre polynomials and Chebyshev polynomials. He noted that none of the polynomial representations were markedly superior to the others. The Legendre polynomials however did simplify the computations.

The method and the various polynomials were tested by using as input data the calculated emission from atmosphere with various temperature profiles. These profiles were taken from actual radiosonde soundings. The derived profiles reproduced well the mean features of the actual atmospheres. Details such as the height of the tropopause did not show up very well. In all of the calculations, the effects of water vapor and ozone on absorption at 15 μ were neglected. No error studies were conducted.

Meeks (1961) first proposed using the millimeter spectrum of oxygen to sound the atmosphere. This idea was elaborated in a later work, Meeks and Lilley (1963), in which details of atmospheric oxygen absorption and emission centered at 60.0 kilo-megacycles per sec was considered. The microwave spectrum of the oxygen molecule O_2^{16} is a result of fine-structure transitions in which the magnetic moment assumes

various directions with respect to the rotational angular momentum of the molecule. In comparison, the fine structure of the 15 μ CO_2 band is due to the rotational fine structure of the molecule while in its vibratory state.

At the microwave frequencies the emission from the earth's atmosphere, which is considered to be a black body at temperatures on the order of 300° K, is adequately represented by the Rayleigh Jeans approximation to black body emission. Thus we can write for J_ν, the source function in the previous equations,

$$J_\nu = 2\,kT/\lambda^2 \tag{19}$$

Also since radiometers are generally calibrated with sources at certain reference temperatures, it is customary to measure power in terms of an equivalent temperature. This so called brightness temperature is defined by the expression

$$I_\nu = 2kT_b(\nu)/\lambda^2 \tag{20}$$

If we now substitute equations (19) and (20) into (8) there obtains

$$T_b(\nu) = T_s(\nu)\, e^{-K_\nu H\mu} + \int_0^H T\,\{K_\nu\, e^{-K_\nu(H-z)\mu}\ \mu\}dz \tag{21}$$

where we have generalized to an arbitrary nadir angle θ, by assuming a horizontally stratified atmosphere with $\mu = \sec\theta$ (see Fig. 1) and where T_s = the brightness of a source lying outside the atmosphere.

As pointed out by Meeks and Lilley (1963), if the brightness temperature of the underlying surface of the atmosphere is close to zero or if the exponent $K_\nu H$ is much greater than 1, then the bracketed quantity of equation (21) can be regarded as a weighting function that specifies the contribution of the state temperature T(h) to the brightness temperature $T_b(\nu)$. Let us now consider the shape of this function when viewing the atmosphere from above and at a frequency which is not on a resonance line. At low altitudes the value of K_ν is very large due to the pressure broadening effects, however, concomitantly the exponential term is very small; hence the weighting function has a small value. As we rise to higher altitudes K_ν decreases, but so does the quantity $K_\nu(H-z)$; hence the value of the exponential term rises and thus so does the value of the weighting function. As z approaches H, the exponential approaches its maximum value 1, but at the same time decreasing effects of pressure broadening are causing K_ν to approach zero; hence the weighting function approaches zero again. A typical weighting function is shown in Fig. 2.

Meeks and Lilley (1963) determined the shapes of twelve weighting functions at six different frequencies and at two nadir angles for each frequency. It is shown that at frequencies of intense absorption, the half width is smaller and the altitude at the peak points is higher than at frequencies of less intense absorption. It is also shown that the altitude at the peak point rises slightly with increasing nadir angle.

The weighting function concept shows us that the brightness temperature at a given frequency is indicative of state temperatures

FIGURE 2

A TYPICAL WEIGHTING FUNCTION

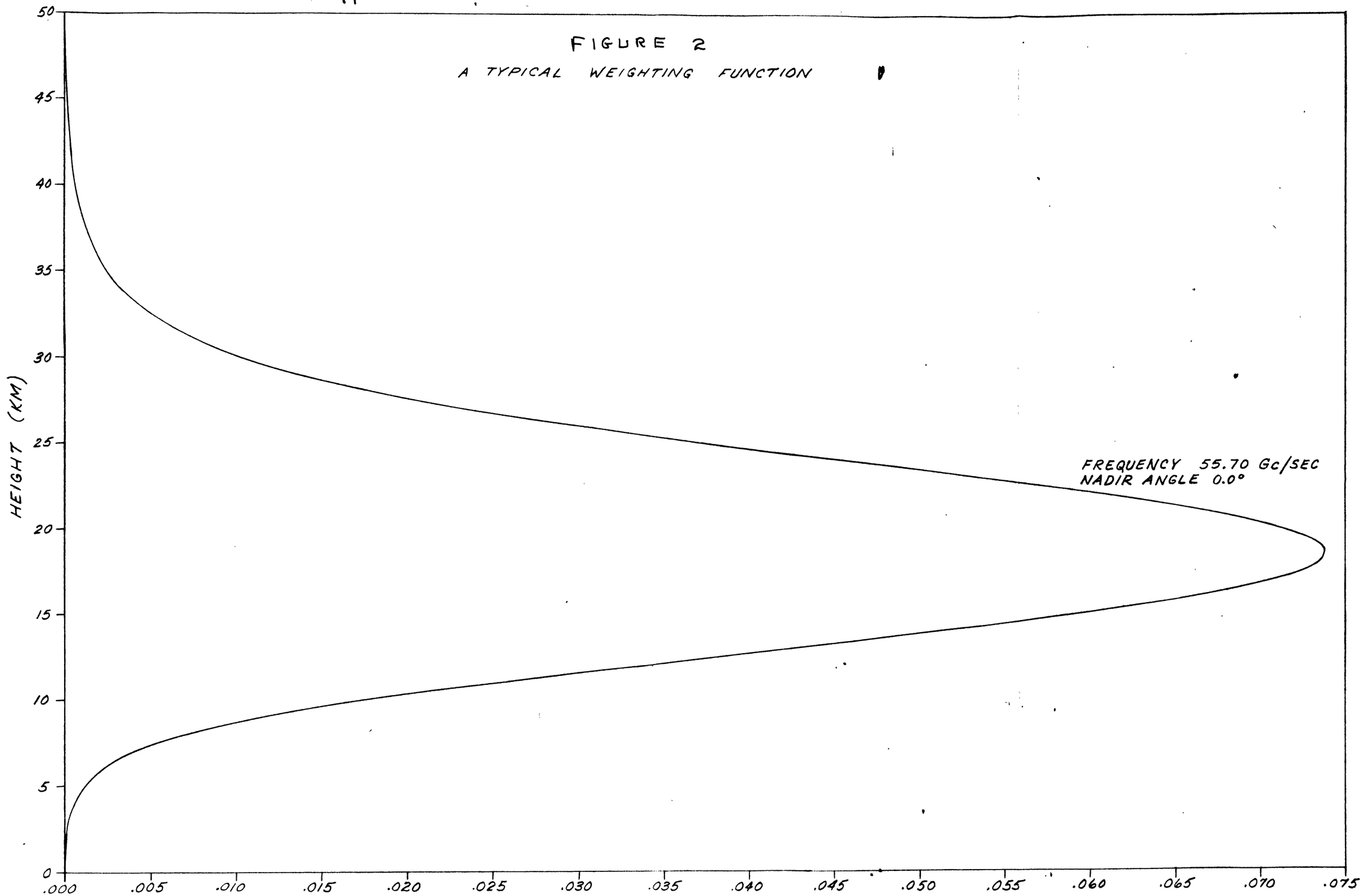

B-19314-2 WEIGHTING FUNCTION

primarily in the region between the half maxima of the weighting function. Consequently Meeks and Lilley proposed that the weighted mean temperatures of atmospheric layers about 10 km thick could be determined from brightness temperature measurements. The mean height of these layers would depend upon the nominal frequency of the measurement. They pointed out that at frequencies between strong lines bandwidth limitations on the radiometer would be more severe than at frequencies between weaker lines or lines more widely separated. This results from the fact that the mean height of the weighting function and its width at half-maximum is strongly dependent upon the absorption coefficient. The absorption in turn is relatively constant over bandwidths on the order of tens of megacycles in between lines. The width of this constant region determines the bandwidth. A set of typical parameters for probing the atmosphere from 0 to 30 km are given in the paper by Meeks and Lilley.

The aforementioned provides a very good starting point for this work - the objective of which is to demonstrate the possibility of using the microwave oxygen emission spectrum to sound the atmosphere. Additional frequencies need to be investigated as possible operational frequencies of measurement. Also it should be demonstrated at least with computed results that weighting functions do not change significantly with different atmospheric temperature profiles. Having obtained a set of frequencies for measurements which are considered to be the best possible in some sense, Yamamoto's inversion technique ought to be tried in the microwave region. Finally, an elementary study of the effects of random errors in the data should be attempted.

There are several reasons why it might prove more desirable to use the microwave spectrum rather than the infrared spectrum in sounding the atmosphere. In the first place in the infrared region there are no amplifiers; there are only direct detection devices. Years of work in radar, communications and radio astronomy has placed the state of the art of millimeter wavelength coherent detectors and amplifiers considerably ahead of that of the micron wavelength region. These facts more than offset the factor of about 1000 in intensity that infrared wavelength emission from the atmosphere has over microwave emission.

In the second place, scattering by atmospheric aerosols from the molecular scale to the scale of water droplets in clouds is less pronounced in the microwave region than in the infrared region. In the case of Rayleigh type scattering, which is the case for dry air, the scattering coefficient at the infrared wavelengths is 10^{12} greater than the microwave scattering coefficient. In the case of fog or stratus type cloud layers which contain water droplets whose radii are on the order of 5 μ, the scattering coefficient for infrared radiation in the 15 μ region is about an order of magnitude or more larger than that for the 5 mm microwave region. However, it should be noted at this point that there is some evidence to indicate that absorption of microwaves by cloud drops and precipitation may be very appreciable (see Hogg and Semplak, 1959).

Another advantage the microwave spectrum has over the infrared spectrum lies in the ability of the observer to discern more details of line structure. This, of course, translates into better resolution in the temperature versus height profile.

There is an advantage in measuring at microwave frequencies which arises from considerations of the minimum attainable error in a radiometer. In the case where $T \gg \hbar w/k$ where $\hbar$ is Planck's constant, w the frequency and k Boltzmann's constant, the minimum error of is given approximately by

$$\Delta T_{rms} \geq \frac{T_{eff}}{\sqrt{\beta\tau}} \tag{22}$$

where ΔT_{rms} = uncertainty in radiometer reading

T_{eff} = source temperature plus receiver noise temperature

τ = integration time

β = bandwidth.

Equation (22) is a statement of the accuracy with which we can measure a noise like signal over bandwidth β in a time τ. It is derived by considering the input signal to be sum of harmonics of a basic signal and then summing the fluctuations in each harmonic. The in phase and quadrature components of each elementary signal are assumed to be independent. The assumption of white noise is also employed. A very good derivation of equation (22) is given in Dicke (1946). However, when $T \sim \hbar w/k$, the in phase and quadrature components of each elementary signal are no longer independent, they are instead non-commuting variables, and their energy can thus assume only discrete values. In this case Hagfors (1963) has shown that the minimum error is given by

$$\Delta T_{rms} = \frac{T_{eff}}{\sqrt{\beta\tau}} \quad \frac{\sin h\, X}{X} \quad \sqrt{1 + 2 \operatorname{Tan} h \frac{X}{2}} \tag{23}$$

where $X = \pi w_o/kT$.

In the classical limit (when $X \to 0$) equation (23) reduces to equation (22). Now if we assume that we are given noiseless instruments at both 15 μ and 5 mm wavelength then we would find that for source temperatures of about 300°K the classical limit obtains at the millimeter wavelengths but not at the infrared wavelengths. Hence at 15 μ there are errors due to quantum effects which are not significant at 5 mm.

The 5 mm oxygen spectrum is also superior to the 15 μ carbon dioxide spectrum for determining the temperature profile in the following respect. Our knowledge of the absorption properties of a gas depend upon how well we know the distribution of that gas. In the troposphere and stratosphere the oxygen distribution is certainly more uniform and better known than the CO_2 distribution in the same region.

Finally, at 5 mm, there are fewer important complications due to other emitting gases than at 15 μ where we have to consider contributions from ozone and water vapor.

SECTION II

STATEMENT OF THE PROBLEM AND THE PROPOSED METHOD OF SOLUTION

In the most concise terms our problem is to convert measurements of brightness temperature versus frequency from the atmosphere into estimates of the kinetic temperature versus height profile. The source of the emission we shall be concerned with is the magnetic moment transitions of molecular oxygen in the atmosphere. The frequencies of these transitions are located near sixty kilo-megacycles.

The satellite radiometer system which we shall have to work with initially will probably have the following characteristics:

1) It will measure the emission at several discrete frequencies.
2) It will have a narrow bandwidth at each frequency, hopefully on the order of one to ten megacycles.
3) The antenna will have a response pattern similar to that shown in Fig. 3. The beamwidth of the half power point of the antenna will be very small, hopefully on the order of a degree.

Equation (21) is the form of the radiative transfer equation most applicable to the data which we shall obtain. It is re-written here for convenience

$$T_b(\nu, \theta) = T_s(\nu)\, e^{-K_\nu H \mu} + \int_0^H T(z)\, K_\nu e^{-K_\nu (H-z)\mu}\, \mu dz \qquad (21)$$

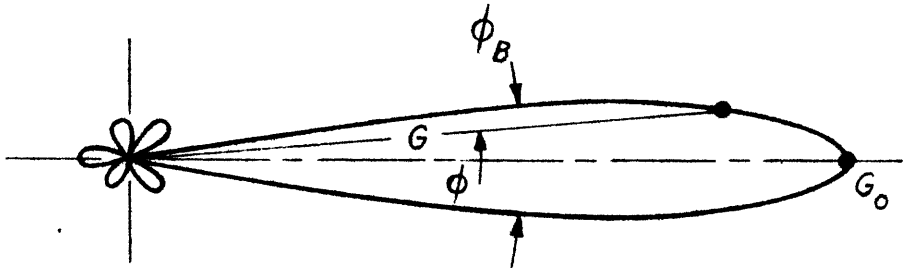

FIG. 3 A POLAR COORDINATE PLOT OF ANTENNA GAIN

G_o = THE ON AXIS GAIN OF THE ANTENNA

ϕ_B = THE BEAMWIDTH AT THE HALF POWER POINT

G = THE ANTENNA GAIN AT ANY ANGLE ϕ FROM THE POSITIVE EXTENSION OF THE ANTENNA'S AXIS

where $T_b(\nu,\theta)$ = brightness temperature at a frequency ν and nadir angle

$T_s(\nu)$ = equivalent temperature of the ground

K_ν = monochromatic absorption coefficient

μ = sec θ, θ = nadir angle

ν = nominal frequency of the measurement

$T(z)$ = kinetic temperature profile

We shall refer to the quantity $K_\nu e^{-K_\nu(H-z)\mu}\,\mu$ of equation (21) as a weighting function or kernel.

If the kernel were not a function of the temperature profile then equation (21) would be linear, but this is not the case. The temperature profile does enter the kernel in a rather complicated fashion through the absorption coefficient as shown below

$$K_\nu = \frac{C_1\ p[T(z)]}{\nu^2\ [T(z)]^3} \sum_N S_n\ [T(r),\ \nu]\ e^{-E_n/kT(z)} \tag{24}$$

where $p[T(z)]$ = pressure profile, assumed hydrostatic

$S_n[T(r),\nu]$ = frequency and line width dependent matrix element (C.F. Meeks and Lilley, 1963)

E_n = excitation energy of the nth line

In deriving equation (21) it is assumed implicitly that there is no scattering. In order to avoid complications due to non zero reflectivity of the ground we shall restrict the investigation to frequencies and nadir angles for which $K_\nu H\,\mu \gg 1$. Thus the equation

whose solution we shall be concerned with is

$$T_B(\nu,\theta) = \int_0^H T(z)\ WF\ [T(z),\ \nu,\ \theta]\ dz \tag{25}$$

where

$$WF[T(z),\ \nu,\ \theta] = K_\nu e^{-K_\nu(H-z)\mu}\ \mu$$

We shall employ a method closely related to that used by Yamamoto (1961) to solve equation (25). Our method is different in that we are dealing with an inversion to the temperature profile and we assume boundary conditions at both $z = 0$ and $z = H$. Also we shall perform the iterations which Yamamoto suggested but did not perform.

First we let $T(z)$ be represented by a polynomial of a finite number of terms each having an undetermined coefficient, i.e.

$$T(z) = a_o + a_1 z + a_2 z^2 + \ldots + a_k z^k \tag{26}$$

The total number of terms must be two less than the total number of independent brightness temperature versus frequency and nadir angle measurements. This polynomial representation of $T(z)$ is substituted into the integrand of equation (25) for the function $T(z)$ which appears explicitly.

Next we assume a fully determined temperature profile and substitute it into the function WF in equation (25). This determined temperature profile is actually our first guess at what the real profile might be. Normally this first guess would be some average

or standard atmosphere such as the U. S. Standard Atmosphere 1962. The first guess might very well be a constant for lack of anything better.

We next assume that the boundary conditions T(0) and T(H) have been determined. Hence by the appropriate substitution of equation (26) into equation (30) there obtains the following linear system:

$$\left\{\begin{array}{l} T(0) = a_o \\ T_B(\nu_1, \theta_1) = a_o \int_0^H z^o (WF)_1 \, dz + \ldots + a_k \int_0^H z^k (WF), \, dz \\ T_B(\nu_2, \theta_2) = \ldots\ldots\ldots\ldots\ldots \\ T_B(\nu_{k-1} \theta_{k-1}) = a_o \int_0^H z^o (WF)_{k-1} \, dz + \ldots + a_k \int_0^H z^{k-1} (WF)_{k-1} \, dz \\ \\ T(H) = a_o + a_1 H + \ldots \quad a_k H^k \end{array}\right\} \tag{27}$$

The integrals in (27) are evaluated using the first guess at the temperature profile and the coefficents a_o through a_k are determined by solving simultaneously the resulting linear equations.

The temperature profiles corresponding to these coefficients are substituted back into the functions $(WF)_i$ $(i = 1, 2 \ldots k)$ of (27) and the system of equations are solved again. Successive iterations of this type are performed until the following condition is satisfied:

$$\left(\frac{1}{H} \int_0^H \left[T^{(P)}(z) - T^{(P-1)}(z) \right]^2 dz \right)^{1/2} \leq M \tag{28}$$

$T^{(P)}(z)$ and $T^{(P-1)}$ are the pth and $p - 1^{th}$ derived temperature profile. M is some arbitrary constant which is a measure of the difference between the pth and $p - 1^{th}$ derived $T(z)$.

By satisfying (28) we guarantee convergence in the sense of (28) to a kth degree polynomial representation of the kinetic temperature profile which satisfies best the radiometric data. We must be aware of the fact that convergence in this context does not mean convergence to the best possible solution of (25).

We intend to investigate certain questions relating to this problem given that we must limit ourselves to five measurements of brightness temperature versus frequency and nadir angle and measurements of the two boundary conditions. This is a total of seven measurements which is reasonable for a satellite experiment. The resulting limitation to a sixth degree polynomial also tends to keep the calculations at reasonable number. Hence the problem can be handled by standard FORTRAN II programming on an available IBM 7094 Data Processing System in a reasonable time (approximately 10 minutes).

We shall consider the following questions:

1) What frequencies and nadir angles are the best at which to make brightness temperature measurements?
2) Do the associated weighting functions change their location on the height axis with different temperature profiles?
3) What is the ultimate in accuracy that we can expect from our method?
4) What is the effect of a poor initial guess for the temperature profile?
5) What are the effects of poorly determined boundary conditions?
6) What are the effects of random errors in the data?

SECTION III

DETERMINATION OF THE BEST FREQUENCIES AND NADIR ANGLES FOR MEASUREMENTS

Let us first examine the effect of different temperature profiles on a weighting function corresponding to a fixed frequency and nadir angle. The characteristic shape of a weighting function is independent of the temperature profile. The shape depends only on the fact that the absorption coefficient is always positive. The width at half maximum points and the altitude of the maximum point are however dependent upon the temperature. Analytic investigation of this problem is virtually impossible because of the complicated manner in which the temperature profile enters into the weighting function.

The following experiment was thus performed to obtain at least a partial solution to the above problem. The altitudes of the maxima or peaks of the weighting functions were computed for several different representations of atmospheres. The results are given in Table I. The temperature profiles used are shown in Fig. 4.

The results seem to indicate that the temperature profile does not have a marked effect on the altitude of the weighting function peaks. Plots of the weighting function show the same is true for its effect on the width of the weighting function. Even though these conclusions were deduced from a small sample of an infinity of temperature profiles which exist in the atmosphere, they are true in general in view of the following. The various temperature structures which have been observed in the earth's atmosphere are not very different from one another. At any given altitude, temperatures at various points

TABLE I

A Comparison of the Altitudes of the Weighting Function Peaks

Frequency Gc/sec.	Nadir Angle Degrees	ATMOS. 1 Peak Alt. Km	ATMOS. 2 Peak Alt. Km	ATMOS. 3 Peak Alt. Km	ATMOS. 4 Peak Alt. Km
55.6500	0.0	14.80	15.20	15.10	14.50
59.3000	0.0	20.94	21.30	21.00	20.70
60.3200	30.0	34.88	34.40	34.50	34.70
60.3300	0.0	31.13	30.50	30.60	30.90
60.3200	0.0	27.15	26.80	26.70	26.90

Description of the T(h) profiles used above.

ATMOSPHERE 1 - A six degree polynomial fit to the U. S. Standard Atmosphere, 1962, 0-50 Km.

ATMOSPHERE 2 - A six degree polynomial fit to Radiosonde and Rocket grenade data taken at Norfolk, Va., July 14, 1961, 0-50 Km.

ATMOSPHERE 3 - A six degree polynomial fit to data representing the mean of the winter 1957 profiles at 12° N, 0-50 Km.

ATMOSPHERE 4 - A six degree polynomial fit to data representing the mean of the winter 1957 profiles at 58° N, 0-50 Km.

These profiles are illustrated in Figure 4.

Note: Gc = 1000 megacycles.

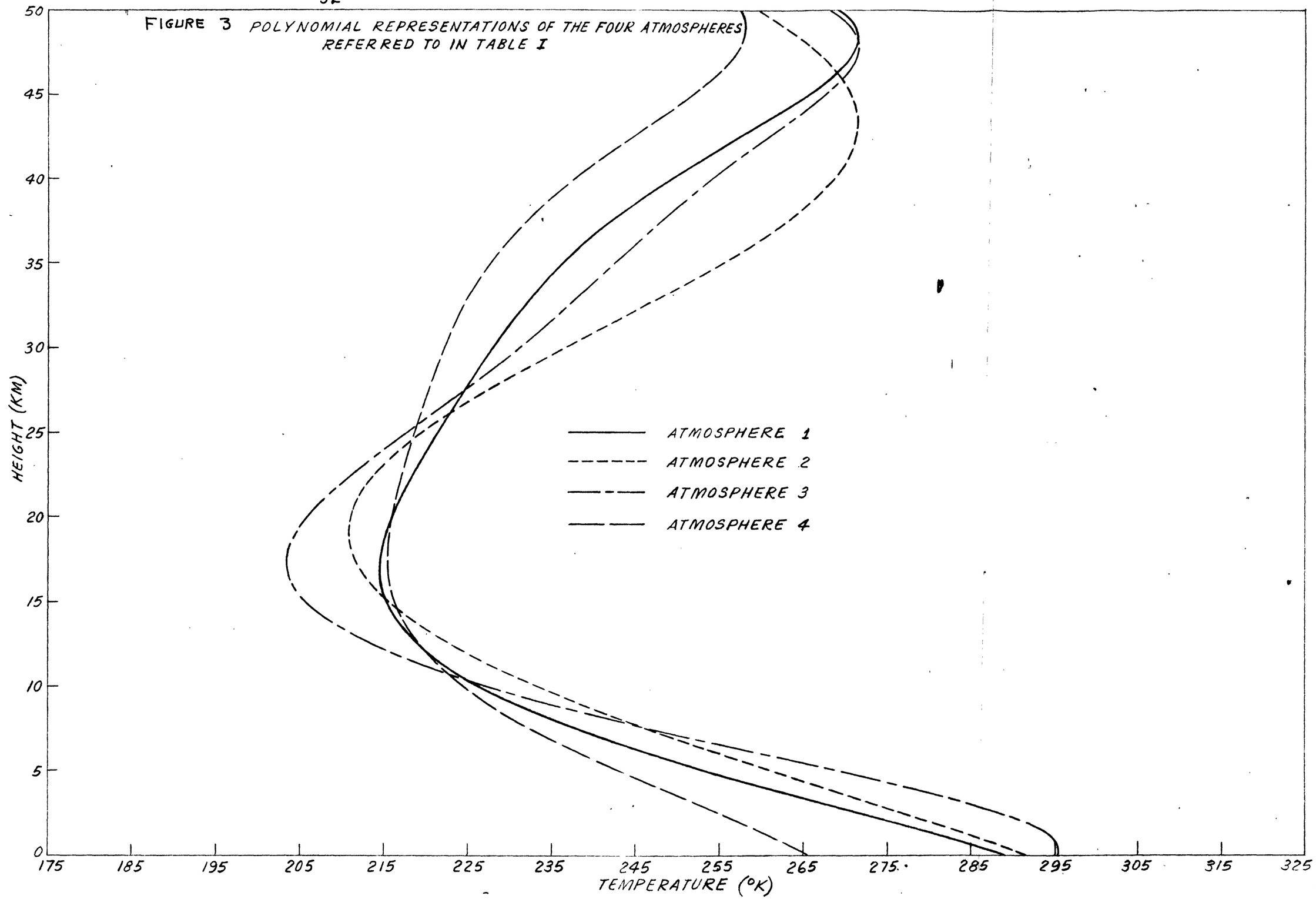

FIGURE 3 POLYNOMIAL REPRESENTATIONS OF THE FOUR ATMOSPHERES REFERRED TO IN TABLE I

on the earth very rarely differ by more than 100°K. The average temperatures of the air columns from 0 to 100 kilometers at these points differ by even less. These facts make our conclusion concerning the effects of temperature profiles at least plausible.

The weighting function peak altitudes and their widths at half maximum are dependent on frequency and nadir angle. With respect to frequency, the closer one is a line center, the higher the altitude at which the weighting function will peak and the wider it will be. With respect to nadir angle the larger it is the higher will be the altitude at which the weighting function will peak and the wider it will be. These results are deduced by inspection of the expression for the weighting function as defined in equation (25). We note that large values of K or μ make the exponential factor more influential at high altitudes, hence the weighting function peaks at higher altitudes. The larger values of K or μ also cause the exponential term to change more rapidly with altitude, thus causing the weighting functions to be narrow.

With ATMOSPHERE 1, Fig. 4 as a model atmosphere and Fig. 5 from Meeks and Lilley (1963) as a guide, the height of the weighting function peak, the kinetic temperature corresponding to the aforementioned height and the brightness temperature were determined for various frequencies and nadir angles. The results are presented in tabular and graphical form in Appendix II. The tabular listing is ordered according to increasing height of the weighting function peak. We shall show that this arrangement is very useful in selecting a set of frequencies and nadir angles at which to take measurements.

The <u>apparent</u> discontinuity in the frequency domain implied by the figures in Appendix II is not real. We decided not to make any computations at frequencies closer than 5 mc/sec. to a line center.

FIGURE 5

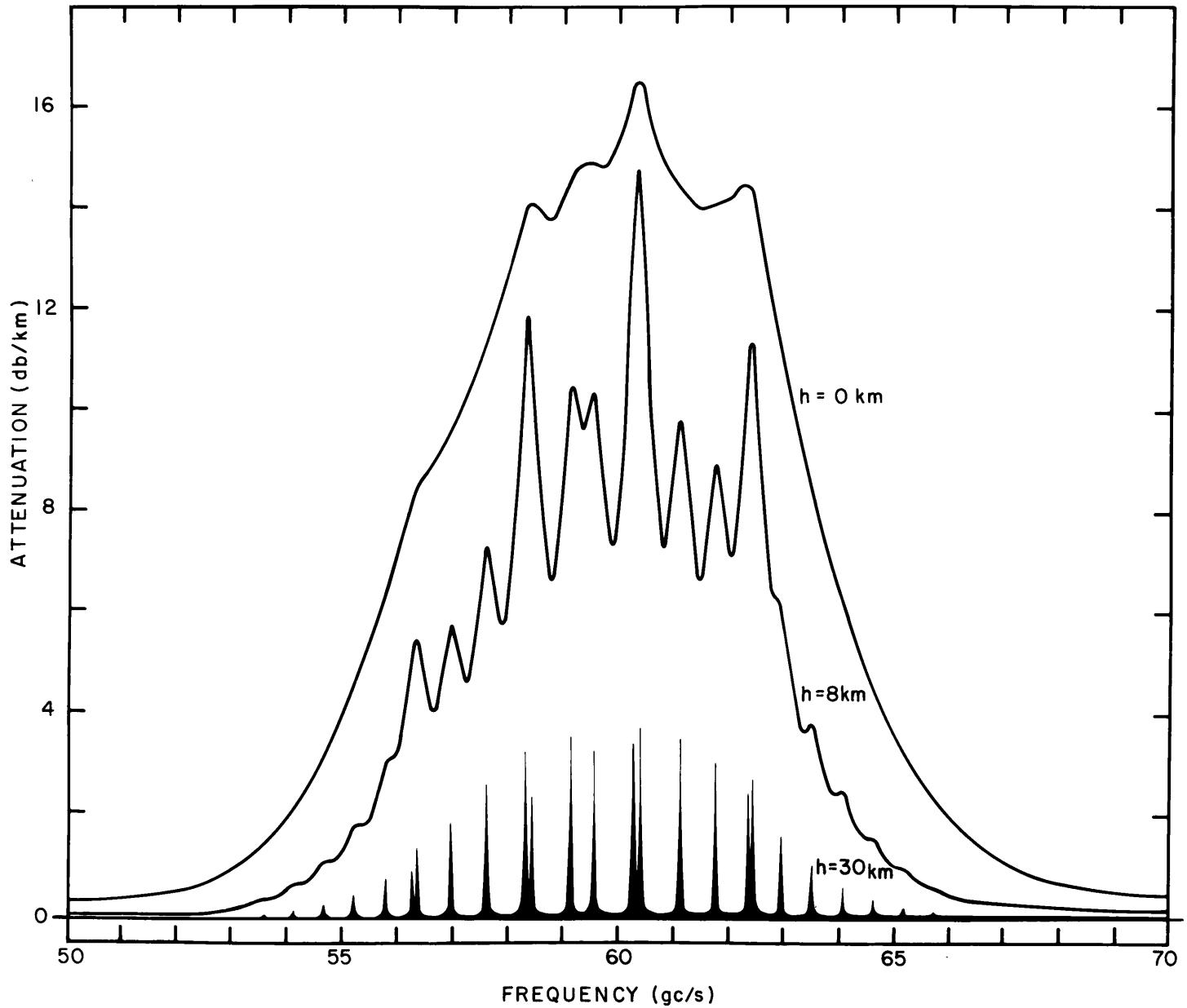
ATTENUATION (db/km)
16
12
8
4
0
50
55
60
65
70
FREQUENCY (gc/s)
h = 0 km
h=8km
h=30km

This was done because the absorption model did not include the Zeeman effect which must be included for frequencies near the line centers. Hence it would be incorrect to extrapolate the results given in Appendix II into the 10 mc/sec band centered on the lines. We emphasize this fact by cross-hatching the 10 mc/sec bands which makes the frequency domain seem discontinuous.

In view of the shape of the weighting function and equation (25) we can see that a brightness temperature for a given frequency and nadir angle is the weighted average of the kinetic temperature profile. The altitudes at which temperatures are weighted most heavily occur between the altitudes of the half maximum points of the weighting function. This means that any brightness temperature by itself contains information mostly about kinetic temperatures in a ten to fifteen kilometer layer centered at the peak of its corresponding weighting function. This is an important fact to bear in mind when selecting the frequencies and nadir angles at which to take measurements.

A simple criterion for the selection of the measuring points is to choose them such that the corresponding weighting functions distribute themselves uniformly over the height region in which the kinetic temperature profile is desired. Such a criterion should provide for a sounding of kinetic temperature that weights equally all altitudes except those near the boundary. It can thus be seen that the table of Appendix II is conveniently arranged for this purpose. There is however, one qualification which must be observed when selecting the measuring points. Any real radiometer which we may use to make these measurements will have a finite non zero bandwidth. This may lead to problems if the chosen frequencies are close to line centers. We must first of all be sure that the band pass of the radiometer

does not cause it to be sensitive at the frequency of a line center. We must also be aware of the fact that the weighting function peak altitudes change very rapidly with frequency near line centers (see the figures in Appendix II). This means that measurements of brightness temperatures near line centers would represent the average kinetic temperature of layers thicker than ten or fifteen kilometers. The exact thickness would depend upon the bandwidth of the radiometer. The larger the bandwidth the larger is the height interval over which we average.

In general, measurements near line centers are to be avoided if possible. Hence, the process of selecting measuring points may involve a compromise between uniformity of weighting function distributions and the proximity of the measuring frequency to a line center. To serve the needs of the latter, we make use of the figures in Appendix II. These figures however show that to make soundings in the regions above thirty kilometers we are forced to make measurements near line centers.

The frequencies and nadir angles selected for the determination of the temperature profile in the first fifty kilometers of the atmosphere, were chosen using the compromise procedure. They are listed together with the altitudes of their weighting function peaks in Table I. The weighting function peaks were determined for the four temperature profiles of Fig. 4. The weighting functions corresponding to these frequencies and nadir angles and computed from the temperatures of ATMOSPHERE 1 are shown in Fig. 6.

It should be thoroughly understood at this point, that to say that five measuring points can be selected at which any temperature profile can be sounded and approximately deduced is nonsense; unless

FIGURE 6

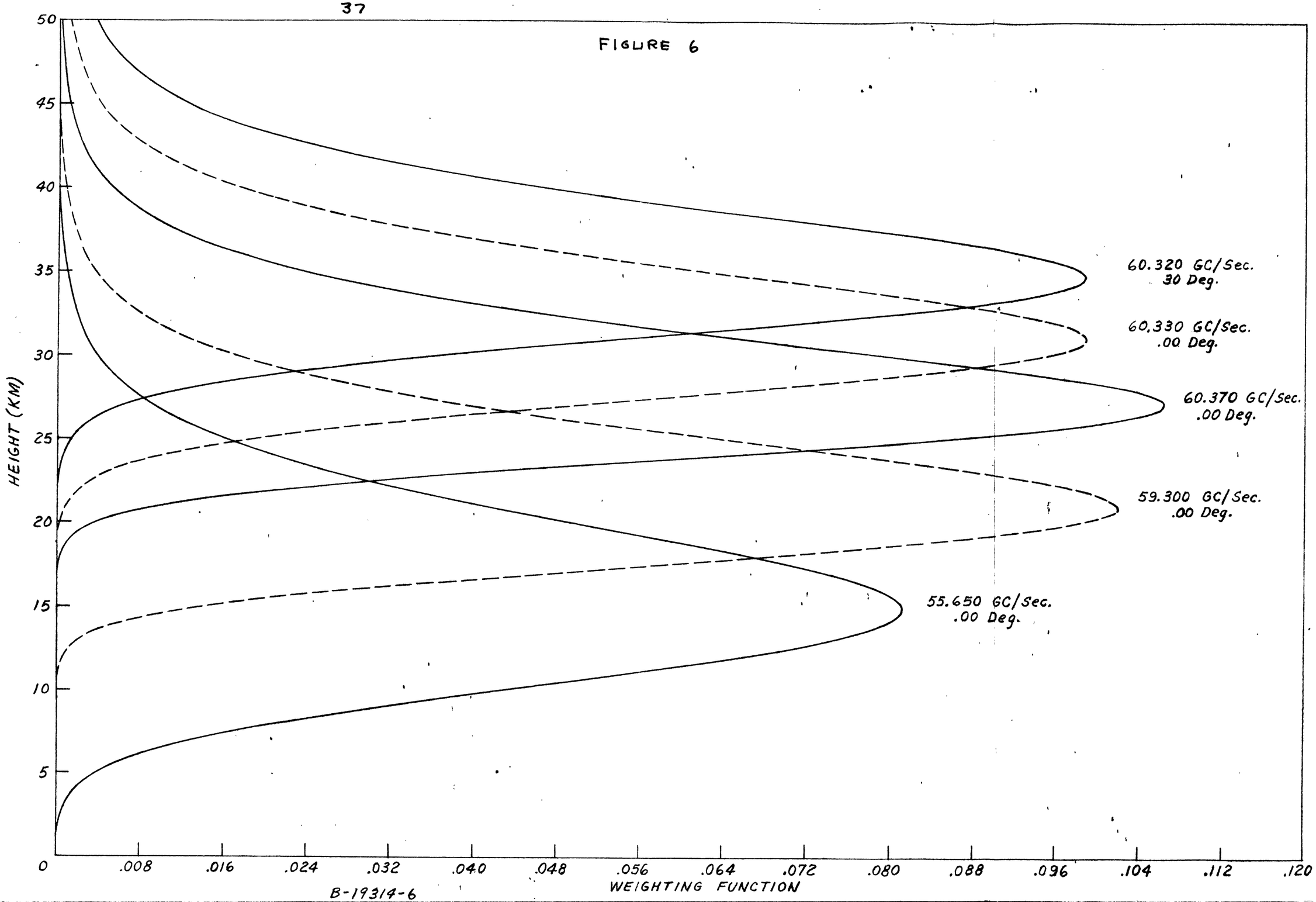

B-19314-6

as we have shown, the atmospheric layer to which each measuring point corresponds is approximately the same for any temperature profile which is likely to be encountered. We recall that Kaplan (1959) made a similar statement.

If we examine the table of Appendix II we note that many of the measuring points would produce nearly identical weighting functions. This means that if we measured brightness temperature versus frequency continuously (except at the 10 mc/sec bands at the line centers) from about 53.0 to 63.0 GC/sec[4], much of our data would be redundant. It is desirable to obtain redundant data for the purpose of checking measurements. However, to utilize redundant data most efficiently there would be required an inversion procedure different from the one described in this work. Since it is not likely that the first generation satellite radiometer will be capable of taking redundant data, we shall not pursue this topic any further.

Let us now consider a group of weighting functions as a set rather than each as separate and complete. Each weighting function shows the relative contribution of the kinetic temperature at every altitude to the brightness temperature corresponding to the frequency and nadir angle of the measurement. If at each altitude we sum the values of each weighting function in a set, then we shall obtain the relative weight of the various kinetic temperatures in the determination of the corresponding set of brightness temperatures. We shall call this function so derived the influence function. For the distribution of weighting functions shown in Fig. 6, the corresponding influence function is shown in Fig. 7.

---

[4] GC (gigacycle) = 10^3 megacycles.

FIGURE 7

INFLUENCE FUNCTION

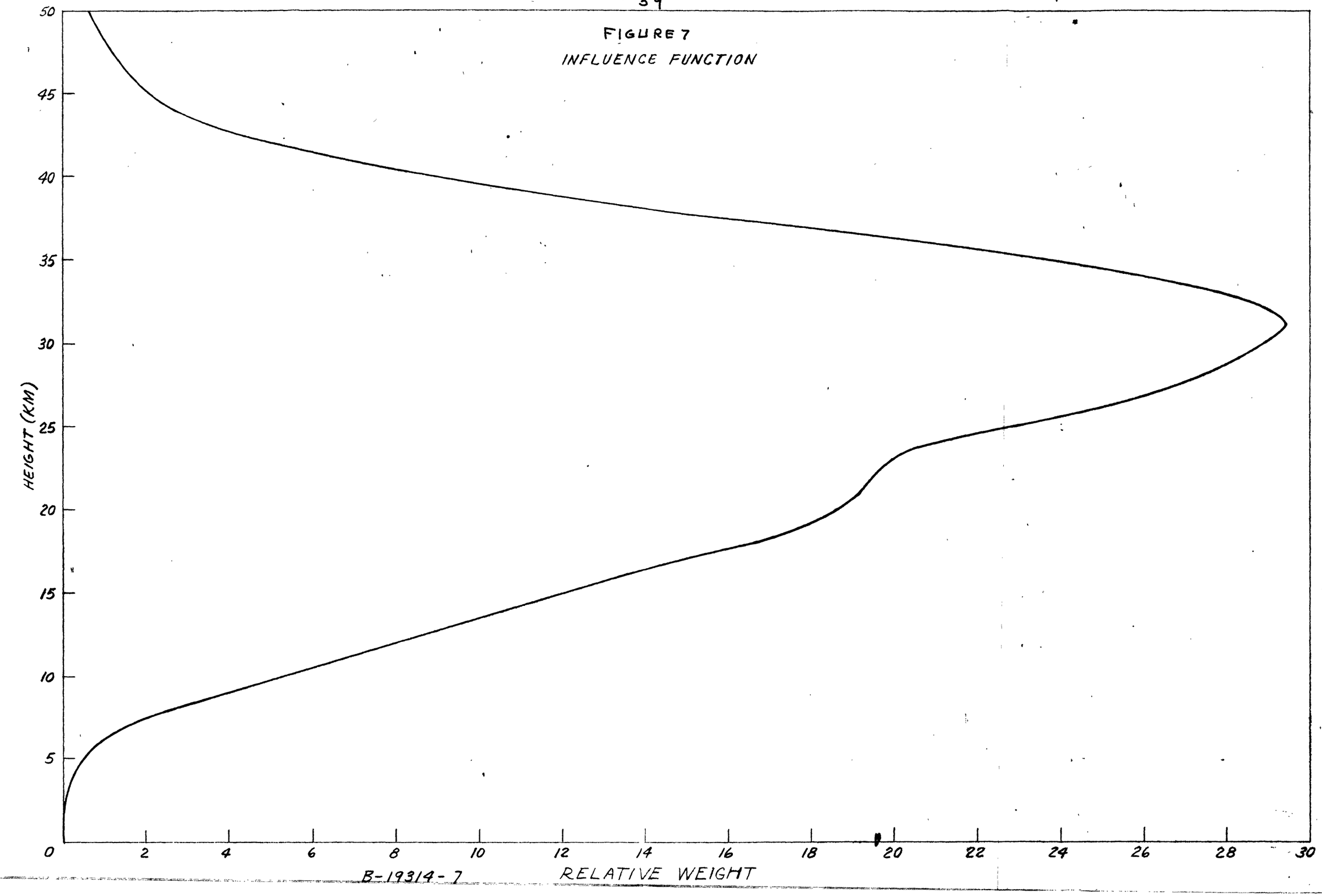

Had it not been necessary to make the compromises described previously, the weighting function distribution of Fig. 6 would have been more uniform and the resulting influence function more nearly constant in the ten to forty kilometer region. It is not unlikely that if we were to delete the 60.330 GC/sec measurement, the influence function would be flatter in the ten to forty kilometer region. A flat influence function would cause all input data to be weighted equally in the inversion process. Of course, there may be instances when this is not desirable.

The local weather forecaster who is primarily interested in the lowest ten kilometers of the atmosphere in detail, would prefer an influence function which peaks in this region. The national and hemispheric forecasters require less detail in the profiles, but they do need to determine a profile over a larger altitude range. A flat influence function from about twenty or thirty kilometers to the surface would be most useful to them. The research meteorologists, especially those interested in the upper atmosphere require varying amounts of detail, but definitely would like to have more regularly scheduled soundings up to one hundred kilometers. The measurements could be selected to give an influence function specifically suited to their needs.

SECTION IV

SOLUTION OF THE INTEGRAL EQUATION

Before we examine in detail the proposed iterative inversion scheme, let us consider a simpler inversion scheme. In this technique we simply assign to the measured brightness temperature a certain altitude. This altitude is that of the peak of the weighting function corresponding to the frequency and nadir angle of the measurement. The temperature which is used in determining this altitude is ATMOSPHERE 1.

The following observations indicate that we ought to try this technique:

1) The weighting functions are very nearly symmetrical about a horizontal axis through their peaks.
2) The brightness temperature is very nearly the weighted average of the kinetic temperature profile in a ten to fifteen kilometer layer centered at the altitude of the weighting function peak.
3) If the weighting function were exactly symmetrical and the temperature profile were a linear function of height in the layer between the half maximum points of the weighting function, then the average temperature in the layer would be equal to the temperature at the height of weighting function peak.
4) The altitude and width of a weighting function are very nearly independent of the temperature profile.

Statement (3) is actually a mathematical fact. It is included in the above in order to emphasize the importance, with regard to this inversion scheme, of the other statements. This simple inversion

scheme will hereafter be referred to as a zero order approximation to the inversion of brightness temperatures or zero order inversion.

An example of the zero order inversion technique is shown in Fig. 8. The solid line is ATMOSPHERE 1. With the temperatures of ATMOSPHERE 1 input to equation (25), the brightness temperatures for some of the frequencies and nadir angles listed in Appendix II are computed. Each point in Fig. 8 corresponds to one of the frequencies and nadir angles listed in Appendix II except those whose weighting functions peak above 39.0 Km.[5] The ordinate of each point is the altitude of the peak of the weighting function; the abscissa is the brightness temperature.

The results of this inversion are good. We note however that in the regions where ATMOSPHERE 1 has considerable curvature the errors are larger. This is because the approximation which states that kinetic temperature at the height of the weighting function peak equals the average kinetic temperature of the layer between the half maximum points of the weighting function, is less valid for regions of large curvature in the temperature profile.

Fig. 8 shows the best result we could hope to obtain with the zero order inversion. The optimum result obtains in this case because the brightness temperatures and weighting function peak altitudes

---

[5] This exclusion was made to avoid errors in brightness temperature which result from the fact that of 50.0 Km, the upper limit of our integrations over height, these weighting functions still have values which are appreciable with respect to their maximum value.

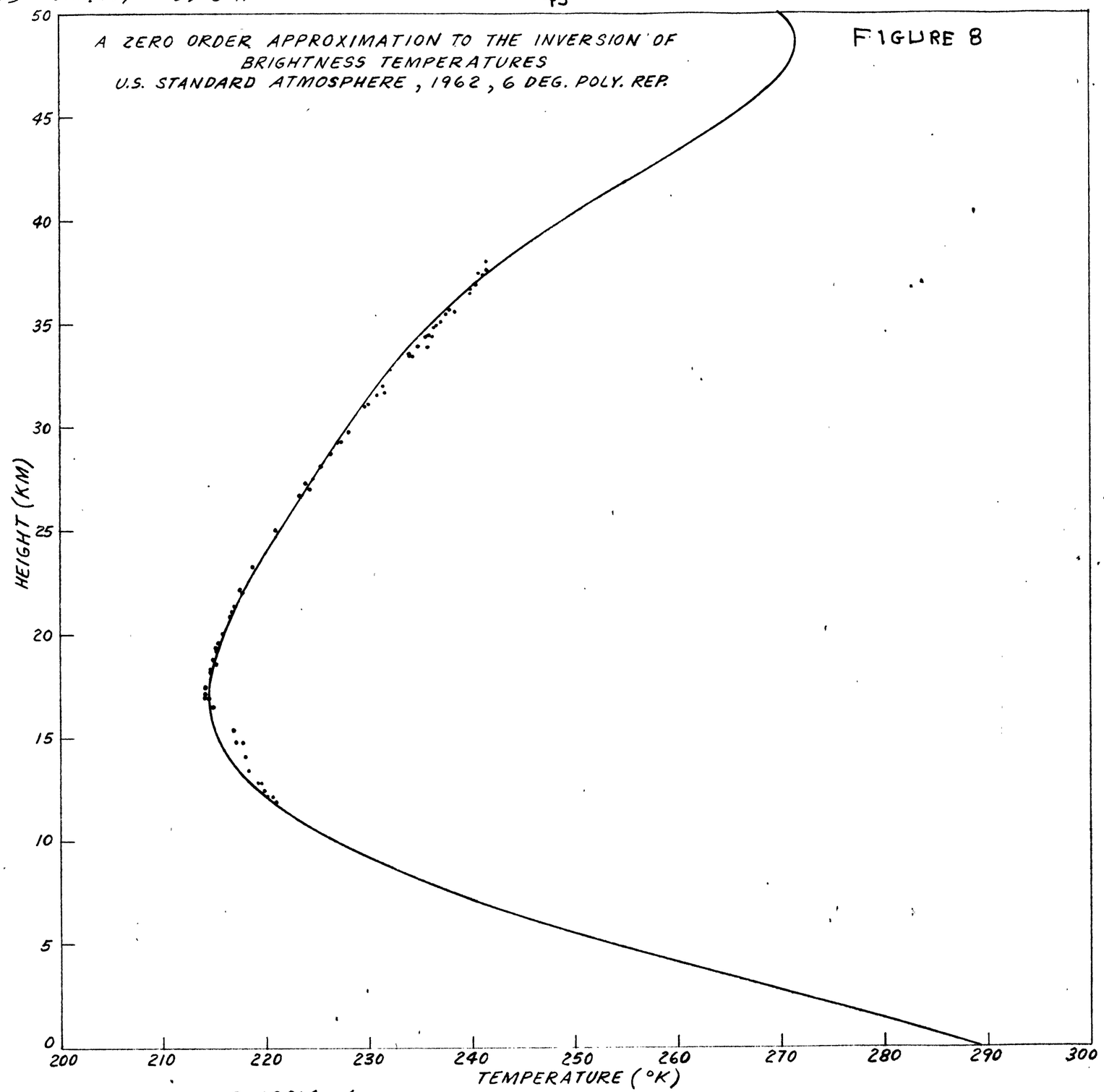

FIGURE 8

B-19314-4

were correlated. Now let us try the zero order inversion in a simulated real situation, i.e. one in which we measure only the brightness temperature and must assign altitudes to these temperatures which correspond to weighting function peaks computed for a standard atmosphere. We shall simulate this real situation by computing brightness temperatures from equation (25) using ATMOSPHERE 2 and the frequencies and nadir angles used in the previous example. The corresponding heights that we shall assign to these brightness temperatures, will be the weighting function peak altitudes as determined with ATMOSPHERE 1, our standard atmosphere.

The results of this inversion are shown in Fig. 9 as the small black dots. The solid line is ATMOSPHERE 2 which is included for comparison. The results of this inversion are surprisingly very good. The larger deviations in the thirty five to forty kilometer region are probably due to termination of the integrations at fifty kilometers. In view of our success with the simple zero order inversion we can proceed with confidence to the more complicated inversion technique described in section II.

We have already discussed the details of the iterative inversion procedure in section II. In the remainder of this section we shall look at some of the intermediate results and interesting details of the procedure.

With the temperatures from ATMOSPHERE 1, brightness temperatures were computed from equation (25) for the frequencies and nadir angles listed in Table I. These brightness temperatures, together with boundary conditions corresponding to T(0) and T(50) of ATMOSPHERE 1, were used as input to the iterative inversion procedure. The initial

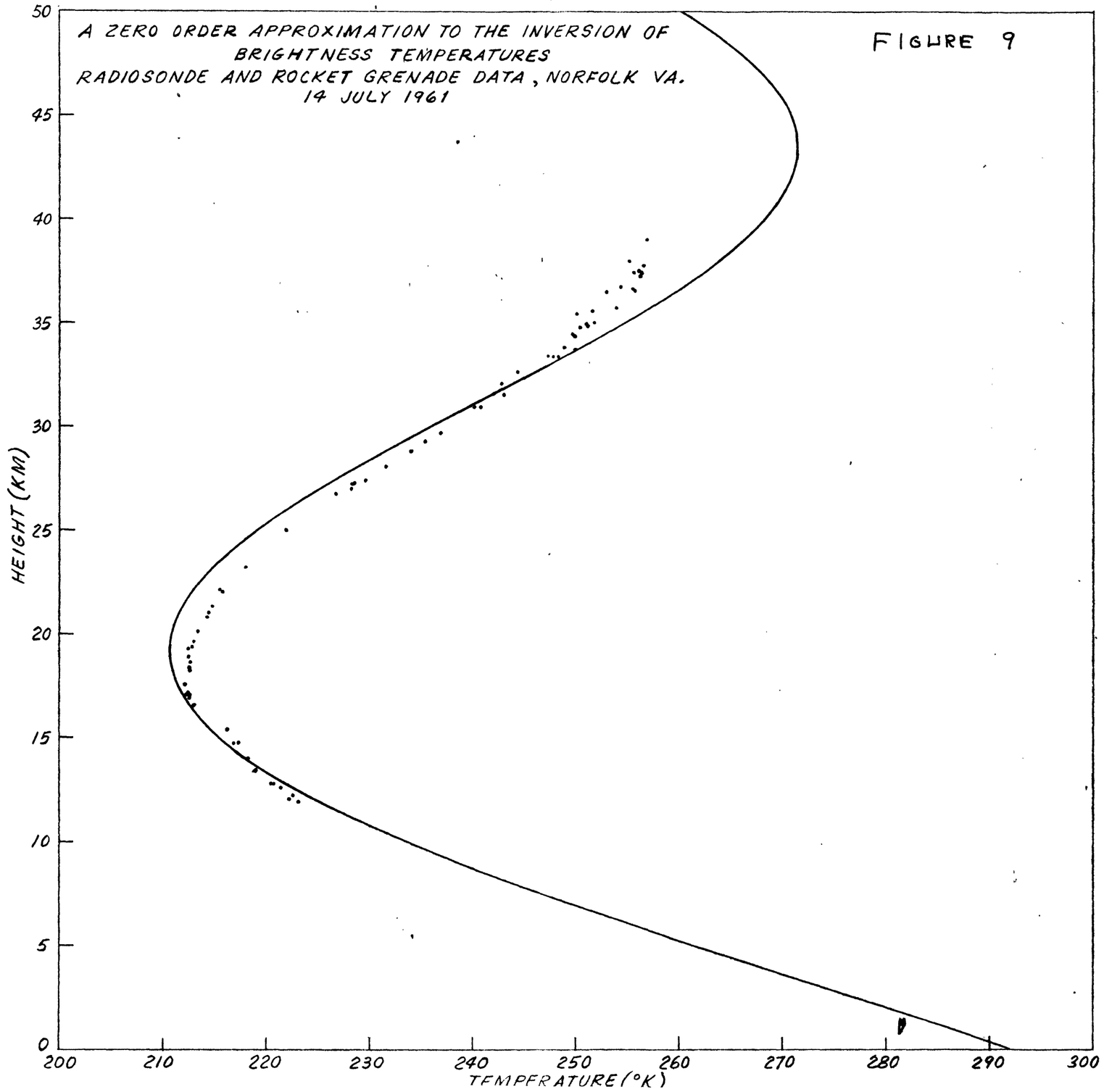

FIGURE 9

11-5-63 Lapierre Graph FOW B-19314-5

or first guess of the temperature profile was an isothermal profile of 289°K. An isothermal profile is assumed to be the worst guess that anyone would ever have to make in practice.

Fig. 10 shows the intermediate and final results of this inversion. This figure is an exact reproduction of the plotted computer output during the inversion. The numbers on the curves designate the order in which they were derived in the series of iterations. The fourth derived profile, which is hardly distinguishable from the third, is a sixth degree polynomial representing the temperature versus height profile which best fits, in the sense of equation (28), the input data. M, the root mean square deviation of the $(p + 1)^{th}$ derived profile from the $(p)^{th}$ derived profile, was set at 0.5°K. We note in Fig. 10, that even the second derived profile is not too different from the third and fourth. The fourth derived profile is virtually identical to ATMOSPHERE 1. Hence we conclude that a poor though reasonable initial guess for T(z) will have very little, if any influence on the final result. Judging from other results not given here, the only effect a poor initial guess for T(z) seems to have is to delay convergence for one or two iterations.

Let us now consider one of the best possible results we might ever hope to obtain with this procedure. We simulate the following conditions and perform an inversion which will give us the answer:

1) We assume a horizontally stratified atmosphere in which the absorption theory set forth by Meeks and Lilley (1963) is exactly obeyed.

2) We assume an infinitely accurate radiometer and antenna system for measuring brightness temperature versus frequency and nadir angle.

3) Finally, by some quirk of nature, we assume that the temperature

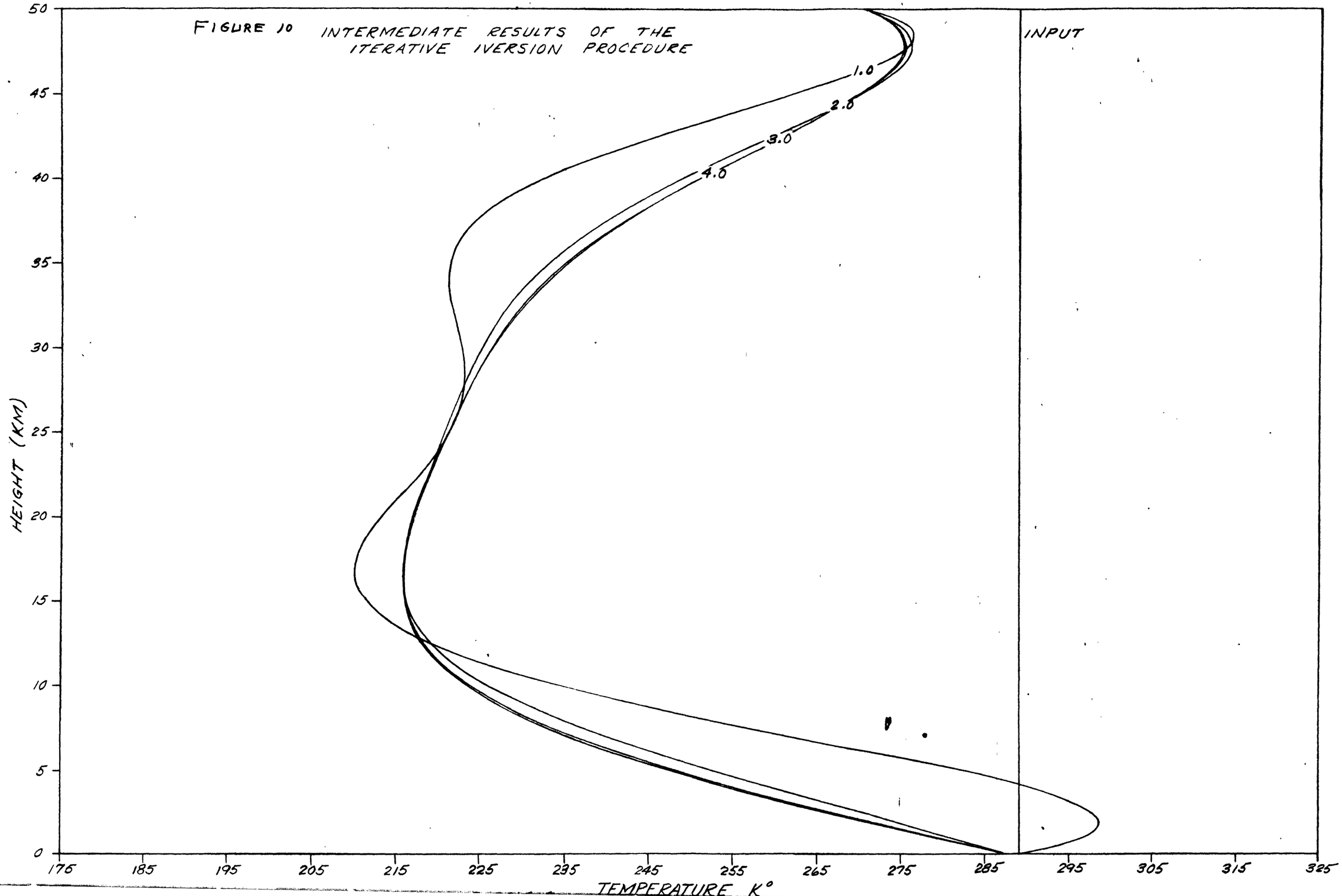

FIGURE 10 INTERMEDIATE RESULTS OF THE ITERATIVE IVERSION PROCEDURE

profile between zero and fifty kilometers is the sixth degree polynomial termed ATMOSPHERE 2.

With these assumptions we compute brightness temperatures from equation (25), with ATMOSPHERE 2 and the frequencies and nadir angles of Table 1 as input data. We use these brightness temperatures and the T(0) and T(50) of ATMOSPHERE 1[6] as input to the iterative inversion scheme. Our initial guess for T(z) is ATMOSPHERE 1.

The results of this inversion are shown in Fig. 11. Also shown in this figure for comparison are ATMOSPHERE 2 and the actual data points from which the polynomial ATMOSPHERE 2 was determined. We conclude after examination of this figure, that this best possible result is indeed excellent. We also note that with measured, rather than assumed, boundary conditions we could do even better.

In the development of the inversion procedure, we discovered that we could not obtain convergence to a solution unless we specified boundary conditions. This might be considered unusual in the light of the following. A linear integral equation has the boundary conditions of its unknown function contained in the statement of the equation (see Hildebrand, "Methods of Applied Mathematics"). Equation (25) is nonlinear, however in the process of substituting and successive approximations for T(z) in WF $\{T(z),\nu\}$ we in a sense linearize the equation. Nevertheless we find that it is necessary

---

[6] In a practical situation in the absence of data at the boundaries we could do no worse than to use the boundary conditions of a standard atmosphere. We here arbitrarily have chosen to illustrate this situation in this experiment.

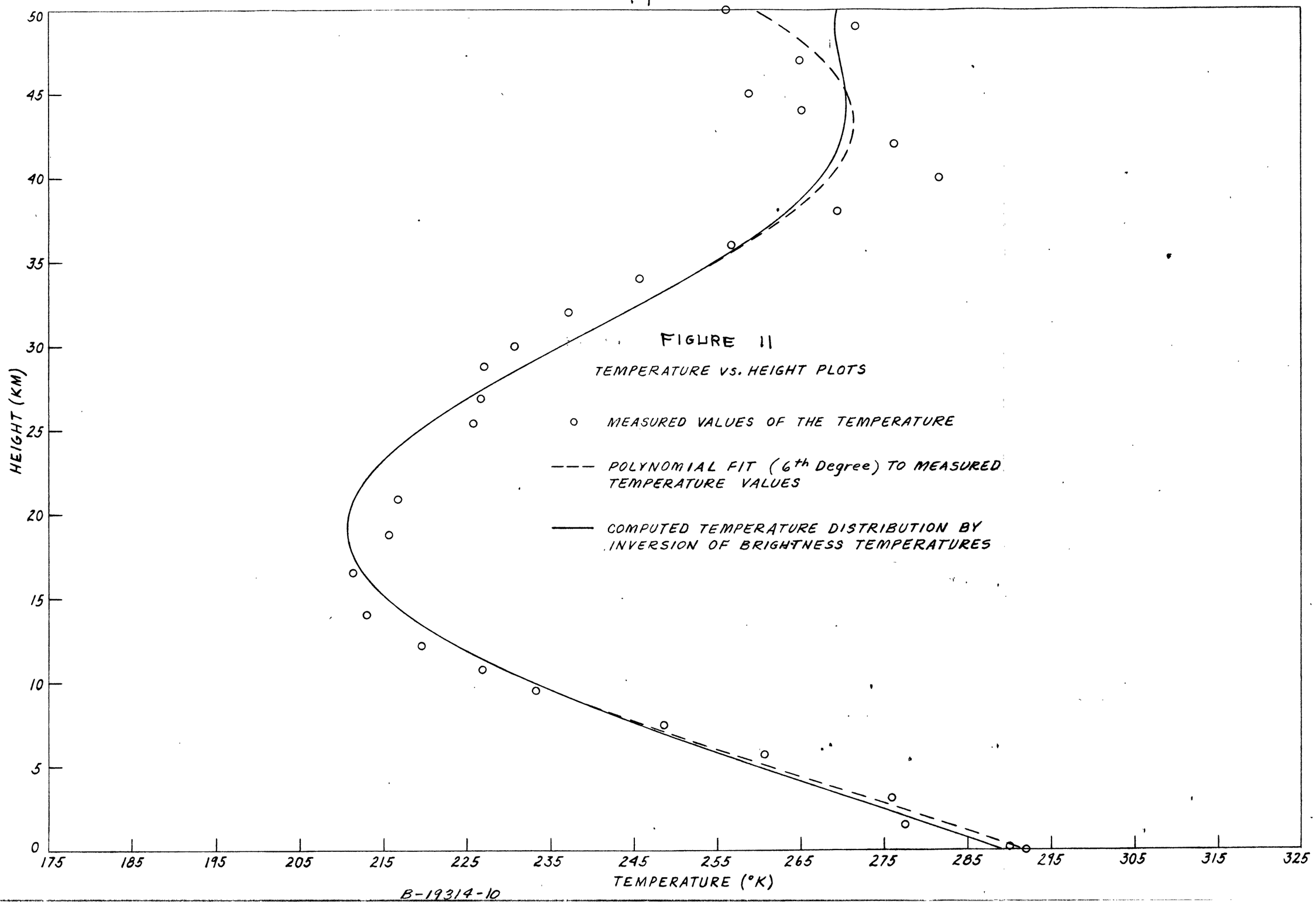

FIGURE 11

TEMPERATURE vs. HEIGHT PLOTS

B-19314-10

to place boundary conditions on T(z) in order to have the iterative solution technique converge to a solution. Thus it seems that a nonlinear integral equation when linearized in the above manner is still intrinsically different from a genuine linear equation. To confirm this conclusion we applied the iterative solution technique to a very simple linear integral equation and an equally simple nonlinear integral equation. In the case of the former convergence to the correct solution occurred without specification of boundary conditions. However in the case of the nonlinear integral equation, divergence from the correct solution occurred in the absence of specified boundary conditions.

We later discovered, quite by accident, that the boundary values we specified at 0 and 50 kilometers had little effect on the inverted profile in the ten to forty kilometer region as the following experiment will illustrate. From equation (25) and the frequencies and nadir angles of Table 1 we computed brightness temperatures with a quadratic interpolation of the raw data of ATMOSPHERE 2 used as the input T(z). From these brightness temperatures together with T(0) and T(50) of the 1962 U. S. Standard Atmosphere as input and boundary conditions respectively, we performed the inversion.

The result of this inversion together with others in which we perturbed the 1962 U. S. Standard Atmosphere boundary conditions by $\pm$ 30.0 $^{\circ}$K in various combinations are shown in Fig. 12. We note that in the central thirty kilometers of these profiles there is little difference between them. Thus we conclude that at points whose distances from the boundaries are at least equal to the width of a weighting function, the boundary values exert little influence.

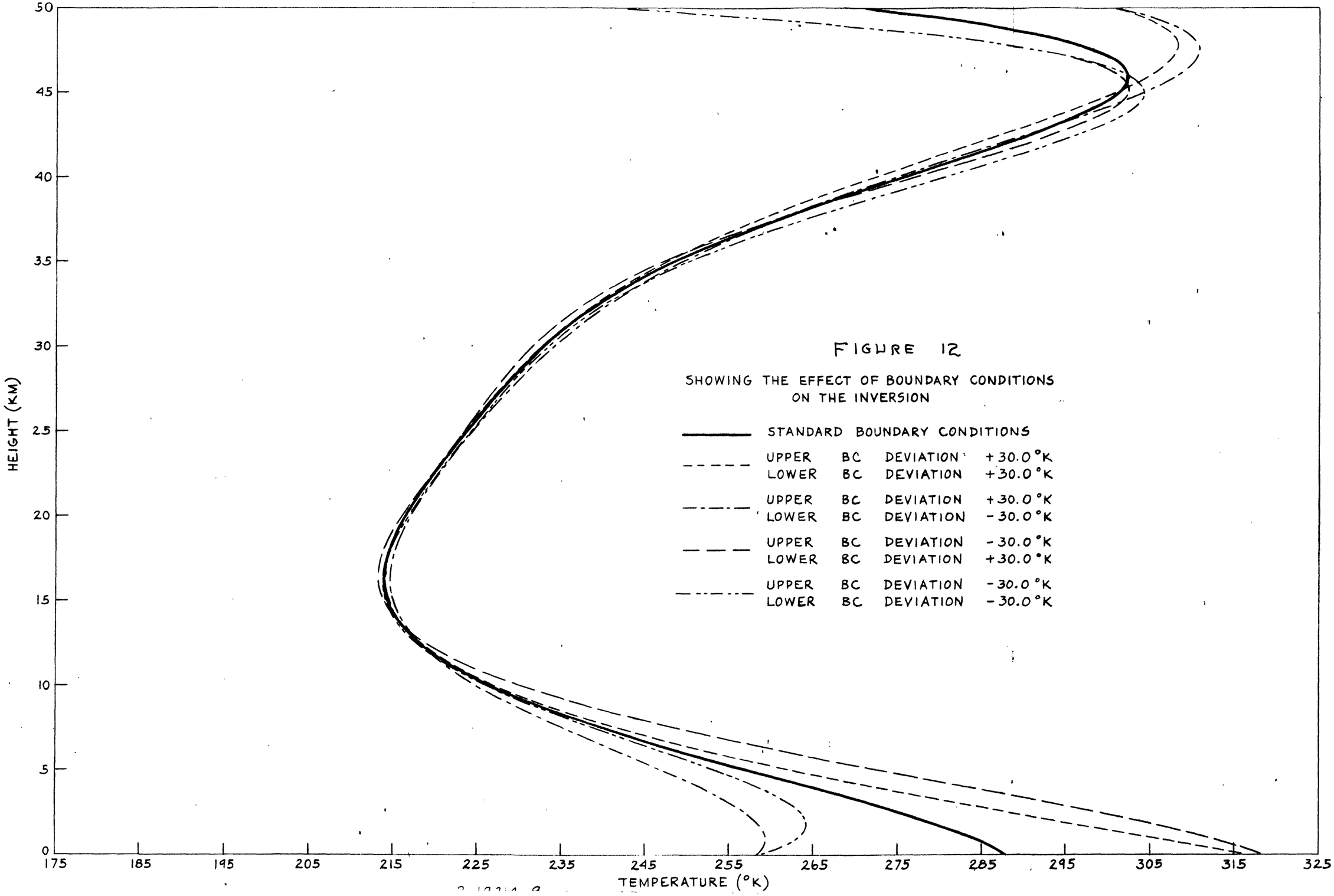

FIGURE 12

SHOWING THE EFFECT OF BOUNDARY CONDITIONS ON THE INVERSION

SECTION V

USE OF THE ITERATIVE INVERSION TECHNIQUE ON IDEAL DATA

Let us now consider a series of experiments which are designed to test the performance of the inversion technique under the assumption of ideal data. We shall also assume, as in the previous experiments, that we are dealing with a horizontally stratified atmosphere in which oxygen is the only emitter at the frequencies of concern and that the absorption theory set forth by Meeks and Lilley (1963) is obeyed exactly. As before, our instrumentation is assumed to have no inherent random errors. Thus we can again use equation (25) to simulate the data that would be received.

The frequencies and nadir angles used with equation (25) are those given in Table 1. For the temperature profile input, a quadratic interpolation of the raw data from which ATMOSPHERES 1 through 4 inclusively were determined is used. These quadratic interpolations appear as the heavy solid lines in Figs. 13 through 16 inclusive. The brightness temperatures thus determined (they correspond to errorless data) were used as input to the inversion routine. The boundary conditions selected were T(0) and T(50) of the U. S. Standard Atmosphere, 1962. The initial guess of the temperature profile was ATMOSPHERE 1.

The results for each set of data and their corresponding interpolated profile are shown as the long dashed curves in Figs. 13 through 16 inclusive. Since the output of the inversion routine is

FIGURE 13 U.S. STANDARD ATMOSPHERE, 1962

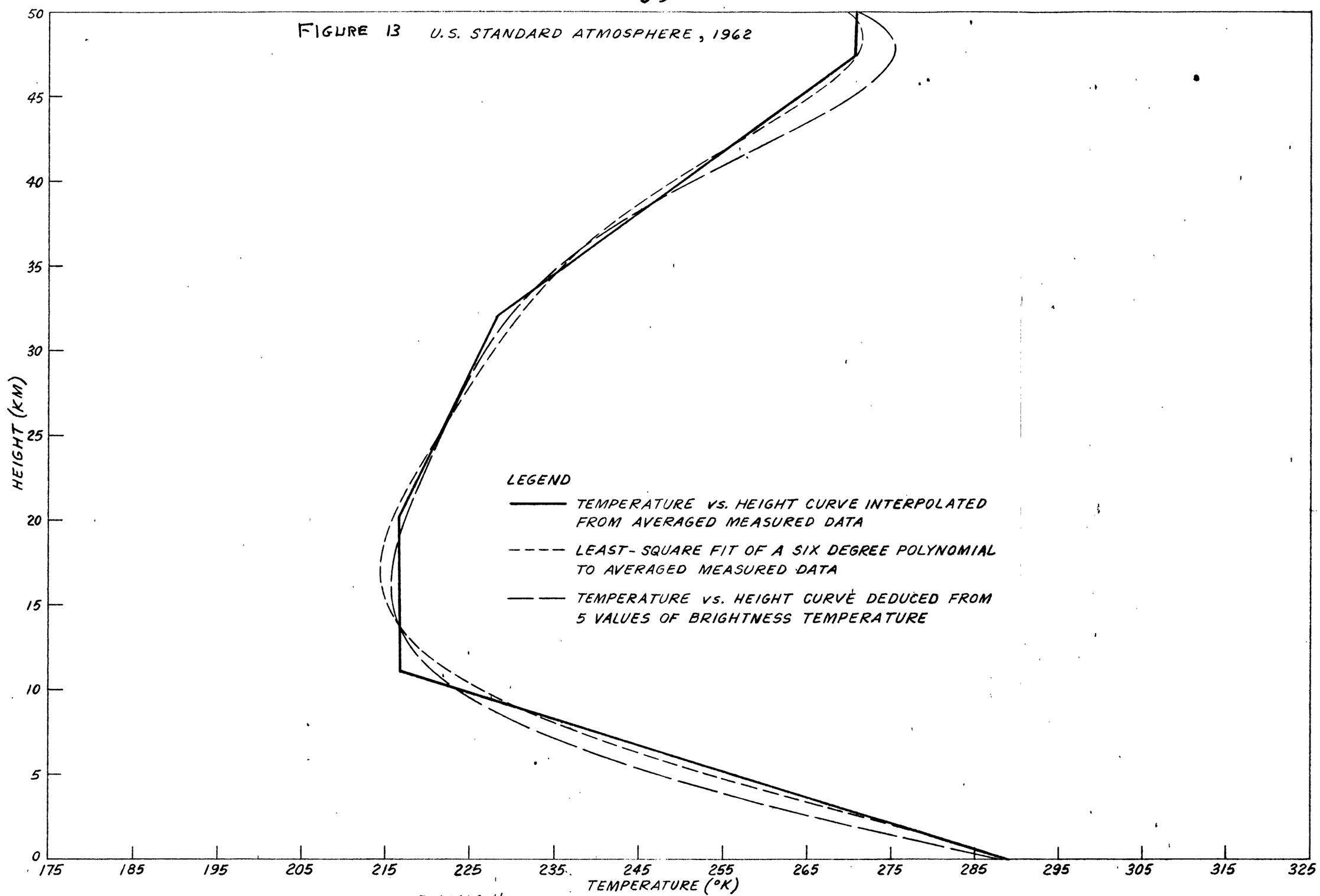

B-19314-11

FIGURE 14 RADIOSONDE AND ROCKET GRENADE DATA
NORFOLK, VA. 14 JULY 1961

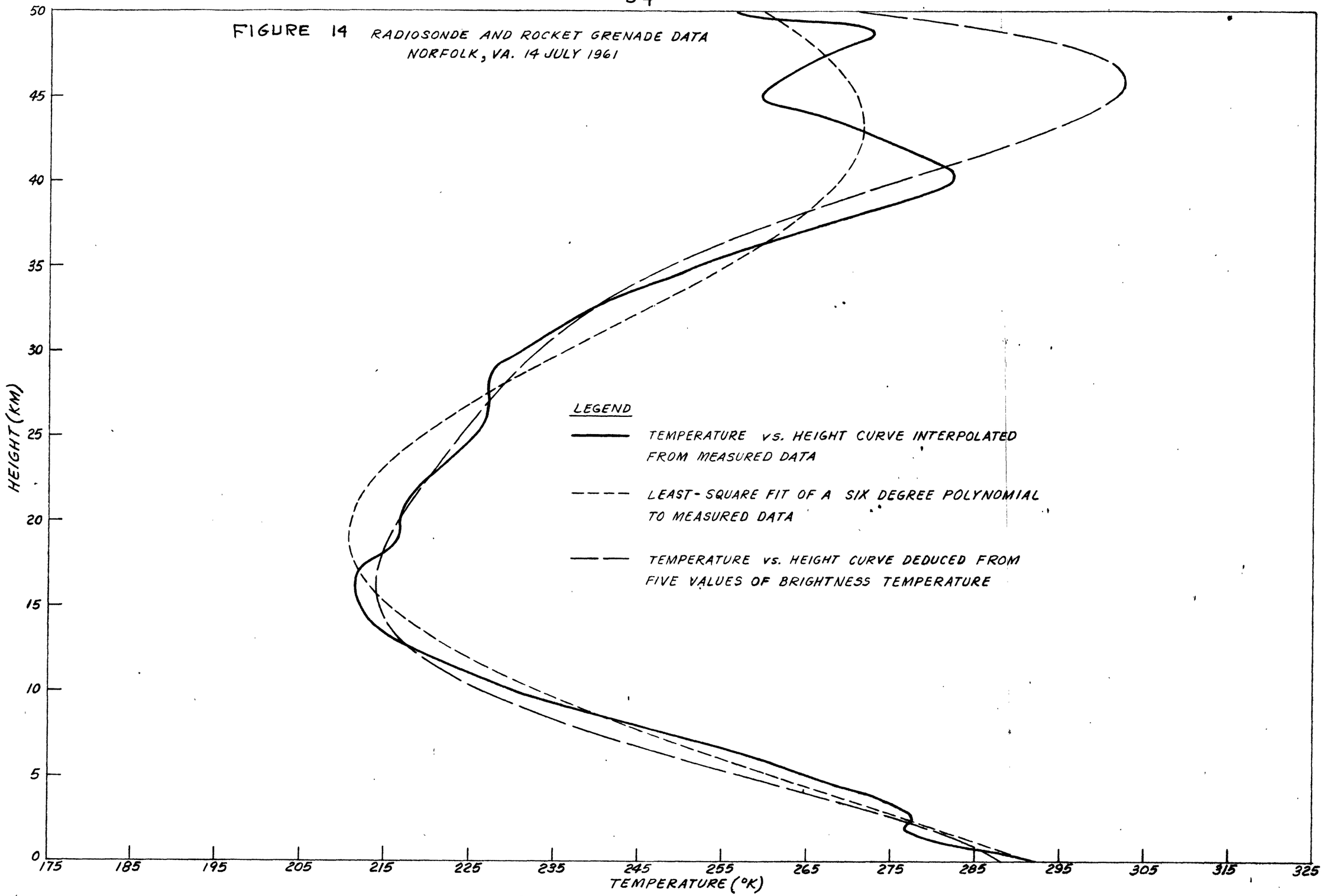

B-19314-12

FIGURE 15 MEAN WINTER 1957, LATITUDE 12° NORTH

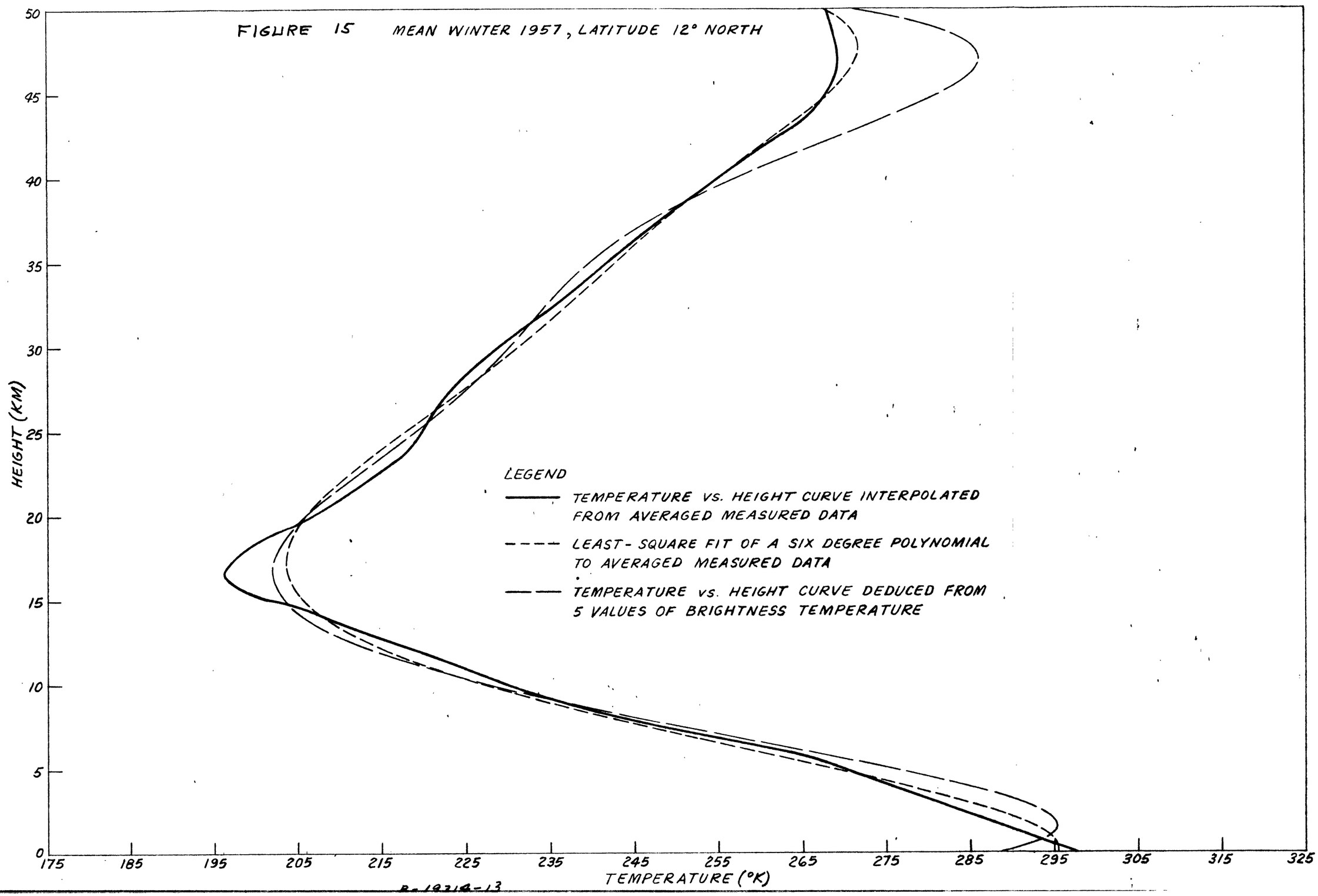

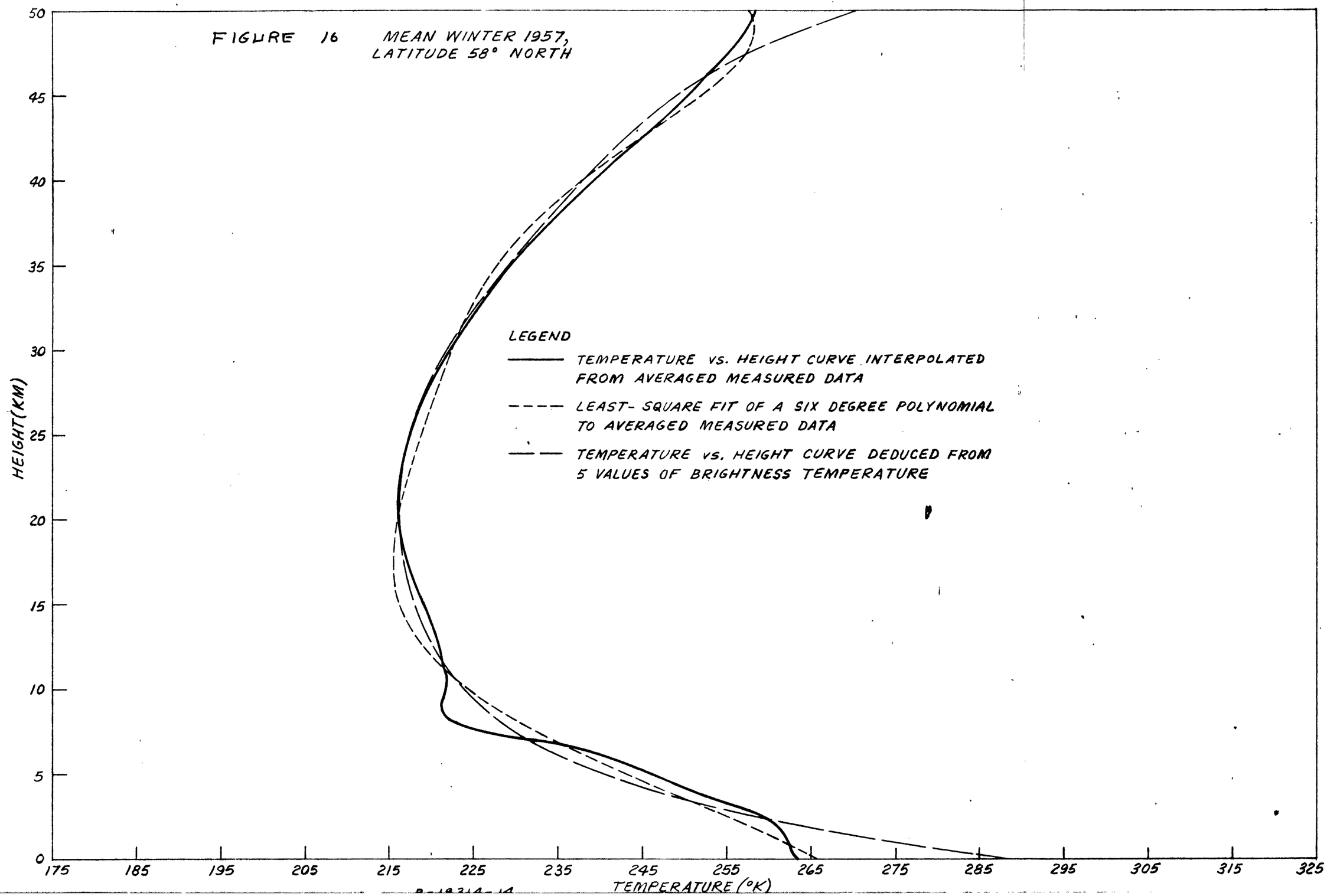

FIGURE 16 MEAN WINTER 1957, LATITUDE 58° NORTH

in essence a six degree polynomial we have included on the appropriate figures, ATMOSPHERES 1 through 4 for the sake of easy comparison. We have also calculated as a measure of comparison the following quantities separately to the zero to fifty and ten to forty kilometer region:

1 - The root-mean-square deviation of the interpolated data from the polynomial curve fit by the method of least squares.

2 - The root-mean-square deviation of the curve obtained by the inversion of brightness temperatures from the interpolated data.

3 - The root-mean-square deviation of the curve obtained by inversion of brightness temperatures from the polynomial curve fit by the method of least squares.

The results of these calculations appear in Table II. We note that the curves deduced from brightness temperature reproduce rather well the interpolated data from which the brightness temperatures were obtained. The fit seems to be better in the ten to forty kilometer region than in the zero to fifty kilometer region. The results in Table II confirm the impressions obtained in our visual inspection of Figs. 13 through 16. The curves deduced from brightness temperatures show a favorable comparison in the ten to forty kilometer region with the curves of polynomials fit to the original data by the method of least squares.

The fact that our results tended to be better in the ten to forty kilometer region than in the zero to fifty kilometer region in part reflects the effect of the influence function. However, the other factor influencing results in the boundaries of the region of our sounding is, of course, boundary conditions. We chose to put into

TABLE II

T(z)	0 to 50 Km Range			10 to 40 Km Range		
	RMS_1 °K	RMS_2 °K	RMS_3 °K	RMS_1 °K	RMS_2 °K	RMS_3 °K
ATMOSPHERE 1	1.49	3.14	2.75	1.53	0.650	1.59
ATMOSPHERE 2	6.45	13.8	10.7	6.58	3.42	5.32
ATMOSPHERE 3	2.07	5.56	5.31	2.33	1.82	1.72
ATMOSPHERE 4	1.86	8.69	7.95	1.63	0.846	1.08

RMS_1 - The root-mean-square deviation of the interpolated data from the polynomial curve fit by the method of least squares.

RMS_2 - The root-mean-square deviation of the curve obtained by the inversion of brightness temperatures from the interpolated data.

RMS_3 - The root-mean-square deviation of the curve obtained by the inversion of brightness temperatures from the polynomial curve fit by the method of least squares.

the inversion routine the standard boundary conditions because it has not been decided at this point whether or not the first satellite radiometer system should be equipped to measure the temperatures of the boundaries. To measure these boundary temperatures radiometrically would require very narrow bandwidth radiometers for the upper boundary and a more thorough understanding of the reflection and emission of the surface and cloud layers for the lower boundary. We thus defer these problems for the present time by using standard boundary conditions.

We also made a few calculations in an attempt to answer the question, "How much do we gain by going from zero order inversion to the iterative inversion procedure?" The zero order inversion and the iterative inversion results on the brightness temperatures corresponding to ATMOSPHERE 2, were compared. Because of the discrete or point like nature of the zero order inversion, the comparison was carried out at five altitudes which correspond to the weighting function peaks for the five frequencies and nadir angles of the measurements. One should recall that according to the rules of the zero order inversion one must use peak altitudes which are computed with a standard atmosphere.

The results of this comparison at the five altitudes is presented in Table III. Also shown are the root-mean-squares of the two sets of deviations. The results tend to indicate that there is gain in accuracy with the use of the iterative technique.

TABLE III

Comparison of Zero and Iterative Inversions

Frequency Gc/sec.	Nadir Angle θ deg.	$H(\nu,\theta)$ Km	$Ta(H)$ °K	$T_B(\nu,\theta)$ °K	ΔT_{Ba} °K	$Ti(H)$ °K	ΔT_{ia} °K
55.65	0.0	14.70	212.419	217.593	+5.174	214.687	+2.268
59.30	0.0	20.90	217.115	218.142	+1.027	217.847	+0.732
60.32	30.0	34.70	249.677	249.913	+0.236	247.214	-2.463
60.33	0.0	31.50	235.678	238.158	+2.480	236.584	+0.906
60.37	0.0	27.10	227.075	228.629	+1.554	227.362	+0.287

$$\sqrt{\frac{\sum_{Hi}^{5} \overline{(\Delta T_{Ba})^2}}{5}} = 2.70\ °K \qquad \sqrt{\frac{\sum_{Hi}^{5} \overline{(\Delta T_{ia})^2}}{5}} = 1.59\ °K$$

ΔT_{Ba} = deviation of brightness temperatures from assumed actual temperature for zero order inversion.

ΔT_{Bi} = deviation of brightness temperature from assumed actual temperature for iterative inversion technique.

$Ta(H)$ = the temperature of ATMOSPHERE 2 at height H; the assumed actual temperature.

H = altitude of weighting function peaks as computed with Atmosphere 1.

$T_B(\nu,\theta)$ = brightness temperature as computed with ATMOSPHERE 2.

$Ti(H)$ = the temperature at height H as obtained by the iterative inversion of the set of $T_B(\nu,\theta)$'s.

SECTION VI

THE INFLUENCE OF INSTRUMENTAL EFFECTS AND UNCERTAINTIES ON THE ITERATIVE INVERSION PROCEDURE

In any real measurement program we shall have to deal with, or limit as much as possible, the effects of our non ideal instruments on the data. We have already discussed radiometer uncertainties in Section I, the Introduction. An uncertainty is an error in our data for which we cannot make any corrections. However, we can make corrections or limit most instrumental effects. Four such effects which might cause trouble if not eliminated or taken into account are bandwidth averaging of the received signal, frequency stability of the radiometer beamwidth averaging by the antenna and side lob reception of the antenna.

The latter of these effects (the side lobe reception) is only serious if the side lobes happen to be directed towards a strong radio source such as the sun. We can, however, take steps to avoid this, thus this effect need not concern us. Insofar as the antenna beamwidth is concerned, presently beamwidths can be made small enough so as to be of little concern unless the horizontal temperature gradients are very large. Only during the passage of the satellite over strong frontal systems might the antenna beamwidth thus be of some concern.

The problems of bandwidth and stability are of more concern to us because they involve an average over frequency. Hence, if the nominal frequency to which the radiometer is tuned is near a line

center, we shall in effect be viewing the average temperature of some very thick layers. Let us now consider the combined effects of bandwidth averaging, the averaging due to the frequency drift of the radiometer and the uncertainty of the radiometer.

We shall assume that the brightness temperature is averaged over frequency according to the equation:

$$\bar{T}_B = \frac{1}{\Delta\nu} \int_{\nu_i}^{\nu_f} T_B(\nu)\, d\nu \tag{28}$$

where $\nu_i = \nu_o - \Delta\nu_s - \frac{\beta}{2}$

$\nu_f = \nu_o + \Delta\nu_s - \frac{\beta}{2}$

ν_o = nominally tuned frequency

$\Delta\nu_s$ = assumed stability of the radiometer at the frequency ν_o

β = bandwidth of the radiometer at frequency ν.

$T_B(\nu)$ was computed using ATMOSPHERE 2 in equation (25). Five values of ν_o corresponding to the five frequencies in Table I were chosen. The corresponding nadir angles of Table I were also used here. For this purpose of computing the uncertainty, we shall assume a radiometer noise temperature of 3000 ^{o}K (this is typical for radiometers which could be built today) and an integration time of 10 seconds. In the real case the uncertainty either adds or subtracts from the signal. We shall arbitrarily assume that the uncertainties subtract from the

signal. Equation (22) is used to compute the uncertainty. All of the calculations are summarized in Table IV.

The result of the inversion run using the input brightness temperatures listed in Table IV and the boundary conditions of ATMOSPHERE 1 is shown as inversion no. 7 in Fig. 17. The result of the inversion run using the actual brightness temperatures, which is the same as the inversion shown in Fig. 111, is depicted as the errorless inversion in Fig. 17. The root-mean-square deviation of inversion no. 7 from the errorless inversion is 21.3 $^{\circ}$K in the zero to fifty kilometer region and 11.8 $^{\circ}$K for the ten to forty kilometer region.

The specifications on the radiometer used to obtain the data for inversion no. 7 are quite loose. Let us now assume a driftless radiometer with a noise temperature of about 100 $^{\circ}$K or slightly less. Proceeding as before we compute average brightness temperatures and uncertainties for the same five frequencies. The results of these calculations are summarized in Table V. The uncertainties are now about an order of magnitude less than before and except for the first frequency they are about an order of magnitude less than the difference between the averaged and actual brightness temperatures. Therefore, let us neglect them in determining the input brightness temperatures.

Hence using the input brightness temperatures listed in Table V and the same boundary conditions as before we obtain a temperature profile which corresponds to inversion no. 8 in Fig. 17. The root-mean-square deviation of this temperature profile from that of the

TABLE IV

Nominal Tuned Frequency Gc/sec.	Band-width B Gc/sec.	Stability Gc/sec.	Initial Freq. Gc/sec.	Final Freq. Gc/sec.	Average T_B °K	ΔT_{rms} °K	Input T_B °K	Actual T_B °K	δT_B °K
55.6500	0.0400	±0.0400	55.5900	55.7100	217.523	±0.165	217.358	217.339	+0.019
59.3000	0.0400	±0.0400	59.2600	59.3600	214.898	±0.165	214.733	214.193	+0.540
60.3200	0.0100	±0.0050	60.3100	60.3300	249.998	±1.030	248.968	250.979	+2.011
60.3300	0.0200	±0.0100	60.3100	60.3500	241.758	±0.233	241.525	240.090	+1.435
60.3700	0.0400	±0.0200	60.3300	60.4200	232.214	±0.165	232.049	228.029	+4.020

$$\sum(\delta T_B)^2 = 22.556$$

$$\frac{\sum(\delta T_B)^2}{5} = 4.511$$

$$\text{RMS Dev.} = \sqrt{\frac{\sum(\delta T_B)^2}{5}} = 2.125$$

$$\delta T_B = T_{B(\text{Input})} - T_{B(\text{Actual})}$$

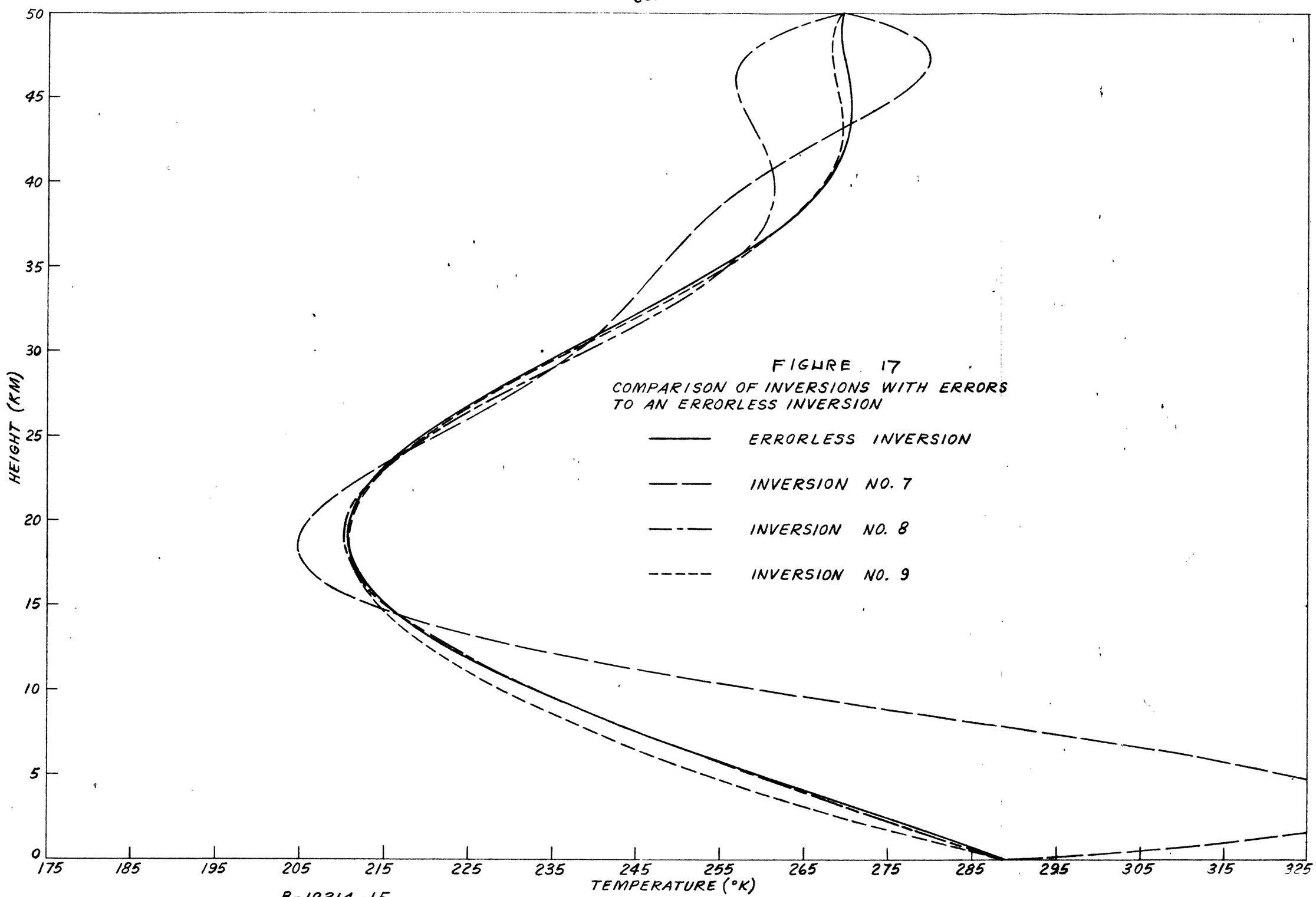

FIGURE 17
COMPARISON OF INVERSIONS WITH ERRORS TO AN ERRORLESS INVERSION

TABLE V

Nominal Tuned Frequency Gc/sec.	Band-width B Gc/sec.	Stability Gc/sec.	Initial Freq. Gc/sec.	Final Freq. Gc/sec.	Average T_B °K	ΔT_{rms} °K	Input T_B °K	Actual T_B °K	δT_B °K
55.6500	0.0400	±0.0000	55.6300	55.6700	217.356	±0.017	217.356	217.339	+0.017
59.3000	0.0400	±0.0000	59.2800	59.3200	214.268	±0.017	214.268	214.193	+0.075
60.3200	0.0100	±0.0000	60.3150	60.3250	249.663	±0.103	249.663	250.979	-1.316
60.3300	0.0200	±0.0000	60.3200	60.3400	240.791	±0.023	240.791	240.090	+0.701
60.3700	0.0400	±0.0000	60.3500	60.3900	229.064	±0.017	229.064	228.029	+1.035

$$\sum(\delta T_B)^2 = 3.307$$

$$\frac{\sum(\delta T_B)^2}{5} = 0.661$$

$$\text{RMS Dev.} = \sqrt{\frac{\sum(\delta T_B)^2}{5}} = 0.871$$

$$\delta T_B = T_{B(\text{Input})} - T_{B(\text{Actual})}$$

errorless inversion is 5.72 °K in the zero to fifty kilometer region and 3.01 °K in the ten to forty kilometer region.

Tables VI and VII give the input brightness temperatures for two inversion runs designed to test for a difference in effect between a positive and negative uncertainty of the same magnitude at the same frequency. The results of these inversion runs are inversion no. 9, Fig. 17 and inversion no. 10, Fig. 18 corresponding respectively to the input data in Table VI and Table VII. The boundary conditions for both are those of ATMOSPHERE 1. The root-mean-square deviation of inversion no. 9 from the errorless inversion is 4.01 °K in the zero to fifty kilometer region and 1.46 °K in the ten to forty kilometer region. For inversion no. 10, the root-mean-square deviation from the errorless inversion in the zero to fifty kilometer region is 3.62 °K and 1.97 °K in the ten to forty kilometer region. The deviations are somewhat greater near the altitudes of influence of the weighting function corresponding to the frequency whose associated brightness temperature is in error. The deviations also appear to have the same sign as the error in the brightness temperature.

Inversion no. 11, Fig. 18, when compared with inversion no. 9, Fig. 17, shows the difference in effect of a one degree error in brightness temperatures corresponding to two different frequencies. The input data for inversion no. 11, is given in Table VIII. The boundary conditions are those of ATMOSPHERE 1. The root-mean-square deviation of inversion no. 11 from the errorless one is 10.2 °K in the zero to fifty kilometer region and 3.60 °K in the ten to forty kilometer region. Again in this case most of the deviations appear to have the same

TABLE VI

Frequency	Nadir Angle	Input T_B	Actual T_B	δT_B
55.6500	0.0	216.339	217.339	-1.000
59.3000	0.0	214.193	214.193	0.000
60.3200	30.0	250.979	250.979	0.000
60.3300	0.0	240.090	240.090	0.000
60.3700	0.0	228.029	228.029	0.000

$$\Sigma(\delta T_B)^2 = 1.000$$

$$\frac{\Sigma(\delta T_B)^2}{5} = 0.2$$

$$\text{RMS Dev.} = \sqrt{\frac{\Sigma(\delta T_B)^2}{5}} = 0.447$$

$$\delta T_B = T_{B(\text{Input})} - T_{B(\text{Actual})}$$

TABLE VII

Frequency	Nadir Angle	Input T_B	Actual T_B	δT_B
55.6500	0.0	218.339	217.339	+1.000
59.3000	0.0	214.193	214.193	0.000
60.3200	30.0	250.979	250.979	0.000
60.3300	0.0	240.090	240.090	0.000
60.3700	0.0	228.029	228.029	0.000

$$\sum(\delta T_B)^2 = 1.000$$

$$\frac{\sum(\delta T_B)^2}{5} = 0.2$$

$$\text{RMS Dev.} = \sqrt{\frac{\sum(\delta T_B)}{5}} = 0.447$$

$$\delta T_B = T_B(\text{Input}) - T_B(\text{Actual})$$

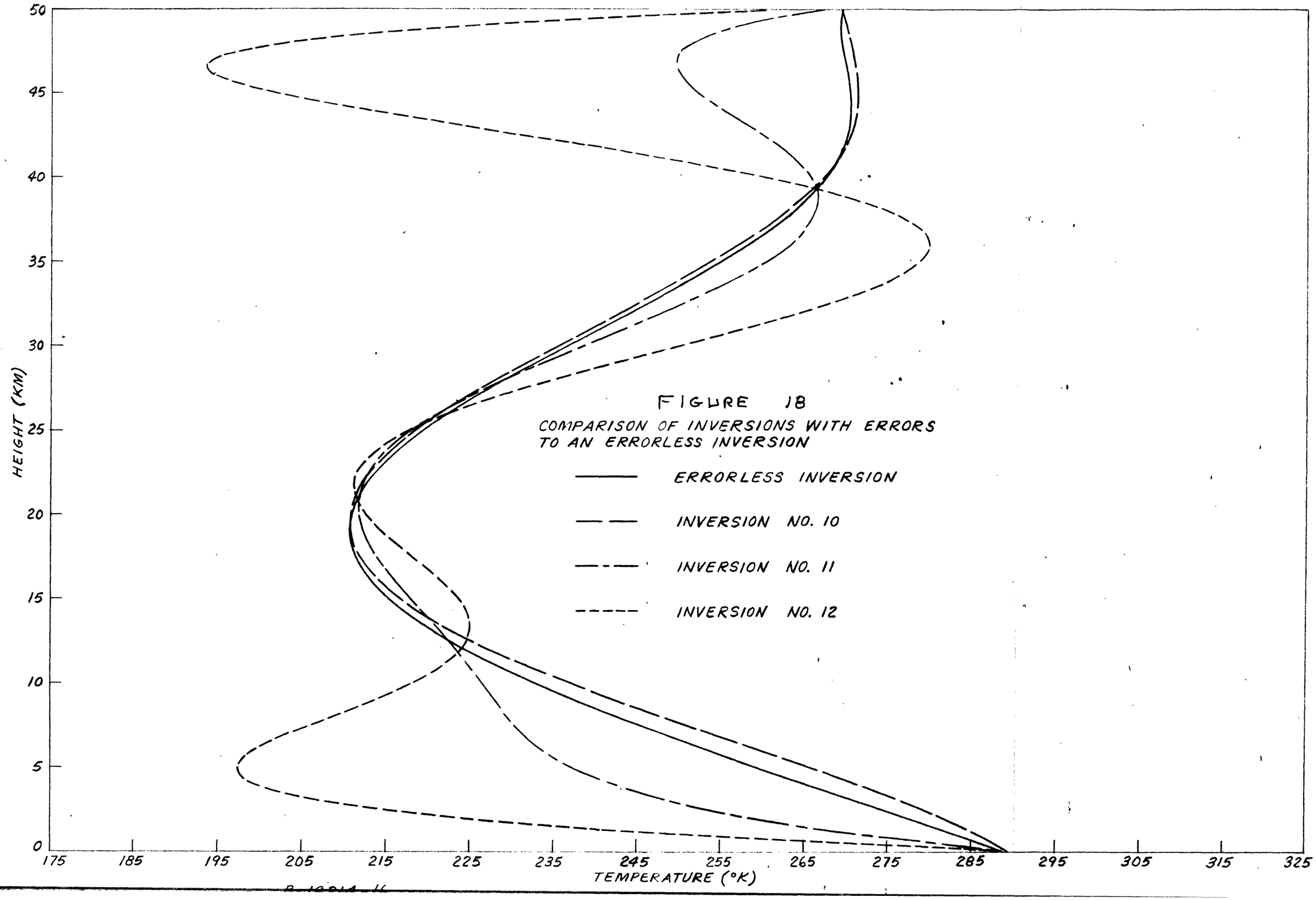

FIGURE 18
COMPARISON OF INVERSIONS WITH ERRORS TO AN ERRORLESS INVERSION

TABLE VIII

Frequency	Nadir Angle	Input T_B	Actual T_B	δT_B
55.6500	0.0	217.339	217.339	0.000
59.3000	0.0	214.193	214.193	0.000
60.3200	30.0	250.979	250.979	0.000
60.3300	0.0	240.090	240.090	0.000
60.3700	0.0	227.029	228.029	-1.000

$$\Sigma(\delta T_B)^2 = 1.000$$

$$\Sigma(\delta T_B)^2 = 0.2$$

$$\text{RMS Dev.} = \sqrt{\frac{\Sigma(\delta T_B)^2}{5}} = 0.447$$

$$\delta T_B = T_{B(\text{Input})} - T_{B(\text{Actual})}$$

sign as the error in brightness temperature. However in this case the greatest deviations tend to be in the boundary regions (0-10 and 40-50 km) rather than in the regions of greatest influence of the weighting function related to the brightness temperature which is in error.

Finally, in inversion no. 12, Fig. 18, we show the effects of errors of the same magnitude but of alternating signs in each of the brightness temperatures. The input data for this inversion run is given in Table IX. Again, the boundary conditions are those of ATMOSPHERE 1. The root-mean-square deviation of inversion no. 12 from the errorless inversion is 30.6 $^{\circ}$K in the zero to fifty kilometer region and 12.6 $^{\circ}$K in the ten to forty kilometer region. The greatest deviations tend to be in the boundary regions. The sign of the deviation at a given altitude tends to be the same as the sign of the error in the brightness temperature which corresponds to the weighting function influential at that altitude.

TABLE IX

Frequency	Nadir Angle	Input T_B	Actual T_B	δT_B
55.6500	0.0	216.339	217.339	-1.000
59.3000	0.0	215.193	214.193	+1.000
60.3200	30.0	249.979	250.979	-1.000
60.3300	0.0	241.090	240.090	+1.000
60.3700	0.0	226.029	228.029	-2.000

$$\sum(\delta T_B)^2 = 8.000$$

$$\frac{\sum(\delta T_B)^2}{5} = 1.6$$

$$\text{RMS Dev.} = \sqrt{\frac{\sum(\delta T_B)^2}{5}} = 1.262$$

SECTION VII

CONCLUSIONS

Various aspects of the problem of the determination of the kinetic temperature profile of the atmosphere from the five millimeter radiative emission of molecular oxygen have been investigated. One of the most important conclusions we have reached is that with only five ideal measurements of this emission, we can deduce a polynomial representation of the actual temperature profile from zero to fifty kilometers which is almost as good as the polynomial representation that could be obtained by a "least square" fit of from thirty to fifty values of kinetic temperature versus height. In fact, in the ten to forty kilometer region we can expect to obtain a better representation of the actual atmospheric temperature profile with an inversion of five measured brightness temperatures than with a polynomial determined from up to fifty kinetic temperature measurements in the zero to fifty kilometer region.

Our investigation of the zero order inversion and a comparison of it with the iterative inversion procedure has led us to the following conclusion. A set of brightness temperatures versus frequencies and nadir angles can yield more information when investigated as a whole set than when each measurement is considered separately. We have come to this conclusion by numerical experimentation. For the limiting case of an infinite number of brightness temperature measurements, we could reach a similar conclusion by abstract mathematical arguments.

We have also concluded that a statement of fixed boundary conditions in the iterative inversion procedure is required. However, we have shown that the chosen boundary conditions do not influence the derived temperature profile outside of the so called boundary region. We might ask ourselves therefore, "Why does the iterative procedure fail to work without boundary conditions?" At present all that we say to answer this question is that without these fixed boundary conditions we do not have a properly specified problem.

The iterative inversion procedure requires an initial guess of the solution. We have shown that the use of a good guess (one which is similar to the unknown actual temperature profile) or a bad guess (a temperature profile having little relation to the actual one) has little effect on the final result. The only effect of a bad guess is to increase the number of iterations required to obtain a solution. We, therefore, conclude that the use of a standard atmosphere for an initial guess is quite satisfactory.

We spent a considerable amount of time investigating the relationship of the frequency and nadir angle dependence of our brightness temperature measurements to the kinetic temperature versus altitude function. To facilitate this investigation, we considered the effect of these parameters on a functional combination of the absorption and transmissivity functions termed by Meeks and Lilley (1963) as weighting functions. We also developed a point of view of a group of weighting functions known as the influence function. We concluded from our studies that the shape and locations of the weighting functions on the height axis were substantially unaffected by the nature of the temperature profile.

Through our investigations of weighting functions and their corresponding influence function we concluded that measurements indicative of temperatures in the ten to thirty kilometer region are easily obtained. However to obtain measurements indicative of temperatures above thirty kilometers would require that these measurements be made at either large nadir angles or at frequencies very close to line centers. The former alternative was concluded to be a poor one because it would destroy horizontal resolution. The latter alternative would impose limitations on allowable bandwidths of the radiometers. This would have adverse ramifications on the root-mean-square undertainties of the measurements. However, we concluded that this is really a technological instrumentation problem that could eventually be solved. To make measurements indicative of temperatures below ten kilometers would involve simply additions to the absorption theory that incorporate ground effects.

From the iterative inversions of ideal data, we learned that the deviations of the derived profile from the actual profile at various altitudes would be negatively correlated to the value of the influence function at the same altitudes. Hence we concluded that an influence function whose value is constant with altitude is desirable in cases where a temperature profile with a uniform deviation is required.

We performed several inversions on data tainted by instrumental effects and uncertainties. These experiments led to the following conclusions:

1 - Deviations of the derived temperature profiles from the actual temperature profile are greater at altitudes where the influence function is small.

2 - Measurements made near line centers must be done with radiometers that are very stable and that have narrow bandwidths and low noise temperatures.

3 - Errors made at brightness temperatures which correspond through frequency and nadir angle to weighting functions that peak at high altitudes are more serious than errors made at brightness temperatures that correspond to weighting functions which peak at low altitudes.

4 - Errors of the same magnitude but different sign at brightness temperatures of the same frequency and nadir angle produce equal root-mean-square deviations of derived profiles from actual profiles. The signs of the former deviations correspond to those of the latter.

5 - There does not seem to be a linear relationship between root-mean-square deviations of ideal data from non ideal data and root-mean-square deviations of the derived profiles from the actual profiles.

SECTION VIII

SUGGESTIONS FOR FUTURE WORK

One of the most important problems and the one most deserving of study in any future work, is that of the effect of errors in the data. The work done in this thesis on this subject is quite incomplete. Two avenues of approach immediately suggest themselves. First, we might try a "least square fit" inversion on a large net of data points. Theory of this method is described in Hildelbrand, "Methods of Applied Mathematics." Such a technique would tend to smooth the data and cause random errors to cancel one another.

A second approach is to divide the inversion from zero to fifty kilometers into inversions over several smaller height ranges. For example, with the same five measurements, we first derive a polynomial valid from zero to fifteen kilometers, then one from fifteen kilometers to thirty five and finally one from thirty five to fifty kilometers. The boundary conditions required at fifteen and thirty kilometers could be the temperatures obtained by a zero order inversion. Dividing the single large inversion up into smaller ones might help to dampen the error multiplying effect which seems to result when the data has errors in it.

Another aspect of this problem which deserves some consideration is the use of orthogonal functions in the inversion procedure. In the least they would reduce the amount of numerical computation necessary. They would also reduce the effect of round off errors in the problem by giving rise to matrices with very strong diagonals.

There also remains to be considered and incorporated into this problem the following:

1) The spectral reflectivity and emission of the ground and sea surfaces.

2) The spectral reflectivity, emission and absorption of clouds and rain.

3) The Zeeman effect.

Finally and most importantly, a program of measurements including the development of suitable airborne radiometers must be undertaken. At present we can build radiometers which are quite stable enough for our purposes. However these radiometers have rather large bandwidths (approximately 100 Mc/sec) and high noise temperatures (approximately 3000 $^{\circ}$K). We need equally stable radiometers with bandwidths of about 5 Mc/sec and noise temperatures of 100 $^{\circ}$K. The rapid development of solid state devices may make it possible to obtain these specifications in radiometers in the not too distant future.

APPENDIX I

POLYNOMIAL CURVE FITTING

Since the result of our inversion procedure is a set of polynomial coefficients, we are naturally led to make a comparison between the polynomials resulting from the inversion of brightness temperatures and those obtained directly from temperature versus height data. Clearly, there are many criterion by which a polynomial can be said to best fit a set of data points. We chose to use the method in which the square of the sum of the deviations of the fitted curve from the data points is minimized. The criterion for this method is

$$\sum_{i=0}^{N} w(z_i) \left\{ T(z_i) - \sum_{k=0}^{n} a_k z_i^k \right\}^2 = \min \qquad \text{(I-1)}$$

where N = number of data points

n = degree of the polynomial

z_i = altitude of ith point

$T(z_i)$ = temperature data at the ith altitude

a_k = k^{th} coefficient of the polynomial

$w(z_i)$ = weight of the ith data point.

The necessary conditions for a minimum in equation (I-1) require that the partial derivatives $\partial/\partial a_k$ $k = 0, 1, 2, \ldots n$ of equation (I-1) all vanish. This leads to the following system of linear equations which can be solved for the coefficients a_o through a_k:

$$a_o \sum_{i=0}^{N} w(z_i)\, z_i^r\, z_i^o + a_1 \sum_{i=0}^{N} w(z_i)\, z_i^r\, z_i^1 + \ldots +$$

$$+ a_n \sum_{i=0}^{N} w(z_i)\, z_i^r\, z_i^n = \sum_{i=0}^{N} w(z_i)\, z_i^r\, T(z_i) \qquad \text{(I-2)}$$

where $r = 0, 1, 2, \ldots n$

Using equation (I-2) with $n = 6$ and a constant $w(z_i)$ we obtained the temperature profiles ATMOSPHERE 1 through ATMOSPHERE 4. The results together with the input data are shown in Fig.(I-1) through Fig. (I-4).

FIGURE I-1
U.S. STANDARD ATMOSPHERE, 1962

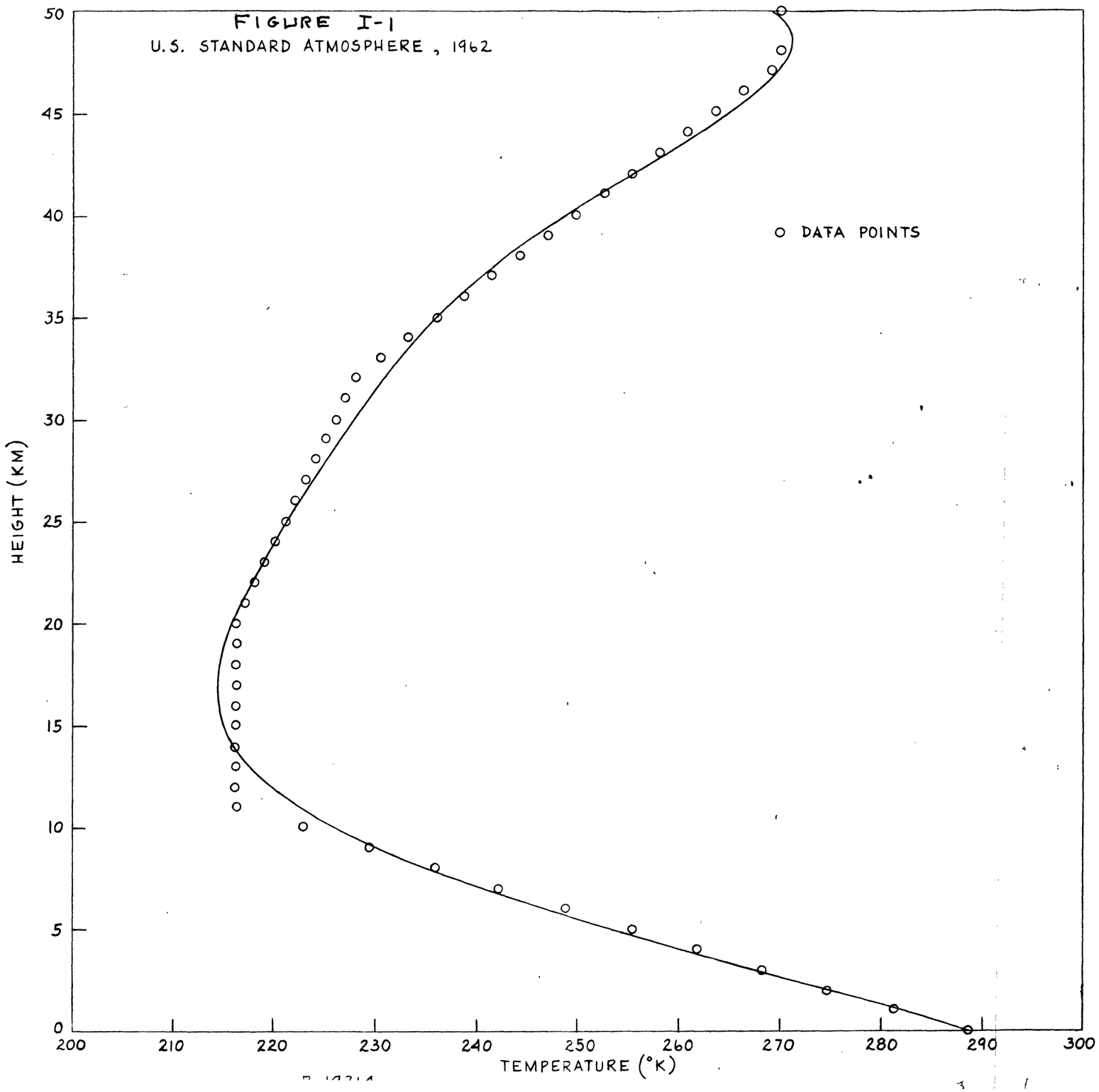

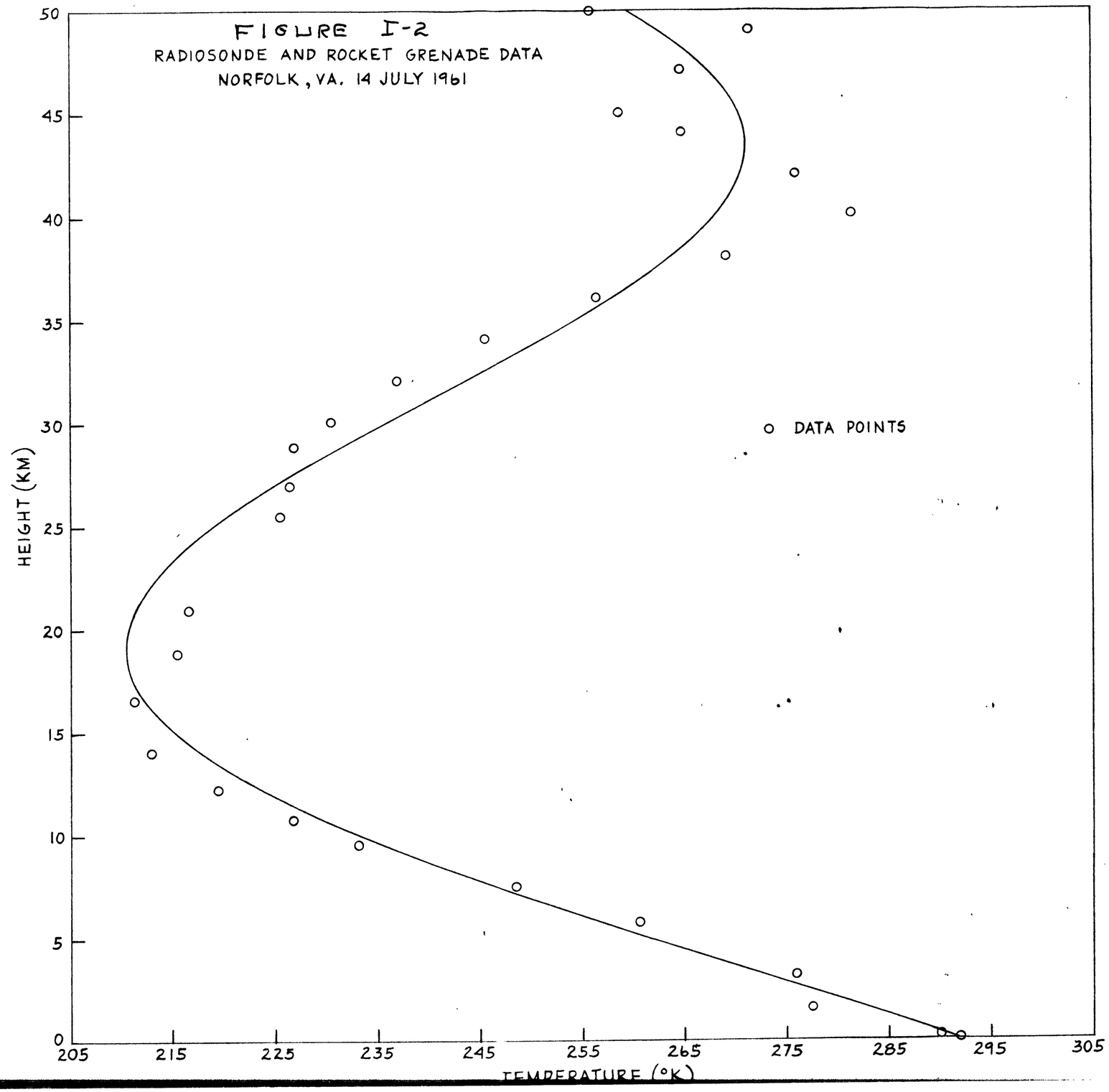

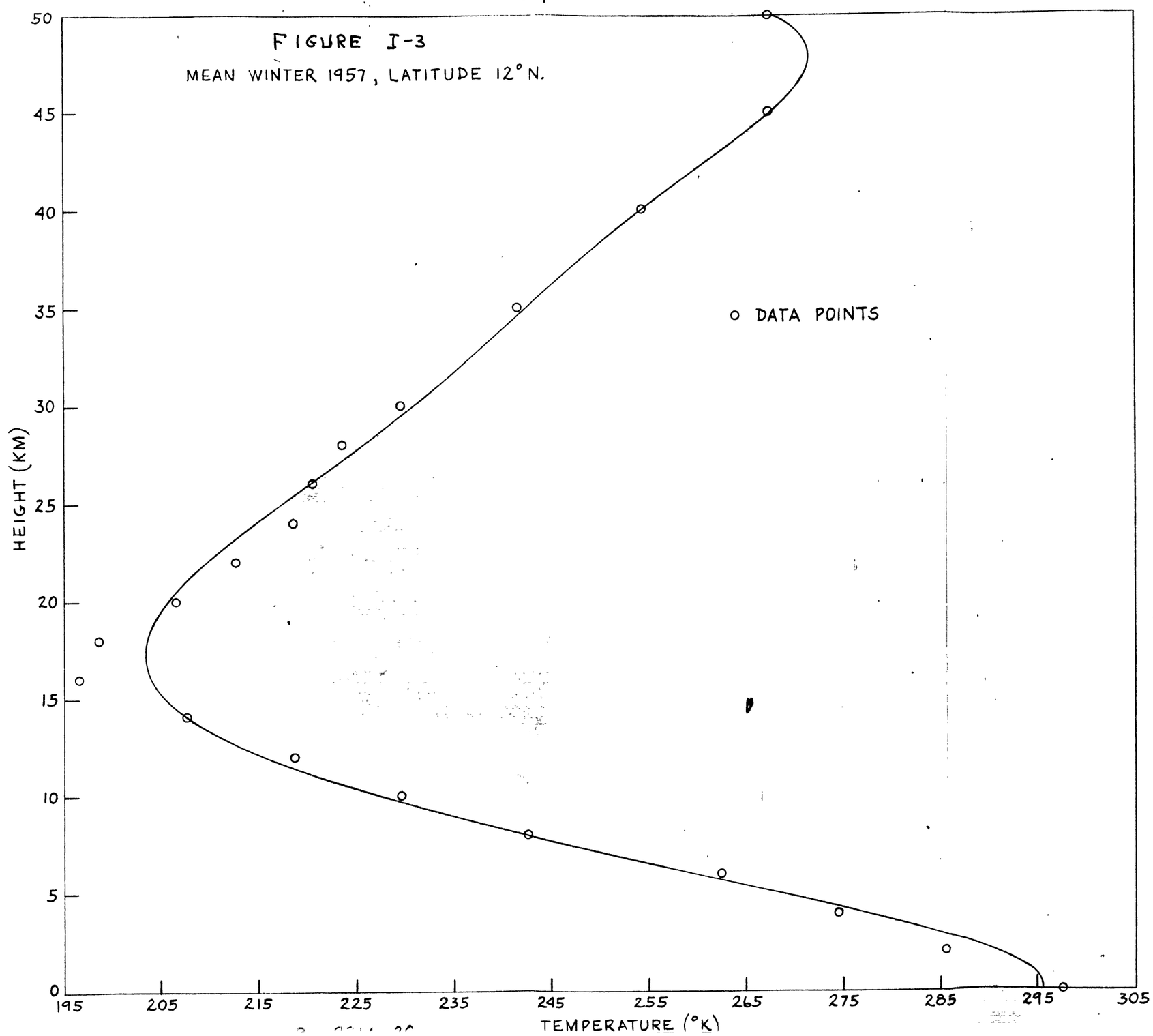

(M)

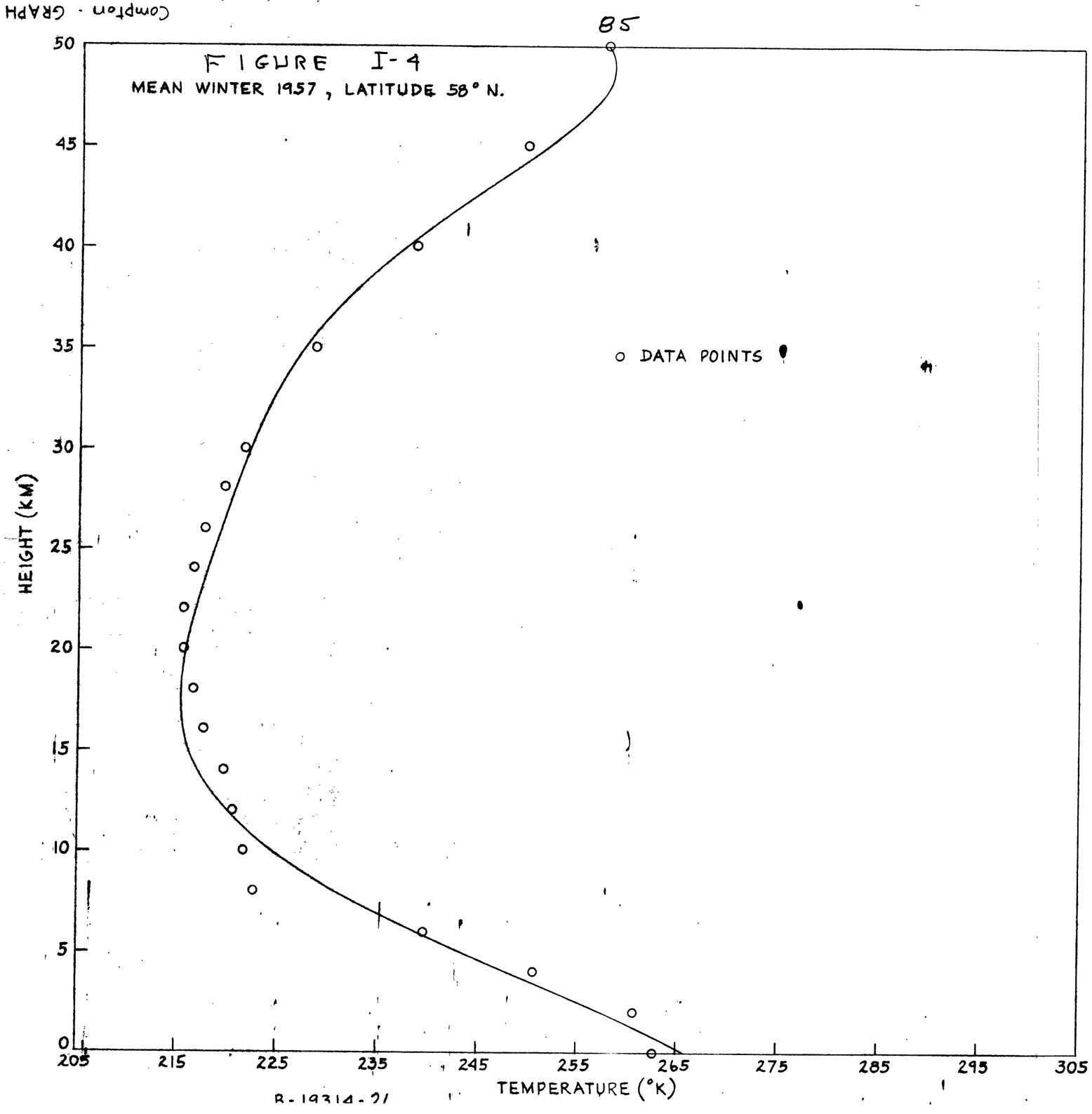

B-19314-21

APPENDIX II

WEIGHTING FUNCTION ANALYSIS

Note - The numbered frequencies in the tables are shown graphically on the charts with arrows.

APPENDIX II

Weighting Function Analysis

Frequency No.	Height of Peak Km	Frequency Gc/sec.	Nadir Angle Deg.	$T_B(3)$ °K	T(h) at.W..F. Peak °K
0	4.05	53.5800	0.0	211.434	260.319
1	11.85	55.4500	0.0	220.940	220.530
2	12.05	55.5100	0.0	220.371	220.020
3	12.15	55.3900	0.0	220.721	219.800
	12.48	55.4500	30.0	219.577	218.981
	12.80	55.3900	30.0	219.373	218.353
	12.80	55.5100	30.0	219.054	218.353
4	12.80	55.5700	0.0	219.184	218.353
	13.45	55.5700	30.0	218.031	217.210
5	14.08	55.6300	0.0	217.718	216.200
6	14.80	55.6500	0.0	217.277	215.475
	14.80	55.6300	30.0	216.846	215.475
	15.40	55.6500	30.0	216.533	215.013
7	16.50	57.9000	0.0	214.406	214.579
	16.90	57.9000	30.0	214.295	214.541
8	17.00	58.8050	0.0	214.215	214.541
	17.00	61.5000	0.0	214.302	214.541
	17.05	61.5000	15.0	214.292	214.542
	17.46	58.8050	30.0	214.189	214.580
	18.29	62.0000	0.0	214.645	214.837
	18.31	62.0000	15.0	214.672	214.837
	18.69	62.0000	30.0	214.786	215.028
	18.80	57.9000	60.0	214.644	215.082
	19.29	58.8050	60.0	214.769	215.390
	19.39	62.0000	45.0	215.099	215.548
9	19.69	59.3775	0.0	215.347	215.676
	20.13	59.3775	30.0	215.655	216.907
10	20.94	59.3000	0.0	216.286	216.760
	21.09	59.3000	15.0	216.378	216.907
	21.32	59.3000	30.0	216.682	217.107
	22.10	59.3000	45.0	217.300	217.953
	22.13	59.3775	60.0	217.211	217.953
	23.27	59.3000	60.0	218.480	219.331
11	25.08	59.1000	0.0	220.843	221.540
12	26.71	58.3950	0.0	223.046	223.574
13	27.15	60.3700	0.0	224.144	224.150
	27.30	58.3950	30.0	223.675	224.348
	27.30	60.3700	15.0	223.724	224.348
	27.52	60.3700	30.0	224.206	224.607
	28.20	60.3700	45.0	225.119	225.522
	28.81	58.3950	60.0	226.178	226.317
	29.31	60.3700	60.0	226.742	226.989
14	29.36	62.4490	0.0	227.054	227.075
	29.78	62.4490	30.0	227.791	227.623
15	31.13	60.3300	0.0	229.767	229.523

APPENDIX II

Weighting Function Analysis

Frequency No.	Height of Peak Km	Frequency Gc/sec.	Nadir Angle Deg.	$T_B(3)$ °K	T(h) at W. F. Peak °K
16	31.18	60.4100	0.0	229.912	229.671
	31.59	62.4490	60.0	230.746	230.272
	31.68	60.3300	30.0	230.569	230.425
17	32.20	58.4300	0.0	231.254	231.204
	32.70	58.4300	30.0	232.110	232.014
	33.42	60.3300	60.0	233.764	233.205
	33.49	60.4100	60.0	233.923	231.686
18	33.50	58.3400	0.0	233.717	233.381
	33.89	58.4300	60.0	235.409	234.102
	33.91	58.3400	30.0	234.604	234.102
19	34.33	58.3100	0.0	235.361	234.489
20	34.41	60.3200	0.0	235.499	235.041
21	34.57	62.4230	0.0	235.698	235.429
	34.80	58.3100	30.0	236.276	235.824
	34.88	60.3200	30.0	236.418	236.025
	34.99	62.4230	30.0	236.669	236.228
22	35.01	58.4570	0.0	236.269	236.228
	35.41	58.4570	30.0	237.225	237.059
	35.60	58.3400	60.0	238.023	237.487
	35.71	58.4370	30.0	237.688	237.704
	36.51	58.3100	60.0	239.743	239.518
	36.60	60.3200	60.0	239.941	239.755
23	36.68	62.4780	0.0	239.702	239.994
	36.85	62.4230	60.0	240.317	240.350
	37.29	58.4570	60.0	240.746	241.477
	37.35	62.4780	30.0	240.650	241.600
24	37.52	57.6200	0.0	241.294	241.989
	37.48	58.4370	60.0	241.200	241.989
25	37.82	58.4400	0.0	241.266	242.776
	38.00	57.6200	30.0	242.211	243.311
	39.05	62.4780	60.0	243.944	246.250
26	39.52	59.5850	0.0	244.299	247.616
	40.02	57.6200	60.0	245.099	249.157
	40.02	59.5850	30.0	244.982	249.157
27	40.08	59.1700	0.0	244.791	249.470
	40.61	59.1700	30.0	245.543	251.065
	41.82	62.4900	0.0	245.501	255.033
	41.90	59.5850	60.0	246.452	255.370
	42.36	62.4900	30.0	245.628	256.900
	42.41	59.1700	60.0	246.335	257.062
	44.32	62.4900	60.0	243.700	263.376

The temperature profile used to make the calculations summarized in this Appendix was ATMOSPHERE 1.

The figures corresponding to the preceding tables are Figure II-1 and Figure II-2.

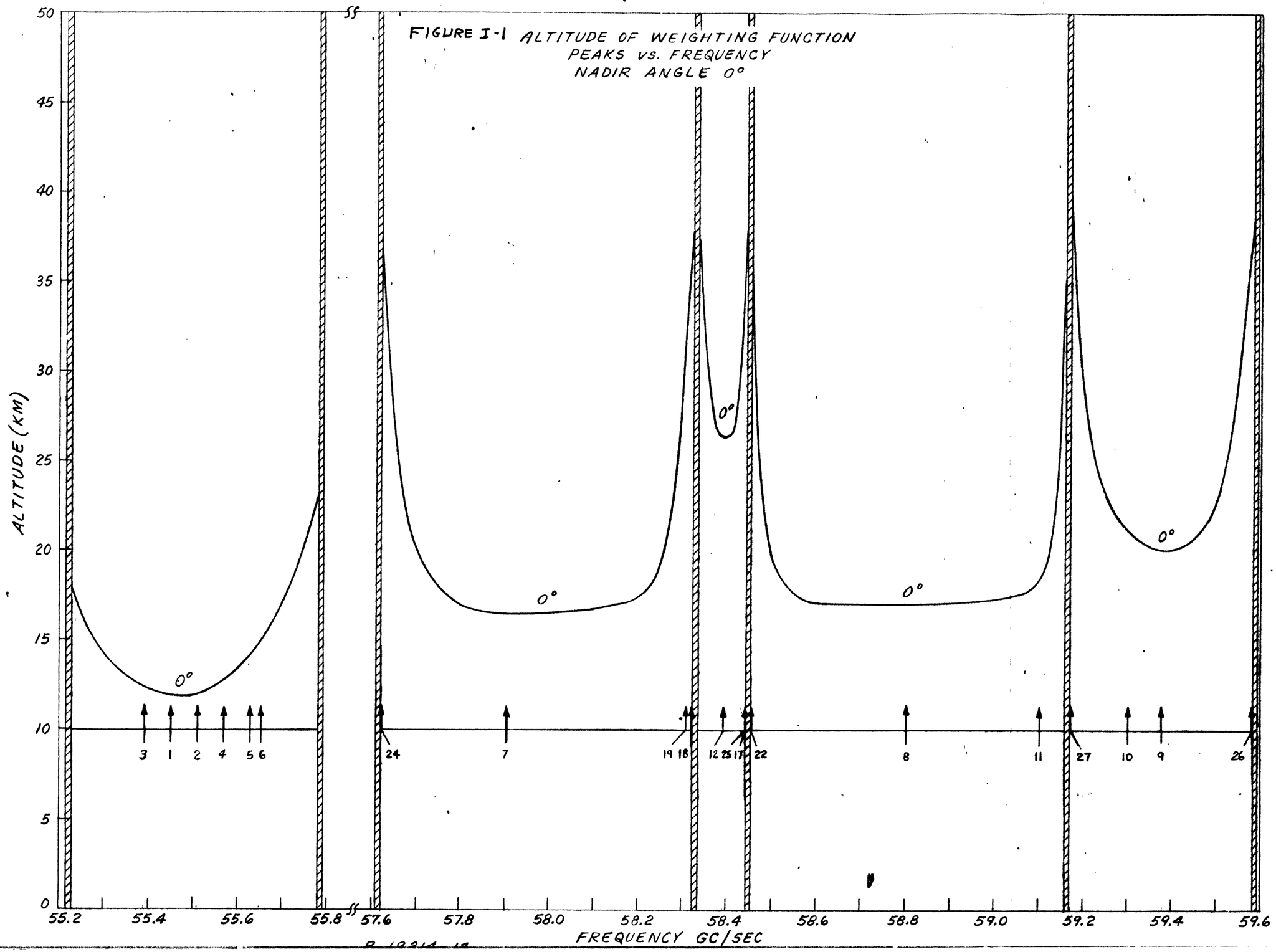

FIGURE I-1 ALTITUDE OF WEIGHTING FUNCTION PEAKS VS. FREQUENCY NADIR ANGLE 0°

FIGURE II-2
ALTITUDE OF WEIGHTING
FUNCTION PEAKS vs. FREQUENCY
NADIR ANGLES 0° AND 60°

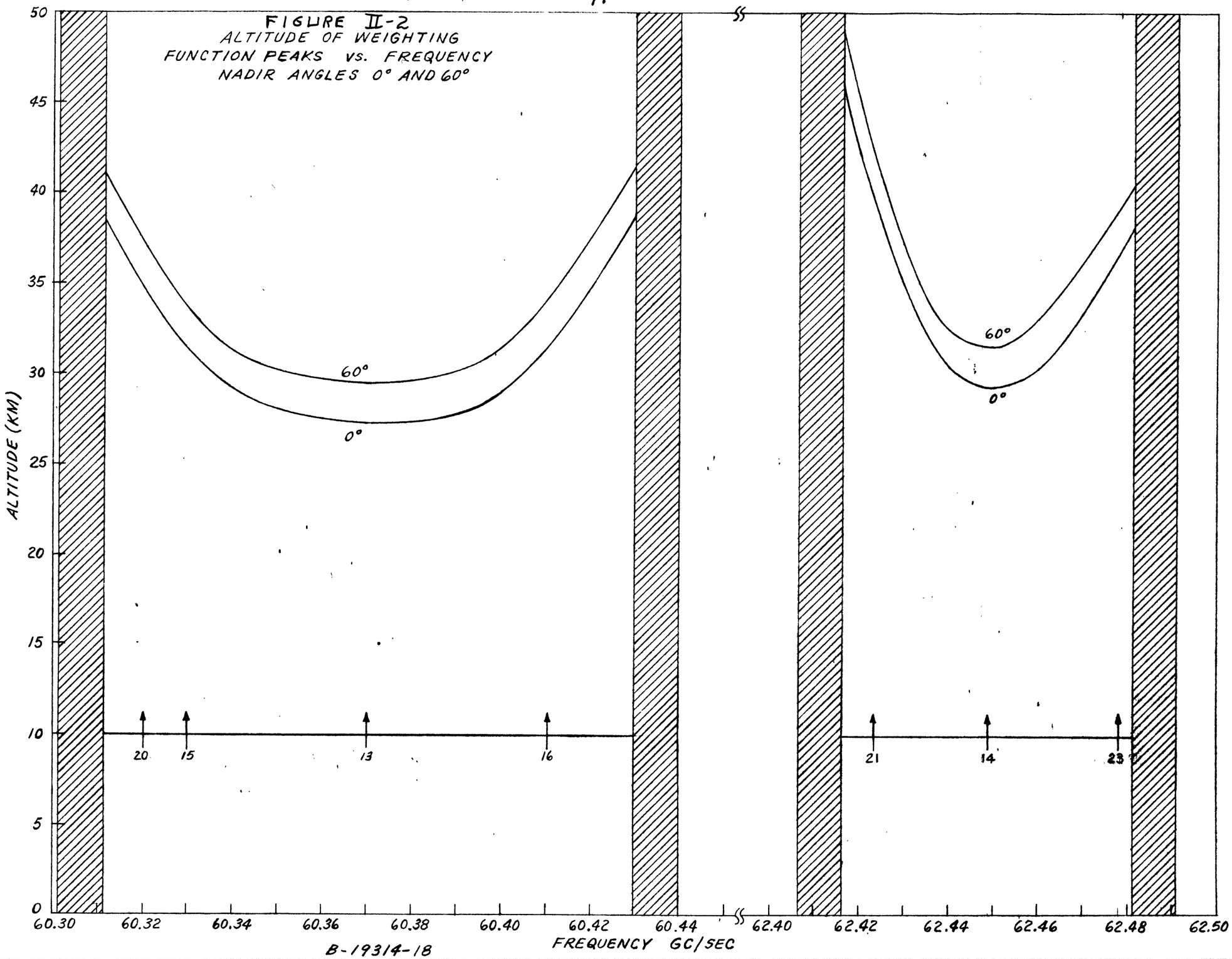

B-19314-18

APPENDIX III

COMPUTER PROGRAMS

This appendix contains the FORTRAN II listings of the principal computer programs used in this work. The computations were done on an IBM 7094 Data Processing System. The plotted output was obtained from a CALCOMP plotter and IBM 1401 Data Processing System.

The comment statements at the very beginning of each program explain the purpose of the program. We have not included programs which differ from the listed programs with respect to the form of the input data and the output results. Likewise, we have not included library or processor subprograms such as the CALCOMP subroutines, since these subprograms were not designed especially for this work.

Below are brief descriptions of the programs listed.

CURVE8 This program fits a polynomial in the sense of least squares to set of kinetic temperature data points. This program was used to obtain ATMOSPHERES 1 through 4.

MISP4 This program computes brightness temperatures and weighting function peak altitudes for a temperature profile represented by a polynomial.

MISP5 This program is the same as MISP4 except for the fact that the temperature profile must be represented by a set of data points.

INVRT1 This program performs the iterative inversion of brightness temperatures.

ATMSP4 This subroutine computes pressure with the hydrostatic equation from a temperature profile represented by a polynomial.

ATMSP5 This subroutine is the same as ATMSP4 except for the fact that the temperature profile must be represented by a set of data points.

KERNL1 This subroutine computes the weighting function for various atmospheric profiles, frequencies and nadir angles.

BTEMP2 This subroutine computes brightness temperatures from the weighting functions determined by KERNL1.

GAMO2E This function routine computes the attenuation coefficient for specified temperatures, pressures and frequency.

```
CATMSP4     B. R. FOW  ID. NO. AAP8 2 AUGUST 1963     SUBROUTINE ATMSP4
C      THIS SUBROUTINE COMPUTES TEMPERATURE AND PRESSURE FOR 1001 HEIGHT
C      LEVELS FROM 0 TO 100 KM.  THE ORDER IN WHICH H(I), T(I), AND P(I)
C      ARE LOADED INTO THE OUTPUT MATRIX IS VARIABLE.
C      THE REQUIRED INPUT DATA IS
C          KD1     THE NUMBER OF POLYNOMIAL COEFFICIENTS NEEDED TO SPECIFY
C                     THE TEMPERATURE PROFILE.  THIS IS ONE MORE THAN THE
C                     DEGREE OF THE POLYNOMIAL.
C          AA(I)   THE COEFFICIENTS OF THE POLYNOMIAL DESCRIBING THE TEMP.
C                  STRUCTURE
C          HMIN    THE MINIMUM HEIGHT FOR WHICH H(I), T(I), AND P(I) ARE
C                  COMPUTED
C          HMAX    THE MAXIMUM HEIGHT FOR WHICH H(I), T(I), AND P(I) ARE
C                  COMPUTED
C          JRD     FOR JRD=1, H(I), T(I), AND P(I) ARE STORED FROM HMIN TO
C                  HMAX.
C                  FOR JRD=2, H(I), T(I), AND P(I) ARE STORED FROM HMAX TO
C                  HMIN.
C          PZERO   GROUND LEVEL PRESSURE IN MM OF HG
C          GZERO   GROUND LEVEL VALUE OF ACCELRATION DUE TO GRAVITY IN CM/
C                  SEC**2
C          VARG    THE RATE OF CHANGE OF GRAVITATIONAL ACCELERATION WITH
C                     ALTITUDE.  THIS NUMBER USUALLY IS 0.3086CM/SEC**2/KM
    1 SUBROUTINE ATMSP4(KD1,AA,HMIN,HMAX,JRD,PZERO,GZERO,VARG)
    5 GGGF(X)=GZERO-(VARG)*(X)
    2 DIMENSION AA(19),J1(1001),H(1001),T(1001),P(1001),GAM(1001),TAU(10
     X01),WAF(1001),I2(1001),HH(1001),TT(1001),PP(1001)
      COMMON T,P,GAM,TAU,WAF,J1,H,JMAX
    3 R=0.28704E+07
    4 PP(1)=PZERO
    6 DO 12 I=1,1001
      I2(I)=I
    7 HH(I)=(FLOATF(I-1))*(0.1)
      TT(I)=AA(1)
      DO 8 M=2,KD1
    8 TT(I)=TT(I)+AA(M)*(HH(I)**(M-1))
   10 IF (I-2) 12,11,11
   11 HS1=HH(I-1)
      HS2=HH(I)
      TS1=TT(I-1)
      TS2=TT(I)
      PP(I)=(PP(I-1))*EXPF((-1.0/((2.0)*R))*(((GGGF(HS1))/(TS1))+((GGGF(
     XHS2))/(TS2)))*(HS2-HS1)*(1.0E+05))
      PS1=PP(I-1)
   12 CONTINUE
   13 KMIN=XINTF((HMIN)*(10.0))+1
   14 KMAX=XINTF((HMAX)*(10.0))+1
   15 JMAX=KMAX+1-KMIN
   16 K2=1001-JMAX
   17 GO TO (18,34),JRD
   18 DO 22 K=KMIN,KMAX
   19 K1=K+1-KMIN
      J1(K1)=K1
   20 H(K1)=HH(K)
   21 T(K1)=TT(K)
   22 P(K1)=PP(K)
   23 IF (K2-1) 41,24,28
   24 H(1001)=1.0
   25 T(1001)=1.0
```

```
26 P(1001)=1.0
   J1(1001)=1001
27 GO TO 41
28 K3=JMAX+1
29 DO 32 K4=K3,1001
   J1(K4)=K4
30 H(K4)=1.0
31 T(K4)=1.0
32 P(K4)=1.0
33 GO TO 41
34 DO 39 K5=1,JMAX
35 K6=KMAX+1-K5
36 H(K5)=HH(K6)
37 T(K5)=TT(K6)
38 P(K5)=PP(K6)
   J1(K5)=K5
39 CONTINUE
40 IF (K2-1) 41,24,28
41 RETURN
   FREQUENCY 10(1,1000,1000),23(1000,1,1000),40(1000,1,1000)
   END
```

```
CATMSP5        B. R. FOW          4 OCTOBER 1963    SUBROUTINE ATMSP5
C      THIS SUBROUTINE COMPUTES TEMPERATURE AND PRESSURE FOR 1001 HEIGHT
C      LEVELS FROM 0 TO 100 KM.  THE ORDER IN WHICH H(I), T(I), AND P(I)
C      ARE LOADED INTO THE OUTPUT MATRIX IS VARIABLE.
C      THE REQUIRED INPUT DATA IS
C          KD1     THE NUMBER OF TEMPERATURE VS HEIGHT DATA POINTS.
C          TD(I)   TEMPERATURE DATA POINT.
C          ZD(I)   CORRESPONDING HEIGHT DATA POINT.
C          HMIN    THE MINIMUM HEIGHT FOR WHICH H(I), T(I), AND P(I) ARE
C                  COMPUTED
C          HMAX    THE MAXIMUM HEIGHT FOR WHICH H(I), T(I), AND P(I) ARE
C                  COMPUTED
C          JRD     FOR JRD=1, H(I), T(I), AND P(I) ARE STORED FROM HMIN TO
C                  HMAX.
C                  FOR JRD=2, H(I), T(I), AND P(I) ARE STORED FROM HMAX TO
C                  HMIN.
C          PZERO   GROUND LEVEL PRESSURE IN MM OF HG
C          GZERO   GROUND LEVEL VALUE OF ACCELRATION DUE TO GRAVITY IN CM/
C                  SEC**2
C          VARG    THE RATE OF CHANGE OF GRAVITATIONAL ACCELERATION WITH
C                     ALTITUDE.  THIS NUMBER USUALLY IS 0.3086CM/SEC**2/KM
    1 SUBROUTINE ATMSP5(KD1,ZD,HMIN,HMAX,JRD,PZERO,GZERO,VARG,TD)
    5 GGGF(X)=GZERO-(VARG)*(X)
    2 DIMENSION ZD(50),J1(1001),H(1001),T(1001),P(1001),GAM(1001),TAU(10
     X01),WAF(1001),I2(1001),HH(1001),TT(1001),PP(1001),TD(50)
      COMMON T,P,GAM,TAU,WAF,J1,H,JMAX
    3 R=0.28704E+07
    4 PP(1)=PZERO
    6 DO  7 I=1,1001
      I2(I)=I
    7 HH(I)=(FLOATF(I-1))*(0.1)
   50 YA=(ZD(2)+ZD(1))/2.0
   51 KZ=YA/0.1
   52 DO 53 J=1,KZ
   53 TT(J)=TD(1)+(((TD(2)-TD(1))/(ZD(2)-ZD(1)))*(HH(J)-ZD(1)))
   54 KDM1=KD1-1
   55 DO 65 K=2,KDM1
   56 YA=(ZD(K+1)+ZD(K))/2.0
   57 MZ=YA/0.1
   58 KZ=KZ+1
   59 TSP=((TD(K+1)-TD(K-1))/(ZD(K+1)-ZD(K-1)))
   60 TDP1=(TD(K+1)-TD(K))/(ZD(K+1)-ZD(K))
   61 TDP2=(TD(K)-TD(K-1))/(ZD(K)-ZD(K-1))
   62 TDP=(2.0*(TDP1-TDP2))/(ZD(K+1)-ZD(K-1))
   63 DO 64 J=KZ,MZ
   64 TT(J)=TD(K)+(TSP*(HH(J)-ZD(K)))+(TDP*((HH(J)-ZD(K))**2)/2.0)
   65 KZ=MZ
   10 DO 12 I=2,MZ
   11 HS1=HH(I-1)
      HS2=HH(I)
      TS1=TT(I-1)
      TS2=TT(I)
      PP(I)=(PP(I-1))*EXPF((-1.0/((2.0)*R))*(((GGGF(HS1))/(TS1))+((GGGF(
     XHS2))/(TS2)))*(HS2-HS1)*(1.0E+05))
      PS1=PP(I-1)
   12 CONTINUE
   13 KMIN=XINTF((HMIN)*(10.0))+1
   14 KMAX=XINTF((HMAX)*(10.0))+1
```

```
15 JMAX=KMAX+1-KMIN
16 K2=1001-JMAX
17 GO TO (18,34),JRD
18 DO 22 K=KMIN,KMAX
19 K1=K+1-KMIN
   J1(K1)=K1
20 H(K1)=HH(K)
21 T(K1)=TT(K)
22 P(K1)=PP(K)
23 IF (K2-1) 41,24,28
24 H(1001)=1.0
25 T(1001)=1.0
26 P(1001)=1.0
   J1(1001)=1001
27 GO TO 41
28 K3=JMAX+1
29 DO 32 K4=K3,1001
   J1(K4)=K4
30 H(K4)=1.0
31 T(K4)=1.0
32 P(K4)=1.0
33 GO TO 41
34 DO 39 K5=1,JMAX
35 K6=KMAX+1-K5
36 H(K5)=HH(K6)
37 T(K5)=TT(K6)
38 P(K5)=PP(K6)
   J1(K5)=K5
39 CONTINUE
40 IF (K2-1) 41,24,28
41 RETURN
   FREQUENCY                    23(1000,1,1000),40(1000,1,1000)
   END
```

```
CBTEMP2   R. R. FOW  I.D.  NO.  AAP8  8 JULY 1963  SUBROUTINE  BTEMP2
C
C          THIS SUBROUTINE COMPUTES THE BRIGHTNESS FOR A SPECIFIED ATMOS
C     PHERE, FREQUENCY AND NADIR OR ZENITH ANGLE.
C
C       INPUT DATA REQUIRED
C             TMS=BRIGHTNESS OF A SOURCE LYING OUTSIDE THE ATMOSPHERE.
C             T=TEMPERATURE IN DEGREES KELVIN.
C             WAF=WEIGHTING FUNCTION.
C             TAU(JMAX)=TOTAL VERTICAL ATTENUATION.
C             THETA=NADIR OR ZEITH ANGLE IN DEGREES.
C            JMAX=THE NUMBER OF LEVELS AT WHICH WAF WAS COMPUTED.
C
C       SUBPROGRAMS REQUIRED
C             ATMSP4 OR ATMSP5 AND KERNL1
C
C       OUTPUT
C             TB=BRIGHTNESS TEMPERATURE IN DEGREES KELVIN.
C
      SUBROUTINE BTEMP2(TMS,TB,THETA)
    2 DIMENSION T(1001),P(1001),GAM(1001),TAU(1001),WAF(1001),J1(1001),H
     2(1001)
      COMMON T,P,GAM,TAU,WAF,J1,H,JMAX
    3 SECTH=1.0/COSF(THETA)
    4 TAUJ=TAU(JMAX)
    5 TB=TMS*EXPF(-TAUJ*SECTH)
      TDUM=TB
    6 DO 11 J=2,JMAX
    7 H1=H(J-1)
    8 H2=H(J)
    9 DELTR=ABSF(H1-H2)
   10 TB=TB+(T(J-1)+T(J))*(WAF(J-1)+WAF(J))*DELTR/4.0
   11 TDM1=TB
   12 RETURN
      END
```

```
CCURVE8
C      CURVE8, A PROGRAM FOR FITTING A POLYNOMIAL FUNCTION TO DATA POINTS
C     XAN INDEPENDENT SET OF DATA POINTS OBTAINED FROM A ROUGH SKETCH OF
C     XTHE FUNCTION AS DETERMINED GRAPHICALLY IS USED TO CHECK THE COMPU-
C     XTED FUNCTION FOR PHYSICALLY UNREASONABLE OSCILLATIONS.
C     XINPUT DATA REQUIRED
C     X  DATA POINTS, TDAT
C     X  DATA POINT POSITIVE UNCERTAINTIES, ERDP
C     X  DATA POINT NEGATIVE UNCERTAINTIES, ERDN
C     X  TEST POINTS, TSTP
C     X  TEST POINT POSITIVE UNCERTAINTIES, ERTP
C     X  TEST POINT NEGATIVE UNCERTAINTIES, ERTN
C     X  NUMBER OF DATA POINTS, IMAX
C     X  NUMBER OF TEST POINTS, JMAX
C     X  DATA IDENTIFICATION NUMBER, IDNT
C     X  MAXIMUM AND MINUMUM TEMPERATURES TO BE PRINTED ON HORIZONTAL AXI
C     X        S OF CALCOMP PLOTTER OUTPUT, TE(2) AND TE(1) RESPECTIVELY.
C     X  MAXIMUM AND MINIMUM ALTITUDES TO BE PRINTED ON VERTICAL AXIS,
C     X        HE(2) AND HE(1) RESPECTIVELY.
C     X  MINIMUM DEGREE POLYNOMIAL DERIVED, KMIN.
C     X  MAXIMUM DEGREE POLYNOMIAL DERIVED, KMAX.
C     X  MINIMUM AND MAXIMUM ALTITUDES AT WHICH THE POLYNOMIAL WILL BE
C     X     EVALUATED, ZMIN AND ZMAX RESPECTIVELY.
C     X  LENGTH OF TEMPERATURE AXIS ON PLOT, XX.
C     X  LENGTH OF ALTITUDE AXIS ON PLOT, YY.
C     X  DATE AND NAME CARD.
C     XSUBROUTINES REQUIRED
C     X      XSIMEQF   THIS SUBPROGRAM IS ON THE SYSTEM TAPE.
C     X      CALCOMP ROUTINES
C     X      SCAIL
      DIMENSION TDAT(50),ERDP(50),ERDN(50),ZD(50),TSTP(25),ERTP(25),ERTN
     X(25),ZT(25),WFD(50),WFT(25),TMPD(50),TMPT(25),DVD(50),DVT(25),TEMP
     X(1001),DTEMP(1001),ALTIT(1001),DATA(750),T(1001),H(1001),FMTR(12),
     XYNMD(3),YNMT(3),       FMT(12),TT(1078),HH(1078),TDA1(50),TST1(25)
     X,ZD1(50),ZT1(25),BB(20,20),CC(20),AA(20),A(20,20),B(20),CBA(20),UW
     XDVD(50),UWDVT(25),TE(2),HE(2)
      EQUIVALENCE(T,TT),(TE,TT(1002)),(TDA1,TT(1004)),(TST1,TT(1054)),(H
     X,HH),(HE,HH(1002)),(ZD1,HH(1004)),(ZT1,HH(1054))
      ASSIGN 951 TO MT
      READ INPUT TAPE 2, 1013,(FMT(I),I=1,12)
 1013 FORMAT (12A6)
      READ INPUT TAPE 2,1011,(TE(I),HE(I),I=1,2)
      WRITEOUTPUTTAPE 3,1011,(TE(I),HE(I),I=1,2)
 1011 FORMAT (4F10.3)
      DO 1 MJ=1004,1078,1
      TT(MJ)=TE(1)
    1 HH(MJ)=HE(2)
      TEX1=TE(1)
      TEX2=TE(2)
      HEX1=HE(1)
      HEX2=HE(2)
      READ INPUT TAPE 2, 1015, ZMIN,ZMAX
      WRITE OUTPUTTAPE3, 1015, ZMIN,ZMAX
 1015 FORMAT(2F15.5)
      READ INPUT TAPE 2,1000,IMAX,JMAX,IDNT,KMAX,KMIN,XX,YY
      WRITEOUTPUTTAPE 3,1000,IMAX,JMAX,IDNT,KMAX,KMIN,XX,YY
 1000 FORMAT(2I5,I15,2I10,2F10.3)
      READ INPUT TAPE 2, 1001, (ZD(I),TDAT(I),ERDP(I),ERDN(I),I=1,IMAX)
```

```
      WRITEOUTPUTTAPE 3, 1001, (ZD(I),TDAT(I),ERDP(I),ERDN(I),I=1,IMAX)
 1001 FORMAT(2(F10.4,F10.2,2F8.2))
      READ INPUT TAPE 2,1002,(ZT(J),TSTP(J),ERTP(J),ERTN(J),J=1,JMAX)
      WRITEOUTPUTTAPE 3,1002,(ZT(J),TSTP(J),ERTP(J),ERTN(J),J=1,JMAX)
 1002 FORMAT(2(F10.4,F10.2,2F8.2))
      CALL PLOTS(DATA(750),750)
    2 KMAX1=KMAX+1
      RDE=0.0
      RTE=0.0
      DO 10 I=1,IMAX
   10 RDE=RDE+(1.0/(ERDP(I)+ERDN(I)))
      DO 13 I=1,IMAX
   13 WFD(I)=(1.0/((ERDP(I)+ERDN(I))*(RDE)))
      DO 16 J=1,JMAX
   16 RTE=RTE+(1.0/(ERTP(J)+ERTN(J)))
      DO 19 J=1,JMAX
   19 WFT(J)=(1.0/((ERTP(J)+FRTN(J))*(RTE)))
      CC(1)=0.0
      DO 211 I=1,IMAX
  211 CC(1)=CC(1)+(WFD(I)*TDAT(I))*(1.0E-15)
      DO 22 M=2,KMAX1
      CC(M)=0.0
      DO 21 I=1,IMAX
   21 CC(M)=CC(M)+(WFD(I)*TDAT(I)*(ZD(I)**(M-1)))*(1.0E-15)
      IF ACCUMULATOR OVERFLOW 100,22
   22 CONTINUE
      DO 26 M=1,KMAX1
      DO 24 N=1,KMAX1
      BB(M,N)=0.0
      DO 23I=1,IMAX
   23 BB(M,N)=BB(M,N)+(WFD(I)*(ZD(I)**(M-1))*(ZD(I)**(N-1)))*(1.0E-15)
      IF ACCUMULATOR OVERFLOW 100,24
   24 CONTINUE
   26 CONTINUE
      GO TO 213
  100 WRITE OUTPUT TAPE 3, 1016,KMAX
 1016 FORMAT(1H1,20X,31HACCUMULATOR OVERFLOW FOR KMAX= ,I2)
      KMAX=KMAX-1
      GO TO 2
  213 BB(1,1)=0.0
      DO 272 I=1,IMAX
  272 BB(1,1)=BB(1,1)+(WFD(I))*(1.0E-15)
  260 WRITE OUTPUT TAPE 3, 1071,IDNT
 1071 FORMAT(1H1,10X,55HTHE AUGMENTED MATRIX OF COEFFICIENTS FOR DATA I.
     X D. NO.,1X,I4,1X,15HIS GIVEN BELOW.//////10X)
      IF (KMAX1 - 9) 261,261,263
  261 DO 262 M=1,KMAX1
      WRITE OUTPUT TAPE 3, 1072, (BB(M,N),N=1,KMAX1),CC(M)
 1072 FORMAT(10X/22X,10E11.4)
  262 CONTINUE
      GO TO 273
  263 DO 264 M=1,KMAX1
      WRITE OUTPUT TAPE 3, 1072, (BB(M,N),N=1,10)
  264 CONTINUE
       WRITE OUTPUT TAPE 3, 1073, IDNT
 1073 FORMAT(1H1,10X,I4/////10X)
      DO 265 M=1,KMAX1
      WRITE OUTPUT TAPE 3, 1074,  (BB(M,N),N=11,KMAX1),CC(M)
 1074 FORMAT(10X/1X,11E11.4)
```

```
  265 CONTINUE
  273 DO 90 K=KMIN,KMAX
      TE(1)=TEX1
      TE(2)=TEX2
      HE(1)=HEX1
      HE(2)=HEX2
      KD=K
      KD1=KD+1
      FID=FLOATF(IDNT)+(0.01)*(FLOATF(KD))
      DO 28 K=1,20
      AA(M)=0.0
   28 CONTINUE
      DO 33 M=1,KD1
      B(M)=CC(M)
      DO 32 N=1,KD1
   32 A(M,N)=BB(M,N)
   33 CONTINUE
      DET=1.0
      M=XSIMEQF(20,KD1,1,A,B,DET,CBA)
      GO TO (36,34,35),M
   34 WRITE OUTPUT TAPE 3,1075,KD
 1075 FORMAT(1H1,77H  ACCUMULATOR UNDERFLOW OR OVERFLOW IN SOLVING THE S
     XYSTEM OF LINEAR EQUATIONS/20X49HFOR THE COEFFICIENTS OF THE POLYNO
     XMIAL OF DEGREE ,I2,2H .)
      GO TO 90
   35 WRITE OUTPUT TAPE 3,1076,KD
 1076 FORMAT(1H1,102HTHE COEFFICIENT MATRIX OF THE LINEAR EQUATIONS INVO
     XLVING THE COEFFICIENTS OF THE POLYNOMIAL OF DEGREE ,I2/30X,12HIS S
     XINGULAR.)
      GO TO 90
   36 DO 47 M=1,KD1
   47 AA(M)=A(M,1)
  274 DVTSQ=0.0
      DVDSQ=0.0
      DO 70 J=1,JMAX
      TMPT(J)=AA(1)
      DO 69 M=2,KD1
   69 TMPT(J)=TMPT(J)+(AA(M))*((ZT(J))**(M-1))
      UWDVT(J)=(TMPT(J)-TSTP(J))
      DVT(J)=UWDVT(J)*WFT(J)
   70 DVTSQ=DVTSQ+(DVT(J))**2
      DO 72 I=1,IMAX
      TMPD(I)=AA(1)
      DO 71 M=2,KD1
   71 TMPD(I)=TMPD(I)+(AA(M))*((ZD(I))**(M-1))
      UWDVD(I)=(TMPD(I)-TDAT(I))
      DVD(I)=UWDVD(I)*WFD(I)
   72 DVDSQ=DVDSQ+(DVD(I))**2
  147 DELTAH=((ZMAX-ZMIN)/1000.0)
      ALTIT(1)=ZMIN
      DO2789NON=2,1001
 2789 ALTIT(NON)=ALTIT(NON-1)+DELTAH
      DO 78 NON=1,1001
  177 TEMP(NON)=AA(1)+(AA(2))*(ALTIT(NON))
      DTEMP(NON)=AA(2)
      DO 77 M=3,KD1
      TEMP(NON)=TEMP(NON)+(AA(M))*((ALTIT(NON))**(M-1))
      MM1=M-1
      AMM1=FLOATF(MM1)
```

```
   77 DTEMP(NON)=DTEMP(NON)+(AMM1)*(AA(M))*((ALTIT(NON))**(M-2))
  178 IF(TEMP(NON)-TEX1) 179,180,180
  179 TEMP(NON)=TEX1
      GO TO 182
  180 IF(TEX2-TEMP(NON)) 181,182,182
  181 TEMP(NON)=TEX2
  182 CONTINUE
   78 CONTINUE
      NP=1
      NOP=KD
   79 WRITE OUTPUT TAPE 3,1004,NOP,NP
 1004 FORMAT(1H1,108X,5HPAGE ,I2,1H-,I1//)
      WRITE OUTPUT TAPE 3,1019,(FMT(I),I=1,12),FID
 1019 FORMAT(20X,12A6,2X,F7.2///)
  791 WRITE OUTPUT TAPE 3,1014,KD
 1014 FORMAT(1H0,7X,85HSUCCESSIVE POLYNOMIAL CURVE FITTING ROUTINE FOR A
     XTMOSPHERIC VERTICAL TEMPERATURE DATA///5X,16HPROGRAM NO   008///5X
     X,23HDEGREE OF POLYNOMIAL   I2///5X,26HCOEFFICIENTS OF POLYNOMIAL/)
      DO 801 K=1,KD1
      KS=K-1
      WRITE OUTPUT TAPE 3,1005,(KS,AA(K))
 1005 FORMAT(5X/10X,2HA(,I2,4H) = ,E14.5)
  801 CONTINUE
      NP=2
   80 WRITE OUTPUT TAPE 3,1050,NOP,NP
 1050 FORMAT(1H1,108X,5HPAGE ,I2,1H-,I1////5X,19HTEST POINT ANALYSIS///1
     X1X,8HALTITUDE,
     X8X,18HWEIGHTING FUNCTION,8X,11HTEMPERATURE,8X,11HTEMPERATURE,13X,1
     X0HDEVIATIONS/54X,8H(SKETCH),10X,10H(COMPUTED),8X,10HUNWEIGHTED,8X,
     X8HWEIGHTED/14X,2HKM,40X,5HDEG K,14X,5HDEG K,12X,5HDEG K,12X,5HDEG
     XK)
   81 WRITE OUTPUT TAPE 3,1006,(ZT(J),WFT(J),TSTP(J),TMPT(J),UWDVT(J),DV
     XT(J),J=1,JMAX)
 1006 FORMAT(12X,F6.2,12X,E12.5,12X,F7.2,12X,F7.2,10X,F7.2,11X,F7.3)
   82 WRITE OUTPUT TAPE 3,1007,DVTSQ
 1007 FORMAT(5X//15X,47HSUM OF THE SQUARES OF THE WEIGHTED DEVIATIONS =,
     XE12.5)
      NP=3
   83 WRITE OUTPUT TAPE 3,1008,(NOP,NP,(ZD(I),WFD(I),TDAT(I),TMPD(I),UWD
     XVD(I),DVD(I),I=1,IMAX))
 1008 FORMAT(1H1,111X,5HPAGE ,I2,1H-,I1/5X,19HDATA POINT ANALYSIS///11X,
     X8HALTITUDE,8X,18HWEIGHTING FUNCTION,8X,11HTEMPERATURE,8X,11HTEMPER
     XATURE,13X,10HDEVIATIONS/54X,8H(SKETCH),10X,10H(COMPUTED),7X,10HUNW
     XEIGHTED,8X,8HWEIGHTED/14X,2HKM,40X,5HDEG K,14X,5HDEG K,12X,5HDEG K
     X,12X,5HDEG K/(12X,F6.2,12X,E12.5,12X,F7.2,12X,F7.2,10X,F7.2,11X,F7
     X.3))
   84 WRITE OUTPUT TAPE 3,1009,DVDSQ
 1009 FORMAT(5X//15X,47HSUM OF THE SQUARES OF THE WEIGHTED DEVIATIONS =E
     X12.5)
      NP=4
   85 WRITE OUTPUT TAPE 3,1010,(NOP,NP,(ALTIT(NON),TEMP(NON),DTEMP(NON),
     XNON=1,1001,10))
 1010 FORMAT(1H1,111X,5HPAGE ,I2,1H-,I1/5X,28HCOMPUTED TEMPERATURE PROFI
     XLE///7X,8HALTITUDE,8X,11HTEMPERATURE,8X,12HDERIV. TEMP.,14X,8HALTI
     XTUDE,8X,11HTEMPERATURE,8X,12HDERIV. TEMP./10X,2HKM,14X,5HDEG K,12X
     X,8HDEG K/KM,19X,2HKM,15X,5HDEG K,12X,8HDEG K/KM,2X/(8X,F6.2,11X,F7
     X.2,10X,E12.5,15X,F6.2,11X,F7.2,10X,E12.5))
      DO 87 I=1,1001
      H(I)=ALTIT(I)
```

```
 87 T(I)=TEMP(I)
    DT=((TE(2)-TE(1))/(XX))*10.0
    DH=((HE(2)-HE(1))/(YY))*10.0
    DTT=DT
    DHH=DH
    DO 88 I=1,IMAX
    TDA1(I)=TDAT(I)
 88 ZD1(I)=ZD(I)
    DO 89 J=1,JMAX
    TST1(J)=TSTP(J)
 89 ZT1(J)=ZT(J)
    IF(JMAX - 25) 880,882,882
880 JM1=JMAX+1
    DO 881 J=JM1,25
    ZT1(J)=HEX1
881 TST1(J)=TEX1
882 CONTINUE
    IF(IMAX-50) 883,885,885
883 IM1=IMAX+1
     DO 884 I=IM1,50
    ZD1(I)=HEX1
884 TDA1(I)=TEX1
885 CONTINUE
    CALL SCAIL(TT,1078,XX,TTMIN,DTT)
    CALL SCAIL(HH,1078,YY,HHMIN,DHH)
    CALL LINE(T,H,1001)
    CALL AXIS(0.0,0.0,19HTEMPERATURE (DEG K),19,XX,0.0,TTMIN,DTT)
    CALL AXIS(0.0,0.0,13HALTITUDE (KM),13,YY,90.0,HHMIN,DHH)
    ALPHA=((TE(2)-TE(1))/XX)
    BETA=((HE(2)-HE(1))/YY)
    XCORA=-0.2*ALPHA*0.859*0.2
    XCORP=-0.45*ALPHA*0.859*0.1
    YCORP=-0.5*BETA*0.10
    DO 93 I=1,IMAX
    TDP=TDA1(I)+XCORA
861 ZDP=ZD1(I)
 93 CALL SYMBL4(TDP,ZDP,0.2,1H*,0.0,1)
    DO 95 J=1,JMAX
    TSP=TST1(J)+XCORP
931 ZST=ZT1(J)+YCORP
 95 CALL SYMBL4(TSP,ZST,0.10,1H+,0.0,1)
    CALL PLOT(-1.5,-1.0,-3)
    CALL PLOT(17.0,0.0,2)
    CALL PLOT(17.0,11.5,2)
    CALL PLOT(0.0,11.5,2)
    CALL PLOT(0.0,0.0,2)
    CALL PLOT(2.5,0.1,-3)
    DO 932 I=1,12
    IR=13-I
932 FMTR(IR)=FMT(I)
    CALL SYMBL4(0.0,0.0,0.2,FMTR(12),0.0,72)
    CALL PLOT(12.25,0.0,-3)
    CALL NUMBER(0.0,0.0,0.2,FID,0.0,2)
    CALL PLOT(-12.75,1.0,-3)
933 YNMD(1)=1HS
    YNMD(2)=6H POINT
    YNMD(3)=6H* DATA
    CALL SYMBL4(0.0,0.0,0.2,YNMD(3),0.0,13)
    CALL PLOT(0.0,0.3,-3)
```

```
      YNMT(1)=1HS
      YNMT(2)=6H POINT
      YNMT(3)=6H+ TEST
      CALL SYMBL4(0.0,0.0,0.2,YNMT(3),0.0,13)
      GO TO MT,(951,952)
  951 ASSIGN 952 TO MT
      CALL PLOT(-0.5,11.1,-3)
      GO TO 954
  952 ASSIGN 951 TO MT
      CALL PLOT(16.5,-11.9,-3)
  954 CONTINUE
      WRITE OUTPUT TAPE 14,2000,KD1
 2000 FORMAT(I5)
      WRITE OUTPUT TAPE 14,2001,(AA(I),I=1,KD1)
 2001 FORMAT(E14.5)
   90 CONTINUE
      FREQUENCY 178(1,1000,1000),180(1,1000,1000)
      CALL EXIT
      END
```

```
CGAMO2E          9 JANUARY 1963 FROM  M. L. MEEKS GAMO2  1962.
C     XFUNCTION GAMO2(T,P,F)      THIS SUBPROGRAM COMPUTES THE ATTENUATION
C     XDUE TO ATMOSPHERIC O2 IN NEPERS/KM FOR A SPECIFIED TEMPERATURE T
C     XIN DEGREES KELVIN,PRESSURE P IN MM OF HG, AND FREQUENCY F IN GC/S.
      FUNCTION GAMO2(T,P,F)
      DIMENSION FK(13),FL(13),EXPW(13)
  300 IF(ITEM-12345) 1,2,1
    1 ITEM = 12345
            ALPHA  = 0.00195
            C1 = 0.61576
            C2 = 2.0684
            C3 = 0.85
            C4 = 300.0
                  FK(1) = 56.2648
                  FK(2) = 58.4466
                  FK(3) = 59.5910
                  FK(4) = 60.4348
                  FK(5) = 61.1506
                  FK(6) = 61.8002
                  FK(7) = 62.4112
                  FK(8) = 62.9980
                  FK(9) = 63.5685
                  FK(10) = 64.1272
                  FK(11) = 64.6779
                  FK(12) = 65.2240
                  FK(13) = 65.7626
            FL(1) = 118.7505
            FL(2) = 62.4863
            FL(3) = 60.3061
            FL(4) = 59.1642
            FL(5) = 58.3239
            FL(6) = 57.6125
            FL(7) = 56.9682
            FL(8) = 56.3634
            FL(9) = 55.7839
            FL(10) =55.2214
            FL(11) =54.6728
            FL(12) =54.1294
            FL(13) =53.5960
    2 IF(P-267.41) 3,4,4
    3 IF(P-18.957) 41,41,42
    4 BETA = 0.25
      GO TO 50
   41 BETA = 0.75
      GO TO 50
   42 BETA = 0.25*(1.0+LOGF(267.41/P)/1.323)
   50 DELT = ALPHA*P*((C4/T)**C3)*(0.2095+0.7809*BETA)
    5 DO 6 I=1,13
    6         EXPW(I) = EXPF(-C2*FLOATF(4*I*I-2*I)/T)
      DELT2 = DELT*DELT
      F2 = F*F
      FZERO = DELT/(F2+DELT2)
      FACTOR = (C1*P*F2)/(T*T*T)
      SUM = 0.0
    7 DO 12 J=1,13
            TSUM = 0.0
            FDIF = FK(J)-F
            TEST = ABSF(FDIF)/DELT
```

```
100         IF(TEST-10000.0) 8,9,9
  8         FDIF2 = FDIF*FDIF
            FADD2 = (FK(J)+F)*(FK(J)+F)
            FNPLUS =DELT*(1.0/(FDIF2+DELT2)+1.0/(FADD2+DELT2))
            UNPLUS = FLOATF((2*J-1)*(4*J+1))/FLOATF(2*J)
            TSUM = FNPLUS*UNPLUS
  9         FDIF = FL(J)-F
            TEST = ABSF(FDIF)/DELT
200         IF(TEST-100.0) 10,11,11
 10         FDIF2 = FDIF*FDIF
            FADD2 = (FL(J)+F)*(FL(J)+F)
            FNMINU = DELT*(1.0/(FDIF2+DELT2)+1.0/(FADD2+DELT2))
            UNMINU = FLOATF(2*J*(4*J-3))/FLOATF(2*J-1)
            TSUM = TSUM+FNMINU*UNMINU
 11         UNZERO = FLOATF((4*J*J-2*J+1)*(4*J-1))/FLOATF(J*(2*J-1))
            TSUM = TSUM+FZERO*UNZERO
            SUM = SUM+TSUM*EXPW(J)
 12         CONTINUE
      GAMO2 = FACTOR*SUM
      FREQUENCY 100(250,1,10),200(250,1,10),300(250,1,1)
      RETURN
      END
```

```
CINVRT1    B. R. FOW    ID NO. AAP8       PROGRAM INVRT1    6 AUGUST 1963
C
C          THIS PROGRAM FINDS THE POLYNOMIAL COEFFICIENTS OF A KINETIC
C       TEMPERATURE PROFILE CORRESPONDING TO A SET OF BRIGHTNESS TEMPERA-
C       TURE VS. FREQUENCY AND NADIR ANGLE READINGS.
C
C          INPUT DATA REQUIRED
C
C            NAME, DATE AND ID CARD
C            KD1=THE NUMBER OF POLYNOMIAL COEFFICIENTS SPECIFYING THE IN-
C                 ITIAL GUESS TEMPERATURE PROFILE.
C            KD2=THE NUMBER OF BRIGHTNESS TEMPERATURE VS. FREQUENCY AND
C                 NADIR ANGLE POINTS.
C            HMIN=THE MINIMUM HEIGHT OF INITIAL AND DERIVED TEMPERATURE
C                 PROFILES, KM.
C            HMAX=THE MAXIMUM HEIGHT OF INITIAL AND DERIVED TEMPERATURE
C                 PROFILES, KM.
C            JRD=SENSE OF RADIOMETER OR ANTENNA.
C                   JRD=1, SENSE IS UP FROM HMIN TO HMAX.
C                   JRD=2, SENSE IS DOWN FROM HMAX TO HMIN.
C            PZERO=GROUND LEVEL VALUE OF PRESSURE, MM OF HG.
C            GZERO=GROUND LEVEL VALUE OF GRAVITATIONAL ACCELERATION,
C                   CM/SEC**2.
C            VARG=RATE OF CHANGE WITH HEIGHT OF GRAVITATIONAL ACCELERA-
C                   TION, CM/SEC**2/KM.
C            TMS=BRIGHTNESS TEMPERATURE OF SOUCE LYING OUTSIDE THE ATMOS-
C                   PHERE, DEG K.
C            YH=LENGTH OF HEIGHT AXIS ON PLOTTED OUTPUT, INCHES.
C            YT=LENGTH OF TEMPERATURE AXIS ON PLOTTED OUTPUT, INCHES.
C            TE(1) AND TE(2)=EXTREME VALUES OF TEMPERATURE AXIS, DEG K.
C            HE(1) AND HE(2)=EXTREME VALUES OF HEIGHT AXIS, KM.
C            IP=THE NUMBER OF ALTITUDE LEVELS BETWEEN PRINTOUTS OF TEMP.
C            AI=THE INITIAL TEMPERATURE PROFILE COEFFICIENTS.
C            TB=INPUT BRIGHTNESS TEMPERATURES, DEG K.
C            FI=INPUT FREQUENCIES, GC/SEC.
C            ZA=INPUT NADIR ANGLES, DEG.
C            IM=MAXIMUM NUMBER OF ITERATIONS.
C            DSM=CRITERION FOR STOPPING ITERATIONS.
C            TMIN=LOWER BOUNDARY CONDITION ON T(H).
C            TMAX=UPPER BOUNDARY CONDITION ON T(H).
C
C          OUTPUT DATA
C
C            A=COFFFICIENTS OF POLYNOMIAL
C            ITC=NUMBER OF ITERATION
C            J1=LEVEL NUMBER
C            H=HEIGHT
C            T=TEMPERATURE
C            DT=DEVIATION OF TEMPERATURE AT J1 FROM THE PREVIOUSLY PRE-
C                DICTED TEMPERATURE AT J1.
C            P=PRESSURE
C            SSDT=SUM OF THE SQUARES OF THE DEVIATIONS.
C            DP=DEVIATION OF PRESSURE AT J1 FROM THE PREVIOUSLY PREDICTED
C                PRESSURE AT J1.
C
C          SUBPROGRAMS REQUIRED-  ATMSP4, KERNL1, GAMO2, CALCOMP.
C
      DIMENSION RATA(800),AR(12),TE(2),HE(2),AI(21),TB(21),FI(21),ZA(21)
```

```
     1,B(21,21),T(1001),P(1001),GAM(1001),TAU(1001),WAF(1001),J1(1001),H
     2(1001),CBA(21),A(21),J2(1001),H2(1001),T2(1001),P2(1001),DT(1001),
     3DP(1001),ARR(12),HH2(1003),TT2(1003),TBR(21),H3(1001)
      COMMON T,P,GAM,TAU,WAF,J1,H,JMAX
      FREQUENCY 350(10,1,1),580(1,5,100),610(1,5,100),730(20,2,1),750(20
     1,1,2)
      EQUIVALENCE (H2,HH2),(T2,TT2)
      CALL PLOTS(BATA(800),800)
   10 READ INPUT TAPE 2,1010,(AR(I),I=1,12)
   20 READ INPUT TAPE 2,1020,KD1,KD2,JRD,IP,INI,IM,YH,YT,DSM,TMS
   30 READ INPUT TAPE 2,1030,HMIN,HMAX,PZERO,GZERO,VARG
   40 READ INPUT TAPE 2,1040,(TE(I),HE(I),I=1,2),TMIN,TMAX
   50 READ INPUT TAPE 2,1050,(AI(I),I=1,KD1)
   60 READ INPUT TAPE 2,1060,(TB(I),FI(I),ZA(I),I=1,KD2)
   70 WRITE OUTPUT TAPE 3,1010,(AR(I),I=1,12)
   80 WRITE OUTPUT TAPE 3,1020,KD1,KD2,JRD,IP,INI,IM,YH,YT,DSM,TMS
   90 WRITE OUTPUT TAPE 3,1030,HMIN,HMAX,PZERO,GZERO,VARG
  100 WRITE OUTPUT TAPE 3,1040,(TE(I),HE(I),I=1,2),TMIN,TMAX
  110 WRITE OUTPUT TAPE 3,1050,(AI(I),I=1,KD1)
  120 WRITE OUTPUT TAPE 3,1060,(TB(I),FI(I),ZA(I),I=1,KD2)
  128 KD3=KD2+1
  129 KD4=KD2+2
  130 CALL ATMSP4(KD1,AI,HMIN,HMAX,JRD,PZERO,GZERO,VARG)
  131 JMX2=JMAX
  132 DO 136 K=1,JMX2
  133 J2(K)=J1(K)
      H3(K)=H(K)
  134 H2(K)=H(K)
  135 T2(K)=T(K)
  136 P2(K)=P(K)
  137 WRITE OUTPUT TAPE 3,2000,(AR(I),I=1,12)
  138 WRITE OUTPUT TAPE 3,2010,(J2(I),H2(I),T2(I),P2(I),I=1,JMAX,IP)
  139 DO 142 K=1,2
  140 JMPK=JMAX+K
  141 HH2(JMPK)=HE(K)
  142 TT2(JMPK)=TE(K)
  143 CALL SCALE(HH2,JMPK,YH,HH2M,DHH2)
  144 CALL SCALE(TT2,JMPK,YT,TT2M,DTT2)
  145 CALL AXIS(0.0,0.0,10HHEIGHT, KM,10,YH,90.0,HH2M,DHH2)
  146 CALL AXIS(0.0,0.0,18HTEMPERATURE, DEG K,18,YT,0.0,TT2M,DTT2)
  147 CALL LINE(T2,H2,JMAX)
  148 XS=T2(5)-0.4
  149 YS=H2(5)
  150 CALL SYMBL4(XS,YS,0.2,5HINPUT,0.0,5)
  151 DO 153 I=1,12
  152 IR=13-I
  153 ARR(IR)=AR(I)
  154 CALL PLOT(2.0,-0.9,-3)
  155 CALL SYMBL4(0.0,0.0,0.2,ARR(12),0.0,72)
  156 CALL PLOT(-3.5,-0.1,-3)
  157 CALL PLOT(17.0,0.0,2)
  158 CALL PLOT(17.0,11.5,2)
  159 CALL PLOT(0.0,11.5,2)
  160 CALL PLOT(0.0,0.0,2)
  161 CALL PLOT(1.5,1.0,-3)
  162 DO 163 J=1,JMX2
  163 T2(J)=T(J)
  164 ITC=ITC+1
  165 DO 320 I=1,KD2
```

```
166 F=FI(I)
170 A=ZA(I)*0.0174533
171 JMAX=JMX2
172 DO 176 M=1,JMAX
173 J1(M)=J2(M)
174 H(M)=H3(M)
175 T(M)=T2(M)
176 P(M)=P2(M)
180 CALL KERNL1(F,A)
181 JMAX=JMAX
190 SEC=1.0/COSF(A)
200 TAK=TAU(JMAX)
210 TS=TMS*EXPF(-TAK*SEC)
220 TBR(I)=TB(I)-TS
230 DO 310 J=1,KD4
240 DO 300 K=2,JMAX
250 HA=H(K-1)
260 HB=H(K)
270 DELTR=ABSF(HA-HB)
280 AVH=(HA+HB)/2.0
290 AVWF=(WAF(K)+WAF(K-1))/2.0
300 B(I,J)=B(I,J)+((AVH**(J-1))*(AVWF)*(DELTR))
310 CONTINUE
320 CONTINUE
321 DO 323 J=2,KD4
322 B(KD3,J)=(HMIN**(J-1))
323 B(KD4,J)=(HMAX**(J-1))
324 B(KD3,1)=1.0
325 B(KD4,1)=1.0
326 TBR(KD3)=TMIN
327 TBR(KD4)=TMAX
330 DET=1.0
    WRITE OUTPUT TAPE 3,9999,KD4,((B(I,J),J=1,KD4),I=1,KD4),(TBR(I),I=
   11,KD4)
340 M=XSIMEQF(21,KD4,1,B,TBR,DET,CRA)
    WRITE OUTPUT TAPE 3,9998,M,KD4,((B(I,J),J=1,KD4),I=1,KD4),(A(I),I=
   11,KD4)
350 GO TO (400,360,380),M
360 WRITE OUTPUT TAPE 3,2020,ITC
370 GO TO 970
380 WRITE OUTPUT TAPE 3,2030,ITC
390 GO TO 970
400 DO 410 I=1,KD4
410 A(I)=B(I,1)
420 CALL ATMSP4(KD4,A,HMIN,HMAX,JRD,PZERO,GZERO,VARG)
429 AJM=FLOATF(JMAX)
430 DO 480 K=1,JMAX
440 DT(K)=T(K)-T2(K)
450 DP(K)=P(K)-P2(K)
460 T2(K)=T(K)
470 P2(K)=P(K)
480 SSDT=SSDT+(DT(K)**2)/AJM
490 WRITE OUTPUT TAPE 3,2040,ITC,ITC
500 DO 520 J=1,KD4
510 KK=J-1
520 WRITE OUTPUT TAPE 3,2050,KK,A(J)
530 WRITE OUTPUT TAPE 3,2060,SSDT,(J1(I),H(I),T(I),DT(I),P(I),DP(I),I=
   11,JMAX,IP)
540 DO 560 K=1,2
```

```
550 JMPK=JMAX+K
560 TT2(JMPK)=TE(K)
570 DO 630 J=1,JMAX
580 IF(T2(J)-TE(1))590,610,610
590 T2(J)=TE(1)
600 GO TO 630
610 IF(TE(2)-T2(J))620,630,630
620 T2(J)=TE(2)
630 CONTINUE
640 CALL SCALE(TT2,JMPK,YT,TT2M,DTT2)
650 CALL LINE(T2,H2,JMAX)
660 KSCB=20*(ITC+1)
670 FITC=FLOATF(ITC)
680 XS=T2(KSCB)
690 YS=H2(KSCB)
700 CALL NUMBER(XS,YS,0.1,FITC,0.0,1)
710 DO 720 K=1,JMAX
720 T2(K)=T(K)
721 DO 724 I=1,21
722 DO 723 J=1,21
723 B(I,J)=0.0
724 TBR(I)=0.0
730 IF (DSM-SSDT) 731,750,750
731 SSDT=0.0
740 IF(ITC-IM)164,750,750
750 CALL PLOT(0.0,11.5,-3)
760 DO 780 K=1,2
770 JMPK=JMAX+K
780 TT2(JMPK)=TE(K)
790 CALL SCALE(TT2,JMPK,YT,TT2M,DTT2)
810 CALL AXIS(0.0,0.0,10HHEIGHT, KM,10,YH,90.0,HH2M,DHH2)
800 CALL AXIS(0.0,0.0,18HTEMPERATURE, DEG K,18,YT,0.0,TT2M,DTT2)
820 CALL LINE(T2,H2,JMAX)
830 XS=T2(5)-0.4
840 YS=H2(5)
850 CALL SYMBL4(XS,YS,0.2,5HFINAL,0.0,5)
860 XS=T2(20)
870 YS=H2(20)
880 CALL NUMBER(XS,YS,0.2,FITC,0.0,1)
890 CALL PLOT(2.0,-0.9,-3)
900 CALL SYMBL4(0.0,0.0,0.2,ARR(12),0.0,72)
910 CALL PLOT(-3.5,-0.1,-3)
920 CALL PLOT(17.0,0.0,2)
930 CALL PLOT(17.0,11.5,2)
940 CALL PLOT(0.0,11.5,2)
950 CALL PLOT(0.0,0.0,2)
960 CALL PLOT(0.0,0.0,3)
970 CALL EXIT
1010 FORMAT(12A6)
1020 FORMAT(6I5,4F10.3)
1030 FORMAT(5F10.3)
1040 FORMAT(6F10.3)
1050 FORMAT(4E18.6)
1060 FORMAT(6F10.5)
2000 FORMAT(1H1,28X,12A6,24X,6HPAGE 0)
2010 FORMAT(10X////5X,2HNO,3X,6HHEIGHT,5X,4HTEMP,8X,8HPRESSURE, 8X,2HNO
     1,3X,6HHEIGHT,5X,4HTEMP,8X,8HPRESSURE, 8X,2HNO,3X,6HHEIGHT,5X,4HTEM
     2P,8X,8HPRESSURE//(2X,I4,3X,F5.1,4X,F7.3,4X,E12.5,6X,I4,3X,F5.1,4X,
     3F7.3,4X,E12.5,6X,I4,3X,F5.1,4X,F7.3,4X,E12.5))
```

```
2020 FORMAT(1H1,10X,56HACCUMULATOR OVERFLOW OR UNDERFLOW IN XSIMEQF DUR
    1ING THE ,I2,1X,10HITERATION.)
2030 FORMAT(1H1,10X,16HMATRIX B IN THE ,I2,1X,22HITERATION IS SINGULAR.
    1)
2040 FORMAT(1H1,10X,17HITERATION NUMBER ,I2,95X,4HPAGE,I2////11X,40HTEM
    1PERATURE POLYNOMIAL COEFFICIENTS ARE-)
2050 FORMAT(15X,2HA(,I2,3H)= ,E14.7//)
2060 FORMAT(4X,114HSUM OF THE SQUARES OF DEVIATIONS OF TEMPERATURES DET
    1ERMINED IN THIS ITERATION FROM THOSE DETERMINED IN THE LAST = ,E12
    2.5///2X,5HLEVEL,2X,6HHEIGHT,3X,5HTEMP.,3X,7HDELTA T,5X,8HPRESSURE,
    37X,11HDELTA PRES.,4X,5HLEVEL,2X,6HHEIGHT,3X,5HTEMP.,3X,7HDELTA T,5
    4X,8HPRESSURE,7X,11HDELTA PRES.///(1X,I4,3X,F5.1,3X,F7.3,3X,F6.2,3X
    5,E12.5,4X,E12.5,4X,I4,3X,F5.1,3X,F7.3,3X,F6.2,3X,E12.5,4X,E12.5))
9998 FORMAT(5X////2I5/(1X,7E15.8))
9999 FORMAT(I5/(1X,7E15.8))
     END
```

```
CKERNL1   R. R. FOW  ID. NO. AAP8  31 JULY 1963   SUBROUTINE KERNL1
C
C          THIS SUBROUTINE COMPUTES THE O2 ATMOSPHERIC ABSORPTION WEIGHT-
C        ING FUNCTION, ZENITH OPACITY, AND ATTENUATION COEFFICIENT.
C
C       INPUT DATA REQUIRED
C            F=FRQUENCY IN GC/SEC
C            J1=HEIGHT LEVEL NO.
C            H=HEIGHT IN KM.
C            T=TEMPERATURE IN DEGREES KELVIN
C            P=PRESSURE IN MM OF HG
C            JMAX=THE NUMBER OF LEVELS AT WHICH  T AND P HAVE BEEN COM-
C                 PUTED.
C            THETA=NADIR OR ZENITH ANGLE IN RADIANS.
C
C       OUTPUT
C            GAM=ATTENUATION COEFFICIENT IN NEPERS/KM.
C            TAU=ZENITH OPACITY IN NEPERS.
C            WAF=WEIGHTING FUNCTION.
C            JMAX=THE NUMBER OF LEVELS AT WHICH WAF WAS COMPUTED.
C            THE FIRST JMAX LOCATIONS IN THE J1, H, T, AND P MATRICES ARE
C                 REPLACED BY THE THE J1, H, T, AND P CORRESPONDING TO
C                 THE LEVELS AT WHICH WAF WAS COMPUTED.
C
C       SUBPROGRAMS REQUIRED
C            ATMSP4 OR ATMSP5 AND KERNL1
C         LEVEL JC REFERS TO THE LAST LEVEL AT WHICH WAF WAS COMPUTED.
C
      SUBROUTINE KERNL1(F,THETA)
      DIMENSION T(1001),P(1001),GAM(1001),TAU(1001),WAF(1001),J1(1001),H
     1(1001)
      COMMON T,P,GAM,TAU,WAF,J1,H,JMAX
      FREQUENCY 18(100,1,5),45(50,1,10),48(100,1,2),62(50,1,2),73(10,1),
     176(50,1,10),79(50,1,5)
    1 JM1=JMAX-1
    2 IGO=1
C     SECTION 1, COMPUTATIONS FOR LEVELS 1 THROUGH 5 IN GAMO2, 1 THROUGH
C        4 IN WAF.
    3 GAM(1)=GAMO2(T(1),P(1),F)
    4 TAU(1)=GAM(1)
    5 SECTH=1.0/COSF(THETA)
    6 TAK=TAU(1)
    7 WAF(1)=(EXPF(-TAK*SECTH))*GAM(1)*SECTH
    9 GAM(2)=GAMO2(T(2),P(2),F)
    8 DO 13 I=2,4
   10 GAM(I+1)=GAMO2(T(I+1),P(I+1),F)
   11 TAU(I)=(((GAM(I-1)+2.0*GAM(I)+GAM(I+1))/4.0)*0.1)+TAU(I-1)
   12 TAK=TAU(I)
   13 WAF(I)=(EXPF(-TAK*SECTH))*GAM(I)*SECTH
   14 DWAF=(((WAF(4)-WAF(2))/0.2)*1.2)+WAF(3)
   15 IC=4
   16 JM13=JMAX-13
   17 JC=4
   18 IF (DWAF-0.0005) 19,49,49
C     SECTION 2, COMPUTATIONS FOR LEVELS JC+9 THROUGH JC+13 IN GAMO2 AND
C        LEVELS JC+10 THROUGH JC+12 IN WAF.
   19 JC=JC+9
      GAM(JC)=GAMO2(T(JC),P(JC),F)
```

```
   20 GJC=GAM(JC)
   21 TAU1=(((GAM(JC)+GAM(JC-8))/2.0)*0.9)+TAU(JC-9)
   22 DO 24 I=1,4
   23 JCI=JC+I
      GAM(JCI)=GAMO2(T(JCI),P(JCI),F)
   24 GJCI=GAM(JCI)
   25 TAU(JC+1)=TAU1+(((GAM(JC)+GAM(JC+1))/2.0)*0.1)
   26 TAK=TAU(JC+1)
   27 WAF(JC+1)=(EXPF(-TAK*SECTH))*GAM(JC+1)*SECTH
   28 DO 32 I=2,3
   29 JCI=JC+I
   30 TAU(JCI)=(((GAM(JCI-1)+2.0*GAM(JCI)+GAM(JCI+1))/4.0)*0.1)+TAU(JCI-
     11)
   31 TAK=TAU(JCI)
   32 WAF(JCI)=(EXPF(-TAK*SECTH))*GAM(JCI)*SECTH
   33 DO 41 I=1,3
   34 ICI=IC+I
   35 JCI=JC+I
   36 J1(ICI)=J1(JCI)
   37 H(ICI)=H(JCI)
   38 T(ICI)=T(JCI)
  381 P(ICI)=P(JCI)
   39 GAM(ICI)=GAM(JCI)
      GIC=GAM(ICI)
   40 TAU(ICI)=TAU(JCI)
      TIC=TAU(ICI)
      WAF(ICI)=WAF(JCI)
   41 WIC=WAF(ICI)
   42 IC=ICI
   43 JC=JCI
   44 GO TO (45,49),IGO
   45 IF (JC-JM13) 47,46,481
   46 IGO=2
   47 DWAF=(((WAF(ICI)-WAF(ICI-2))/0.2)*1.2)+WAF(ICI-1)
   48 IF (DWAF-0.0005) 19,49,49
  481 IGO=2
C     SECTION 3, COMPUTATIONS FOR LEVEL JC+2 IN GAMO2 AND LEVEL JC+1 IN
C        WAF.
   49 JCI=JC+1
   50 GAM(JCI+1)=GAMO2(T(JCI+1),P(JCI+1),F)
   51 TAU(JCI)=(((GAM(JCI-1)+2.0*GAM(JCI)+GAM(JCI+1))/4.0)*0.1)+TAU(JCI-
     11)
   52 TAK=TAU(JCI)
   53 WAF(JCI)=(EXPF(-TAK*SECTH))*GAM(JCI)*SECTH
   54 ICI=IC+1
   55 J1(ICI)=J1(JCI)
   56 H(ICI)=H(JCI)
   57 T(ICI)=T(JCI)
   58 P(ICI)=P(JCI)
   59 GAM(ICI)=GAM(JCI)
   60 TAU(ICI)=TAU(JCI)
   61 WAF(ICI)=WAF(JCI)
  611 IC=ICI
  612 JC=JCI
   62 IF (JCI-JM1) 73,63,63
C     SECTION 4, COMPUTATIONS FOR LEVEL JMAX IN ALL PARAMETERS.
   63 ICI=IC+1
   64 J1(ICI)=J1(JMAX)
   65 H(ICI)=H(JMAX)
```

```
66 T(ICI)=T(JMAX)
67 P(ICI)=P(JMAX)
68 GAM(ICI)=GAM(JMAX)
69 TAU(ICI)=(((GAM(JMAX)+GAM(JM1))/2.0)*0.1)+TAU(JC)
70 TAK=TAU(ICI)
71 WAF(ICI)=(EXPF(-TAK*SECTH))*GAM(ICI)*SECTH
72 GO TO 80
73 GO TO (76,49),IGO
76 IF (JC-JM13) 78,77,481
77 IGO=2
78 DWAF=(((WAF(ICI)-WAF(ICI-2))/0.2)*1.2)+WAF(ICI-1)
79 IF (DWAF-0.0005) 19,49,49
80 JMAX=ICI
81 RETURN
   END
```

```
CMISP4    B. R FOW  ID NO. AAP8  PROGRAM MISP4  22 AUGUST 1963
C
C         THIS PROGRAM COMPUTES BRIGHTNESS TEMPERATURE AND FINDS THE ALTI-
C       TUDE OF THE PEAK OF THE WEIGHTING FUNCTION FOR A GIVEN ATMOSPHERE,
C       FREQUENCY, NADIR ANGLE AND EXTERNAL SOURCE TEMPERATURE.
C
C          INPUT DATA REQUIRED
C
C             NAME, DATE AND ID CARD
C             KD1=THE NUMBER OF TEMPERATURE POLYNOMIAL COEFFICIENTS.
C             KD2=THE NUMBER OF BRIGHTNESS TEMPERATURE VS. FREQUENCY AND
C                  NADIR ANGLE POINTS.
C             HMIN=THE MINIMUM HEIGHT OF INITIAL AND DERIVED TEMPERATURE
C                  PROFILES, KM.
C             HMAX=THE MAXIMUM HEIGHT OF INITIAL AND DERIVED TEMPERATURE
C                  PROFILES, KM.
C             JRD=SENSE OF RADIOMETER OR ANTENNA.
C                    JRD=1, SENSE IS UP FROM HMIN TO HMAX.
C                    JRD=2, SENSE IS DOWN FROM HMAX TO HMIN.
C             PZERO=GROUND LEVEL VALUE OF PRESSURE, MM OF HG.
C             GZERO=GROUND LEVEL VALUE OF GRAVITATIONAL ACCELERATION,
C                    CM/SEC**2.
C             VARG=RATE OF CHANGE WITH HEIGHT OF GRAVITATIONAL ACCELERA-
C                    TION, CM/SEC**2/KM.
C             TMS=BRIGHTNESS TEMPERATURE OF SOUCE LYING OUTSIDE THE ATMOS-
C                    PHERE, DEG K.
C             TB=INPUT BRIGHTNESS TEMPERATURES, DEG K.
C             FI=INPUT FREQUENCIES, GC/SEC.
C             ZA=INPUT NADIR ANGLES, DEG.
C
C          OUTPUT DATA
C
C          JWFM=LEVEL NO OF WEIGHTING FUNCTION PEAK.
C          HWFM=HEIGHT OF WEIGHTING FUNCTION PEAK, KM.
C          TWFM=KINETIC TEMPERATURE AT THE LEVEL OF THE WEIGHTING FUNCTION
C                PEAK, DEG. K.
C          PWFM=PRESSURE AT THE LEVEL OF THE WEIGTING FUNCTION PEAK, MM OF
C                HG.
C          TBR=BRIGHTNESS TEMPERATURE.
C          WFM=MAXIMUM VALUE OF WEIGHTING FUNCTION.
C
C          SUBPROGRAMS REQUIRED   ATMSP4,KERNL1, AND BTEMP2.
C
      DIMENSION AR(12),AI(20),        FI(30),ZA(30),T(1001),P(1001),GAM(1
     1001),TAU(1001),WAF(1001),J1(1001),H(1001),J2(1001),H2(1001),T2(100
     21),P2(1001),HH2(1003),TT2(1003),ARR(12),BATA(800),HE(2),TE(2)
      EQUIVALENCE (H2,HH2),(T2,TT2)
      COMMON T,P,GAM,TAU,WAF,J1,H,JMAX
      CALL PLOTS(BATA(800),800)
   10 READ INPUT TAPE 2,1010,(AR(I),I=1,12)
   30 READ INPUT TAPE 2,1030,HMIN,HMAX,PZERO,GZERO,VARG,KD1,KD2,JRD,TB
   40 READ INPUT TAPE 2,1040,(TE(I),HE(I),I=1,2),YH,XT
   50 READ INPUT TAPE 2,1050,(AI(I),I=1,KD1)
   60 READ INPUT TAPE 2,1060,(FI(I),ZA(I),I=1,KD2)
   70 WRITE OUTPUT TAPE 3,1010,(AR(I),I=1,12)
   90 WRITE OUTPUT TAPE 3,1030,HMIN,HMAX,PZERO,GZERO,VARG,KD1,KD2,JRD,TB
  100 WRITE OUTPUT TAPE 3,1040,(TE(I),HE(I),I=1,2),YH,XT
  110 WRITE OUTPUT TAPE 3,1050,(AI(I),I=1,KD1)
```

```
120 WRITE OUTPUT TAPE 3,1060,(FI(I),ZA(I),I=1,KD2)
130 CALL ATMSP4(KD1,AI,HMIN,HMAX,JRD,PZERO,GZERO,VARG)
131 JMX2=JMAX
132 DO 136 K=1,JMX2
133 J2(K)=J1(K)
134 H2(K)=H(K)
135 T2(K)=T(K)
136 P2(K)=P(K)
137 WRITE OUTPUT TAPE 3,2000,(AR(I),I=1,12)
165 DO 320 I=1,KD2
166 F=FI(I)
170 A=ZA(I)*0.0174533
171 JMAX=JMX2
172 DO 176 M=1,JMAX
173 J1(M)=J2(M)
174 H(M)=H2(M)
175 T(M)=T2(M)
176 P(M)=P2(M)
180 CALL KERNL1(F,A)
190 CALL BTEMP2(TB,TBR,A)
199 Z=ZA(I)
200 WFM=WAF(1)
201 M=1
210 DO 270 J=2,JMAX
220 WAFJ=WAF(J)
230 IF(WAFJ-WFM)270,250,250
250 M=J
260 WFM=WAFJ
270 CONTINUE
280 JWFM=J1(M)
290 HWFM=H(M)
300 TWFM=T(M)
310 PWFM=P(M)
320 WRITE OUTPUT TAPE 3,2010,F,Z,TBR,WFM,JWFM,HWFM,TWFM,PWFM
330 JM1=JMX2+1
340 JM2=JMX2+2
350 HH2(JM1)=HE(1)
360 HH2(JM2)=HE(2)
370 TT2(JM1)=TE(1)
380 TT2(JM2)=TE(2)
390 CALL SCALE(HH2,JM2,YH,HH2M,DHH2)
400 CALL SCALE(TT2,JM2,XT,TT2M,DTT2)
410 CALL AXIS(0.0,0.0,10HHEIGHT, KM,10,YH,90.0,HH2M,DHH2)
420 CALL AXIS(0.0,0.0,18HTEMPERATURE, DEG K,18,XT,0.0,TT2M,DTT2)
430 CALL LINE(T2,H2,JMX2)
440 DO 460 I=1,12
450 IR=13-I
460 ARR(IR)=AR(I)
470 CALL PLOT(-1.0,-0.75,-3)
480 YB=YH+1.5
490 XB=XT+1.5
500 CALL PLOT(0.0,YB,2)
510 CALL PLOT(XB,YB,2)
520 CALL PLOT(XB,0.0,2)
530 CALL PLOT(0.0,0.0,2)
540 CALL PLOT(2.0,0.05,-3)
550 CALL SYMBL4(0.0,0.0,0.15,ARR(12),0.0,72)
560 CALL PLOT(XB,0.0,-3)
570 CALL EXIT
```

```
1010 FORMAT(12A6)
1030 FORMAT(5F10.3,3I4,F10.3)
1040 FORMAT(6F10.3)
1050 FORMAT(4E18.6)
1060 FORMAT(6F10.5)
2000 FORMAT(1H1,28X,12A6)
2010 FORMAT(5X///5X11HFREQUENCY =,F8.4,7HGC/SEC.,//5X13HNADIR ANGLE =,F
     16.2,8HDEGREES.//5X24HBRIGHTNESS TEMPERATURE =,F8.3,15HDEGREES KELV
     2IN.//5X35HMAXIMUM VALUE OF WEIGHT. FUNCTION =,E12.5//5X,108HLEVEL,
     3 HEIGHT, KINETIC TEMPERATURE, AND PRESSURE AT THE HEIGHT CORRESPON
     4DING TO THE WEIGHTING FUNCTION PEAK.//5X11HLEVEL NO. =,I3//5X8HHEI
     5GHT =,F6.2,3HKM.//5X13HTEMPERATURE =,F7.3,7HDEG. K.//5X10HPRESSURE
     6 =,E12.5,9HMM OF HG.)
      END
```

```
CMISP5     B. R. FOW            PROGRAM MISP5     4 OCTOBER 1963
C
C        THIS PROGRAM COMPUTES BRIGHTNESS TEMPERATURE AND FINDS THE ALTI-
C      TUDE OF THE PEAK OF THE WEIGHTING FUNCTION FOR A GIVEN ATMOSPHERE,
C      FREQUENCY, NADIR ANGLE AND EXTERNAL SOURCE TEMPERATURE.
C
C          INPUT DATA REQUIRED
C
C            NAME, DATE AND ID CARD
C          KD1     THE NUMBER OF TEMPERATURE VS HEIGHT DATA POINTS.
C          TD(I)  TEMPERATURE DATA POINT.
C          ZD(I)  CORRESPONDING HEIGHT DATA POINT.
C            KD2=THE NUMBER OF BRIGHTNESS TEMPERATURE VS. FREQUENCY AND
C                  NADIR ANGLF POINTS.
C            HMIN=THE MINIMUM HEIGHT OF INITIAL AND DERIVED TEMPERATURE
C                  PROFILES, KM.
C            HMAX=THE MAXIMUM HEIGHT OF INITIAL AND DERIVED TEMPERATURE
C                  PROFILES, KM.
C            JRD=SENSE OF RADIOMETER OR ANTENNA.
C                    JRD=1, SENSE IS UP FROM HMIN TO HMAX.
C                    JRD=2, SENSE IS DOWN FROM HMAX TO HMIN.
C            PZERO=GROUND LEVEL VALUE OF PRESSURE, MM OF HG.
C            GZERO=GROUND LEVEL VALUE OF GRAVITATIONAL ACCELERATION,
C                    CM/SEC**2.
C            VARG=RATE OF CHANGE WITH HEIGHT OF GRAVITATIONAL ACCELERA-
C                    TION, CM/SEC**2/KM.
C            TMS=BRIGHTNESS TEMPERATURE OF SOUCE LYING OUTSIDE THE ATMOS-
C                    PHERE, DEG K.
C            TB=INPUT BRIGHTNESS TEMPERATURES, DEG K.
C            FI=INPUT FREQUENCIES, GC/SEC.
C            ZA=INPUT NADIR ANGLES, DEG.
C
C          OUTPUT DATA
C
C          JWFM=LEVEL NO OF WEIGHTING FUNCTION PEAK.
C          HWFM=HEIGHT OF WEIGHTING FUNCTION PEAK, KM.
C          TWFM=KINETIC TEMPERATURE AT THE LEVEL OF THE WEIGHTING FUNCTION
C                  PEAK, DEG. K.
C          PWFM=PRESSURE AT THE LEVEL OF THE WEIGTING FUNCTION PEAK, MM OF
C                  HG.
C          TBR=BRIGHTNESS TEMPERATURE.
C          WFM=MAXIMUM VALUE OF WEIGHTING FUNCTION.
C
C           SUBPROGRAMS REQUIRED   ATMSP5,KERNL1, AND BTEMP2.
C
      DIMENSION AR(12),ZD(50),TD(50),FI(30),ZA(30),T(1001),P(1001),GAM(1
     1001),TAU(1001),WAF(1001),J1(1001),H(1001),J2(1001),H2(1001),T2(100
     21),P2(1001),HH2(1003),TT2(1003),ARR(12),BATA(800),HE(2),TE(2)
      EQUIVALENCE (H2,HH2),(T2,TT2)
      COMMON T,P,GAM,TAU,WAF,J1,H,JMAX
      CALL PLOTS(BATA(800),800)
   10 READ INPUT TAPE 2,1010,(AR(I),I=1,12)
   30 READ INPUT TAPE 2,1030,HMIN,HMAX,PZERO,GZERO,VARG,KD1,KD2,JRD,TB
   40 READ INPUT TAPE 2,1040,(TE(I),HE(I),I=1,2),YH,XT
   50 READ INPUT TAPE 2,1050,(ZD(I),TD(I),I=1,KD1)
   60 READ INPUT TAPE 2,1060,(FI(I),ZA(I),I=1,KD2)
   70 WRITE OUTPUT TAPE 3,1010,(AR(I),I=1,12)
   90 WRITE OUTPUT TAPE 3,1030,HMIN,HMAX,PZERO,GZERO,VARG,KD1,KD2,JRD,TB
```

```
100 WRITE OUTPUT TAPE 3,1040,(TE(I),HE(I),I=1,2),YH,XT
110 WRITE OUTPUT TAPE 3,1050,(ZD(I),TD(I),I=1,KD1)
120 WRITE OUTPUT TAPE 3,1060,(FI(I),ZA(I),I=1,KD2)
130 CALL ATMSP5(KD1,ZD,HMIN,HMAX,JRD,PZERO,GZERO,VARG,TD)
131 JMX2=JMAX
132 DO 136 K=1,JMX2
133 J2(K)=J1(K)
134 H2(K)=H(K)
135 T2(K)=T(K)
136 P2(K)=P(K)
137 WRITE OUTPUT TAPE 3,2000,(AR(I),I=1,12)
138 WRITE OUTPUT TAPE 3,2030
139 WRITE OUTPUT TAPE 3,2031,(J1(I),H(I),T(I),P(I),I=1,JMAX)
165 DO 320 I=1,KD2
166 F=FI(I)
170 A=ZA(I)*0.0174533
171 JMAX=JMX2
172 DO 176 M=1,JMAX
173 J1(M)=J2(M)
174 H(M)=H2(M)
175 T(M)=T2(M)
176 P(M)=P2(M)
180 CALL KERNL1(F,A)
190 CALL BTEMP2(TB,TBR,A)
199 Z=ZA(I)
200 WFM=WAF(1)
201 M=1
210 DO 270 J=2,JMAX
220 WAFJ=WAF(J)
230 IF(WAFJ-WFM)270,250,250
250 M=J
260 WFM=WAFJ
270 CONTINUE
280 JWFM=J1(M)
290 HWFM=H(M)
300 TWFM=T(M)
310 PWFM=P(M)
320 WRITE OUTPUT TAPE 3,2010,F,Z,TBR,WFM,JWFM,HWFM,TWFM,PWFM
330 JM1=JMX2+1
340 JM2=JMX2+2
350 HH2(JM1)=HE(1)
360 HH2(JM2)=HE(2)
370 TT2(JM1)=TE(1)
380 TT2(JM2)=TE(2)
390 CALL SCALE(HH2,JM2,YH,HH2M,DHH2)
400 CALL SCALE(TT2,JM2,XT,TT2M,DTT2)
410 CALL AXIS(0.0,0.0,10HHEIGHT, KM,10,YH,90.0,HH2M,DHH2)
420 CALL AXIS(0.0,0.0,18HTEMPERATURE, DEG K,18,XT,0.0,TT2M,DTT2)
430 CALL LINE(T2,H2,JMX2)
440 DO 460 I=1,12
450 IR=13-I
460 ARR(IR)=AR(I)
470 CALL PLOT(-1.0,-0.75,-3)
480 YB=YH+1.5
490 XB=XT+1.5
500 CALL PLOT(0.0,YB,2)
510 CALL PLOT(XB,YB,2)
520 CALL PLOT(XB,0.0,2)
530 CALL PLOT(0.0,0.0,2)
```

```
  540 CALL PLOT(2.0,0.05,-3)
  550 CALL SYMBL4(0.0,0.0,0.15,ARR(12),0.0,72)
  560 CALL PLOT(XB,0.0,-3)
  570 CALL EXIT
 1010 FORMAT(12A6)
 1030 FORMAT(5F10.3,3I4,F10.3)
 1040 FORMAT(6F10.3)
 1050 FORMAT(6F10.3)
 1060 FORMAT(6F10.5)
 2000 FORMAT(1H1,28X,12A6)
 2010 FORMAT(5X///5X11HFREQUENCY =,F8.4,7HGC/SEC.,//5X13HNADIR ANGLE =,F
     16.2,8HDEGREES.//5X24HBRIGHTNESS TEMPERATURE =,F8.3,15HDEGREES KELV
     2IN.//5X35HMAXIMUM VALUE OF WEIGHT. FUNCTION =,E12.5//5X,108HLEVEL,
     3 HEIGHT, KINETIC TEMPERATURE, AND PRESSURE AT THE HEIGHT CORRESPON
     4DING TO THE WEIGHTING FUNCTION PEAK.//5X11HLEVEL NO. =,I3//5X8HHEI
     5GHT =,F6.2,3HKM.//5X13HTEMPERATURE =,F7.3,7HDEG. K.//5X10HPRESSURE
     6 =,E12.5,9HMM OF HG.)
 2030 FORMAT(1H1)
 2031 FORMAT(4(1X,I3,1X,F5.1,2X,F7.3,1X,E12.5))
      END
```

1258

ACKNOWLEDGMENTS

I would first like to thank Dr. M. L. Meeks for suggesting and encouraging me to pursue this research. Dr. Meeks also made generous contributions of his time in discussing technical matters with me, directing my research efforts and in obtaining technical and financial support for this work.

I would also like to thank my thesis advisor, Professor Reginald E. Newell for his interest in this work and his invaluable assistance in the writing of this manuscript.

There have been many other people who have given me encouragement and technical assistance in various aspects of this work. I would especially like to thank Dr. Sander Weinreb and Dr. Tor Hagfors of Lincoln Laboratory, M.I.T., and Professor F. B. Hildebrand of M.I.T.

The computational aspects of this work were performed at the M.I.T. Lincoln Laboratory Computation Center. I appreciate very much the assistance of the people in the computer group and I would especially like to thank Mr. Joseph A. Obrien, Mr. Keith T. Russell and Miss Betty M. Lee for the assistance in programming.

Also, I would like to thank the Drafting Department at Lincoln Laboratory for preparing the figures in this work.

The temperature measurements used to obtain ATMOSPHERE 2 were obtained from an unpublished manuscript by W. Nordberg and W. Smith of National Aeronautics and Space Administration entitled "Rocket Measurements of the Structure of the Upper Stratosphere and Mesosphere." (This manuscript was supplied to Professor Newell in April 1963.)

The temperatures used to obtain ATMOSPHERE 3 and ATMOSPHERE 4 were from cross-sections drawn by Mrs. Dorothy Berry for Professor Newell's Upper Atmosphere class.

Finally, I would like to express my appreciation to Mrs. Carol A. Jordan and Miss E. Judith Porter who typed the manuscript.

REFERENCES

Dicke, R. H., "The Measurement of Thermal Radiation at Microwave Frequencies," Rev. Sci. Instr., 17, 7, pp 268-275, July 1946.

Fryberger, D. and E. F. Uretz, "Some Considerations Concerning the Measurement of the Atmospheric Temperature Field by Electromagnetic Means," IRE Transactions on Mil Electronics, pp 279-285, Oct. 1961.

Hagfors, T., Notes on Quantum Effects in Radiometer Observations, private communication.

Hildebrand, F. B., Introduction to Numerical Analysis, Chapter 7, McGraw-Hill, 1956.

Hildebrand, F. B., Methods of Applied Mathematics, Prentice-Hall, 1958.

Hogg, D. C., and R. A. Semplak, "The Effect of Rain and Water Vapor on Sky Noise at Centimeter Wavelengths," Bell System Technical Jour., XL, No. 5, p 1331, 1961.

Kaplan, L. D., "Inference of Atmospheric Structure from Remote Radiation Measurements," J. Optical Soc. Am., 49, pp 1004-1007, 1959.

Kaplan, L. D., "The Spectroscope as a Tool for Atmospheric Sounding by Satellites," Tech. Report No. 5, Atmos. Rad. Proj., M.I.T. Paper given at the Fall Instrument-Automation Conference and Exhibit of the Instrument Society of America, Sept. 26-30, 1960.

King, J. I. F., "Deduction of Vertical Thermal Structure of a Planetary Atmosphere from a Satellite," Aerosciences Lab., Gen. Elec.Co., Tech. Info. Ser. R59SD477, Dec. 1959.

King, J. I. F., "Meteorological Inferences from Satellite Radiometry I," Journal of Atmos. Sci., 20, No. 4, pp 245-250, July 1963.

Meeks, M. L., "Atmospheric Emission and Opacity at Millimeter Wavelengths Due to Oxygen," J. Geophys. Res., 66, No. 11, pp 3749-3757, Nov. 1961.

Meeks, M. L., and A. E. Lilley, "The Microwave Spectrum of Oxygen in the Earth's Atmosphere," J. Geophys. Res., 68, No. 6, pp 1683-1703, March 1963.

Steinberg, J. L. et J. Lequeux, Radioastronomie, Collection Science et Progrés No. 4, Dunod, Paris, 1960.

Wark, D. Q., "On Indirect Temperature Soundings of the Stratosphere from Satellites," J. Geophys. Res., 66, pp 77-82, 1960.

Yamamoto, G., "Numerical Method for Estimating the Stratospheric Temperature Distribution from Satellite Measurements in the CO_2 Band," J. of Meteor., 18, No. 5, pp 581-588, Oct. 1961.